IS-T--1564

DE91 018286

Tribological and Arc Erosion Behaviors of Copper-refractory Metal In Situ Composites

by

Liu, Ping

PHD Thesis submitted to Iowa State University

Ames Laboratory, U.S. DOE

Iowa State University

Ames, Iowa 50011

Date Transmitted: August 6, 1991

PREPARED FOR THE U.S. DEPARTMENT OF ENERGY

UNDER CONTRACT NO. W-7405-Eng-82.

DISCLAIMER

Tribological and arc erosion behaviors of copper-refractory metal in situ composites

Ping Liu

Under the supervision of Shyam Bahadur
From the Department of Mechanical Engineering and
John D. Verhoeven from the Department of Materials Science and Engineering
Iowa State University

Tribological and arc erosion behaviors of Cu-Nb and Cu-Cr in situ composites were investigated in this dissertation. Dry sliding tests were performed in a pin-on-disk wear tester with the composites rubbing against a rotating tool steel disk under ambient conditions with a pressure of 0.68 MPa, sliding speeds up to 2.5 m/s, and electrical current densities up to 2.89 MA/m^2. Electrical arc erosion tests were performed in a make-and-break test set-up and a high-energy stationary arc gap test facility.

Sliding friction and wear behaviors of Cu-Nb composites with and without electrical loads were studied in terms of the effects of composition, filament orientation, true deformation strain, sliding speed and annealing temperature. The Cu-20vol.%Nb composite had the best wear resistance among the compositions studied in both cases. Subsurface deformation was revealed by the presence of filaments and was one of the wear mechanisms for the composites. No debonding was observed in the composites during sliding. The presence of electrical current increased the temperature and promoted oxidation on wear surfaces.

The contact behavior of Cu-Nb composites against tool steel was studied in terms of the contact resistance and temperature rise. Surface oxide film development, wear

particle accumulation, and unsteady contact caused by sliding were found to be the major factors governing electrical contact resistance and, therefore, temperature rise. Arc erosion behavior of the composites was also investigated. It was concluded that, in low-energy make-and-break contacts, oxidation was the major mode of surface deterioration; and, in high-energy contact situation, melting was the major cause of surface damage. The Cu-refractory metal in situ composites had better arc erosion resistance in high-energy contacts than the commercially used Cu-W composite.

Tribological and arc erosion behaviors of copper-refractory metal in situ composites

by

Ping Liu

A Dissertation Submitted to the
Graduate Faculty in Partial Fulfillment of the
Requirements for the Degree of
DOCTOR OF PHILOSOPHY

Major: Mechanical Engineering

Approved:

_____

_____
In Charge of Major Work

_____
For the Major Department

_____
For the Graduate College

Iowa State University
Ames, Iowa
1991

TABLE OF CONTENTS

INTRODUCTION

Copper refractory metal in situ composites were prepared by consumable electrode arc melting and casting followed by extensive deformation processing. As a result of this processing technique, refractory metal filaments were formed in the copper matrix since the constituent elements such as Cu and Nb have hardly any solid solubility at room temperature. Because of the resultant superior combination of conductivity and mechanical strength, these alloys have drawn a lot of research efforts. These composites are promising candidates for application in electrical sliding contacts, where high electrical/thermal conductivity, wear resistance and arc erosion resistance are critical for their normal function and longevity of service life.

Electrical sliding contact is essential for transferring electrical current from moving parts to stationary ones. Recently, extensive research has been focused on sliding contacts due to their use in advanced homopolar electrical machines operating at much higher rotating speeds and electrical currents. The problems associated with electrical sliding contacts are friction and wear, electrical contact resistance, temperature rise and arc erosion.

Explanation of Dissertation Format

In this dissertation, tribological and arc erosion behaviors of copper-refractory metal in situ composites, such as Cu-Nb and Cu-Cr, were studied in five independent parts. Each part is written in the format for direct publication in a technical journal.

Part I deals with the mechanical and tribological behavior of Cu-Nb composites. The mechanical behavior and material structure were studied to provide a basis for understanding the tribological behavior. The effects of Nb proportion and true deformation strain on friction and wear were investigated. The wear mechanisms were studied by scanning electron microscopy of the worn surfaces.

Part II further discusses the friction and wear behavior of Cu-20vol.%Nb sheet composites in terms of the substrate deformation, annealing behavior, sliding speed and filament orientation. Subsurface deformation was revealed by the changes in filament orientation and morphology of the substrate. A wear mechanism of subsurface deformation flow was proposed for this composite. The wear mechanisms were studied by optical and scanning electron microscopy.

Part III investigates the friction and wear behavior of Cu-Nb in situ composites under electrical load. The effects of Nb proportion, electrical current density, sliding speed and filament orientation were studied and compared with those for non-electrical sliding. Oxidation was found to be the major factor affecting the friction and wear behavior. The wear mechanisms were studied by optical and scanning electron microscopy.

Part IV studies the sliding contact behavior of Cu-Nb composites against tool steel. The effects of sliding speed, true deformation strain, Nb proportion and filament orientation on the electrical contact resistance and the temperature rise were

investigated. The surface films formed during electrical sliding were analyzed by X-ray diffraction, and optical and scanning electron microscopy.

Part V presents the arc erosion and contact behaviors of Cu-15vol.%Nb and Cu-15vol.%Cr composites for the low-energy make-and-break contact and high-energy stationary contact situations. The arc erosion mechanism was studied by examining the surfaces and the cross-sections of the eroded electrodes. It was found that, in low-energy condition, oxidation was the major factor for surface deterioration whereas, in the high-energy contact situation, melting was the major failure mode.

The conclusions are summarized at the end of this dissertation.

PART I.

THE MECHANICAL AND TRIBOLOGICAL BEHAVIORS OF Cu-Nb *in situ* COMPOSITES

ABSTRACT

The mechanical and tribological behaviors of Cu-Nb in situ composites were studied. These composites were prepared by consumable arc melting of Cu and Nb electrodes, casting and successive deformation of the cast ingot. Sliding friction and wear tests were performed in a pin-on-disk wear tester with the composite specimen rubbing under dry atmospheric conditions against a flat, hardened tool steel disk surface. The effect of the Nb proportion on the tribological behavior of composites was studied by varying the volume percentage of Nb from zero to 30. It was found that the coefficient of friction decreased slightly with increasing Nb proportion and that Cu-20vol.%Nb composite had the best wear resistance. The effect of true deformation strain on the friction and wear of the composites was also investigated. The micromechanisms of wear were studied by scanning electron microscopy and energy dispersive spectrometry. It was inferred that the deformation-induced fracture was the major mechanism in the wear of these in situ composites.

INTRODUCTION

The in situ composites which are prepared by the successive large-scale deformation of ductile two-phase structures have lately drawn considerable attention. The in situ process for fabricating Cu-Nb composites was developed because of the need for an alternative method for producing A-15 type superconductors, namely Nb_3Sn-Cu [1]. During the early research it was discovered that Cu-Nb composites exhibited unique mechanical properties. Recent studies have been concentrated on correlating the high strengths developed in these composites during cold working with their microstructure.

The Cu-Nb alloy was first made by a casting process. It yielded almost pure Nb dendrites in a nearly pure Cu matrix because Cu and Nb are mutually insoluble at room temperature [2]. The two-phase alloy was so ductile that it could be subjected to reduction ratios of more than 100 % under ambient conditions [3]. As a consequence of this deformation, Nb dendrite arms were drawn into ribbon-like filaments of irregular cross-section. The filaments were aligned along the deformation axis yielding a metal matrix composite with excellent fiber alignment.

Bevk et al. [4] found that the tensile strength of the finest Cu-Nb wires was 2.23 GPa at 293 K which is as high as that of the best Cu whiskers [5]. In support of the development of such a high strength, it was hypothesized that the structure of these fine wires consisted of two high-strength phases with different defect structures. Nb filaments had virtually no dislocations and therefore exhibited whisker-like behavior, while the Cu matrix was highly dislocated with a dislocation density of $10^{13} cm^{-2}$. Recently, Spitzig and Krotz [6] showed that the strength of heavily cold worked Cu-Nb wire increased as the spacing between Nb filaments decreased. It

was found that the composite obeyed a Hall-Petch type relationship indicating that the filaments acted as planar barriers to the dislocation motion between Cu and Nb. Spitzig et al. [7] found that, in the course of rolling, the Cu matrix in the composites of Cu-12vol.%Nb and Cu-20vol.%Nb underwent a deformation-recovery-recrystallization cycle and Trybus [8] observed that dislocation densities of the Cu matrix were on the order of $10^{10} cm^{-2}$.

Cu-Nb in situ composites exhibit the unique combination of high mechanical strength coupled with high thermal/electrical conductivity. With the expectation of finding use in radiation heat transfer applications, Downing et al. [9] showed that the emissivity of an etched alloy surface could be increased from 0.08 to more than 0.9. A study by Renaud et al. [10] on Cu-18vol.%Nb strip demonstrated a tensile strength of 1082 MPa with an electrical conductivity of 67%$IACS$ (International Annealed Copper Standard). This attractive strength/electrical conductivity combination offers the potential for application of these in situ composites in electrical sliding contacts where high electrical conductivity, high thermal conductivity and good wear resistance are required. It is from this aspect that the tribological behavior of Cu refractory metal in situ composites was investigated in this work.

In tribology most studies on composites have been conducted on polymer composites. It has been summarized [11] that the ideal polymer matrix should have a structure with weak bonds acting through the surface but with strong bonds and, therefore, high cohesion in the interior. A material with such characteristics does not presently exist. The role of the reinforcement component is dependent upon its type, geometry and arrangement. Internal lubricants are helpful in reducing adhesive wear but can cause an increase in wear rate when abrasion is the dominant mecha-

nism of material removal. In most cases, the best wear resistance was obtained with the orientation of fibers normal to the sliding direction, but for this condition the frictional coefficients were usually the highest, as observed in Kevlar-epoxy composites [12]. As an exception to this, both the wear and the coefficient of friction of graphite fiber-epoxy composites were minimum at normal fiber orientation [12]. For hybrid carbon/glass fiber epoxy composite materials, Hawthorne [13] indicated that the effect of fiber orientation on wear behavior and the optimum orientation for wear resistance depended on the composite composition. The wear behavior of hybrid composites appeared to be influenced by the abrasiveness, fatigue resistance, film transfer characteristics and relative load-bearing capability of the two constituent phases. Clerico and Patierno [14] showed that the wear mechanism of semicrystalline polymer composites was similar to the delamination mechanism observed in metals, involving subsurface deformation, crack nucleation at the matrix-hard particle or matrix-glass fiber interface, and crack propagation parallel to the surface.

Amateau et al. [15] studied the tribological behavior of continuous graphite fiber reinforced metal matrix composites. Here the fibers were incorporated into copper and silver alloys by means of the liquid-metal infiltration technique. The study indicated that the type of graphite fiber in the composite was the most significant factor in wear and friction behavior. In some high-modulus fiber tin-bronze composites, the fiber fraction influenced the wear rate, but not the coefficient of friction. However, the effect of fiber fraction in a wide range could not be studied because of the limitation of infiltration techniques. Das and Prasad [16] studied the microstructure and the wear behavior of cast Al-Si alloy-graphite composites and found that the distribution of dispersed graphite particles and the morphology of silicon influenced

the tribological behavior. The wear resistance of the composites in the heat treated condition was superior to that in the cast condition. It was also better than that of the matrix alloy. Nath et al. [17] studied the tribological properties of mica-dispersed Al-4%Cu-1.5%Mg composite and found that the wear rate of the composite increased with both mica content and bearing pressure. They also noted that the dispersion of mica in the matrix decreased the temperature rise during wear and improved the ability of the composite to resist seizure. Tsuya et al. [18] studied the effects of varying composition on the coefficient of friction, wear rate, electrical resistance, hardness, porosity and structure of copper-based and copper-tin based composites containing tungsten disulfide and molybdenum disulfide as the lubricating phases. They found that the optimum content of tungsten disulfide was 20% for effectively reducing the wear rate and the coefficient of friction in air and in vacuum up to 600 ^{o}C. Eliezer et al. [19] investigated the high speed tribological properties of graphite fiber/Cu-Sn matrix composites. They reported that the coefficient of friction and the wear rate of the composites depended on the proportion of Sn, orientation of fibers, sliding velocity, graphite grain size, and the degree of liquid-metal infiltration within the fibers.

As indicated earlier, Cu-Nb composites offer a great combination of mechanical and electrical properties, which makes them suitable candidates for sliding electrical contact applications. It was, therefore, decided to study in this paper the mechanical and the tribological behavior of these composites under dry sliding conditions.

EXPERIMENTAL

Materials

The ingots of Cu-Nb composites were prepared by consumable arc melting of the electrodes made from the corresponding constituents [3]. The ingots were successively deformed to either the sheet or the rod form. The sheet was produced by milling a 73 mm diameter ingot with diametrically opposite flats of 51 mm thickness and later rolling at room temperature into a flat of 1.6 mm thickness. The reduction in each pass was about 10%.

In order to achieve higher true deformation strain, the bundling technique was used. Here an ingot of 76.7 mm diameter was put into a pure copper can which was evacuated to 10^{-6} $torr$ and sealed. The ingot with copper jacket around it was extruded into hexagonal wires. The copper on the outside surface of these wires was removed by etching with 50vol.% aqueous solution of HNO_3. Seventy-two of these hexagonal wires were bundled and placed into another pure copper can. The latter was evacuated and sealed. The can was then further extruded to provide rods with higher true deformation strains. The outside Cu jacket was later removed by either machining or chemical etching.

Data Acquisition System for Friction and Wear Test

The data acquisition system, as shown in Figure 1, was developed for sliding friction and wear tests. It consisted of a digital multimeter and a switch/control unit, which were controlled by a microcomputer through an IEEE-488 interface bus (IB). The microcomputer used here was the DEC PRO-380 which is IB compatible

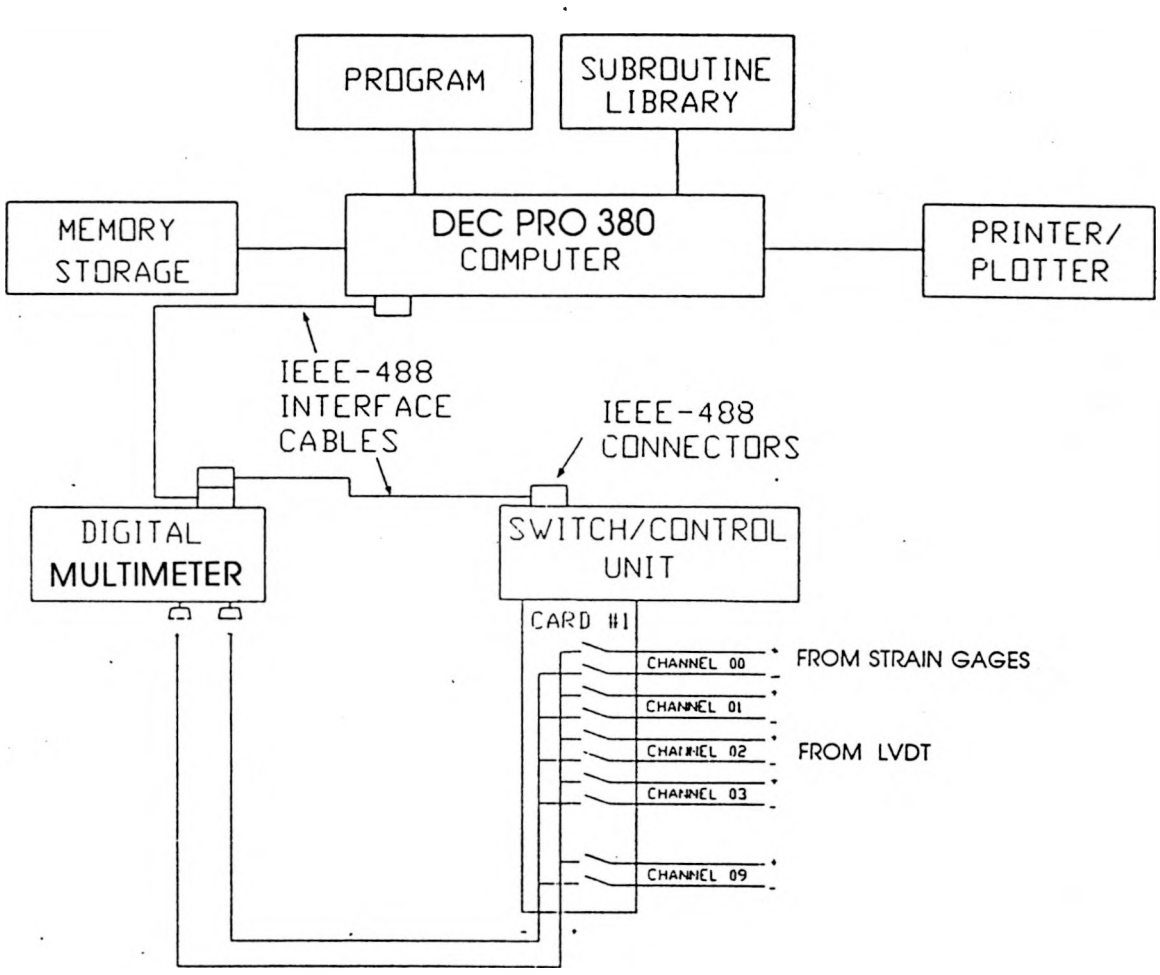

Figure 1: Configuration of the data acquisition system for sliding friction and wear test

and contains a special IB card. It could send commands and receive, manipulate, and output data according to the program.

The switch/control unit acted as an electronic switch (or multiplexer) and thus enabled one digital multimeter to measure several values in a set sequence. Although there were five slots available to insert different types of multiplexer cards, only one relay multiplexer card was used for tribological measurements. The card had 10 different channels which could be individually addressed over the IB by a computer program with the help of a subroutine library. One of the switch channels could be opened or closed so as to measure the output from either a strain gage amplifier or a linear variable differential transformer (LVDT).

The data were read by a multimeter which received instructions from the computer. The measured data were transmitted to the computer over IB as a character string consisting of numerals only, and were then stored and output. The multimeter featured 3.5– 5.5 digit resolution for DC voltage and its range was 100 nanovolt to 300 volts.

The subroutine library used with the PRO-380 was the PRO/Tool Kit Real-Time Interface Library (PRTIL) [20]. The PRTIL software provided a number of routines to enable access to all the functions of the IEEE-488 interface bus. These subroutines oversaw the handshaking operation and also controlled the start-up, the transmittal of commands, and the reception of data over IB.

In our experiments, the signals from the strain gage amplifier and the LVDT were directed to different channels at the switch/control unit. The way the program worked was that the switch/control unit closed channels sequentially so that the multimeter could measure output from either the strain gage or the LVDT in sequence. The

digital multimeter was set to measure DC voltage in the 30 V range with the 4.5 digit display and external trigger. In order to optimize the reading rate, the autozero feature was turned off. The device number or address of the HP3478A multimeter, as set by the manufacturer, was 23 and that of the switch/control unit was 9. The data acquisition system read outputs of the strain gage amplifier and the LVDT. These data were stored and later used for calculation of the coefficient of friction and the wear volume.

Friction and Wear Tests

The arrangement of the friction and wear test set-up is shown in Figure 2. It consists of a test specimen secured to an aluminum cantilever arm and resting on a rotating disk. The latter was made of O2 tool steel (0.90%C, 1.60%Mn, $\leq$0.50%Si, $\leq$0.35%Cr, $\leq$0.30%Ni, $\leq$0.30%Mo, $\leq$0.30%V and balance Fe) and ground mildly after heat treating to 60 RC. The cantilever arm with the specimen in it was balanced by adjusting the position of the balance weight on the arm. The latter had two strain gages mounted on the opposite vertical sides of it. With the loaded specimen rubbing against the disk surface, the deflection of the cantilever beam provided the measurement of friction force in terms of the strain gage output.

The free armature of a linear variable differential transformer (LVDT), which was firmly secured to a table, rested over the far end of the cantilever beam. The LVDT was excited by a 15 V DC power supply. The drop in cantilever end as the sample wore out was measured from the LVDT output. This provided an estimate of the wear loss.

The orientation of Nb filaments was perpendicular to the plane of sliding. There

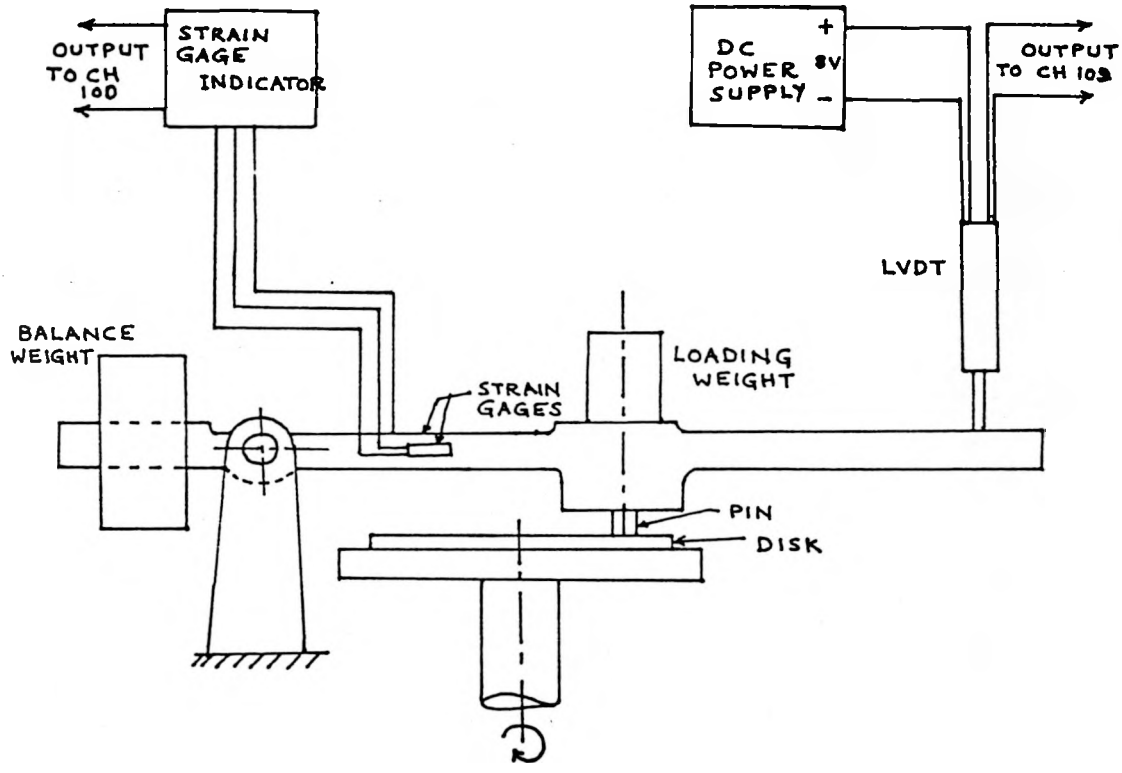

Figure 2: Pin-on-disk sliding friction and wear test set-up

were two kinds of contact geometries used in this study: the rectangular for sheet composites and the circular for rod composites. Rectangular specimens were cut out of the rolled flats and machined to a cross-section of 1.6 $mm \times 4.5$ mm. Cylindrical specimens were machined from rod composites to a diameter of 2.4 mm. These specimens were finished by polishing with 600 grit emery paper. The tests were performed under dry ambient conditions (22^{o}C, 40% relative humidity) with a contact pressure of 0.68 MPa. This required a normal load of 4.9 N for the rectangular specimens and 3.08 N for the cylindrical specimens. The sliding speed was varied in the range of 0.028 to 2.5 m/s. The coefficient of friction and wear volume were recorded as a function of time or sliding distance, and the specimen was weighed before and after the wear test so as to check the weight loss with that estimated from the measurements by LVDT. The coefficient of friction data were taken at 20 s and the wear data at 5 min intervals.

RESULTS AND DISCUSSION

Morphology and Shear Properties

In the as-cast condition, Nb was present as a dendritic array within a Cu matrix. Nb dendrites were approximately 6 μm in diameter and the dendritic arms grew in three orthogonal [100] directions which were randomly oriented with respect to the ingot axis [7]. During rolling deformation, the Nb dendrites flattened and elongated along the rolling direction and thereby developed a ribbon-like structure, as revealed in Figure 3 for Cu-20vol.%Nb sheet composite. Whereas the spacing of Nb dendrites in the initial composite casting was about 25 μm, it was reduced to about 2 μm for a true deformation strain $\eta = 3.5$, as determined from Figure 3. Here $\eta = ln(A_O/A)$ where A_O and A are the initial and the final areas of cross-section before and after deformation, respectively. The irregular fiber morphology is expected to contribute to the strengthening in tension and shear.

Figure 4 gives the stress-strain curves obtained from shear tests on Cu-10vol.%Nb and Cu-20vol.%Nb, both with a true deformation strain of 3.5. Here specimens with a double shear configuration [21] were used and the orientation of Nb filaments in the specimen was perpendicular to the shear planes. The non-linearity in the initial part of elastic deformation was presumably because of the slippage between the specimen and the grip surfaces. The shear modulus of elasticity of both composites was about the same. As for the shear strength, it increased with the increased percentage of Nb, giving a value of 269.7 MPa for Cu-10vol.%Nb versus 310.0 MPa for Cu-20vol.%Nb. The shear-fracture surfaces of Cu-10vol.%Nb and Cu-20vol.%Nb sheet composites are shown in Figure 5. The fracture surface of Cu-10vol.%Nb exhibited tearing while the

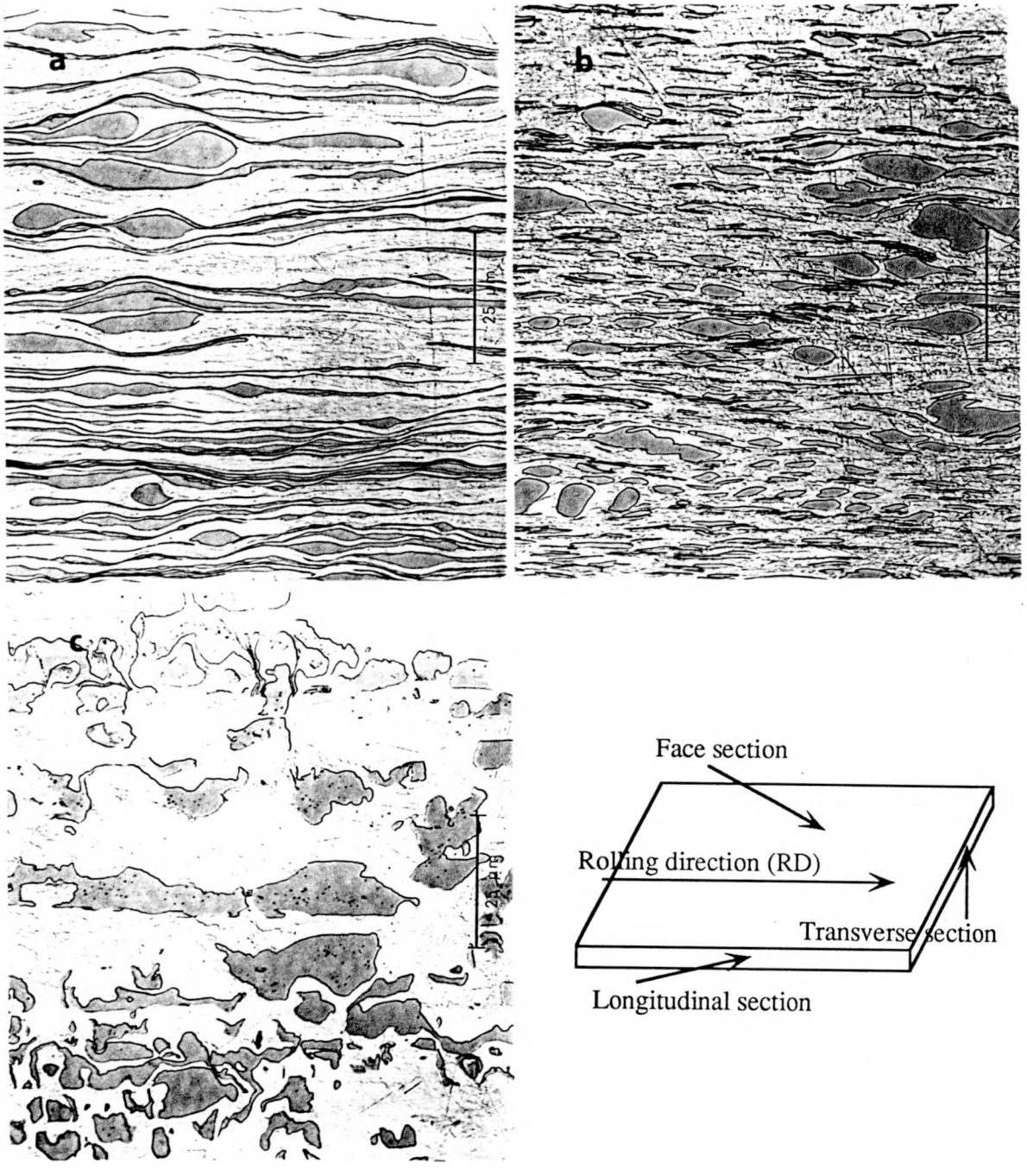

Figure 3: Optical micrographs of Cu-20vol.%Nb sheet composites at $\eta = 3.5$: (a) longitudinal section; (b) transverse section; (c) face section. The section nomenclature is defined in the schematic diagram

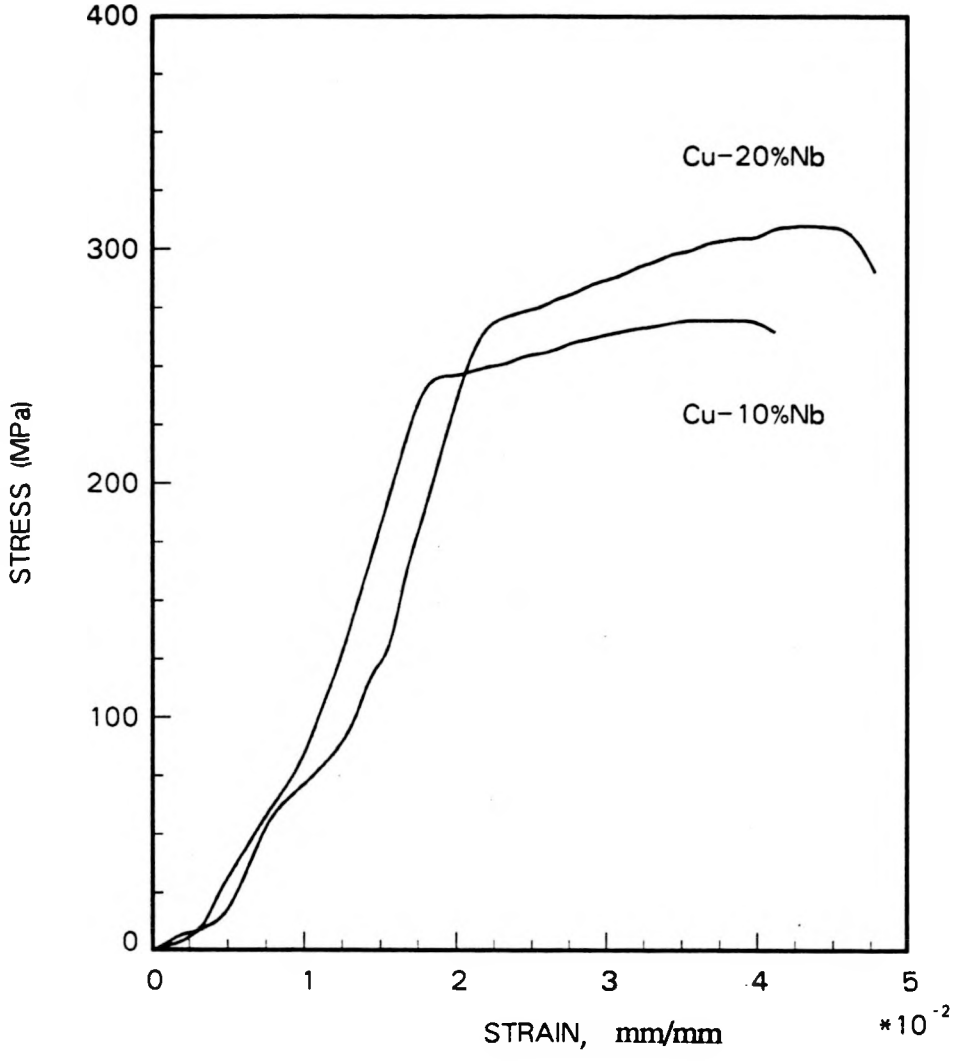

Figure 4: Stress-strain curves from the shear tests on Cu-Nb sheet composites with $\eta = 3.5$ and Nb filaments perpendicular to shear plane

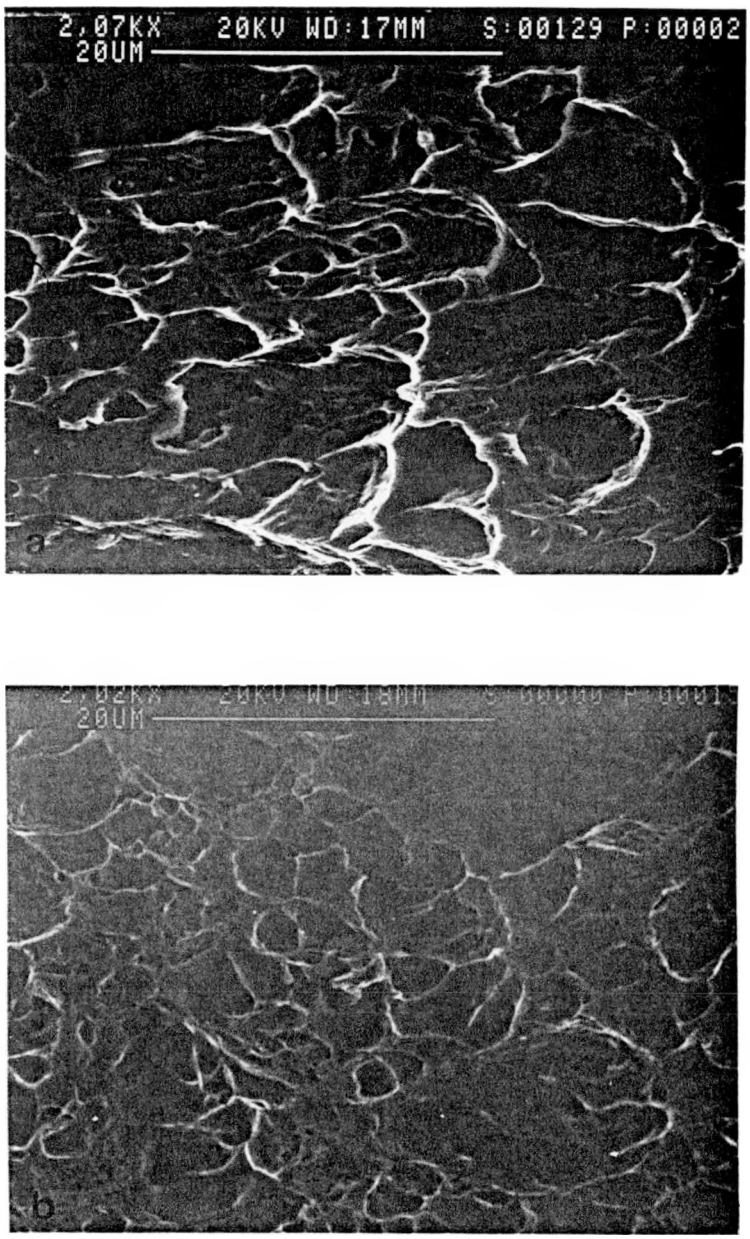

Figure 5: SEM photographs of shear fracture surfaces of sheet composites: (a) Cu-10vol.%Nb; (b) Cu-20vol.%Nb; both with $\eta = 3.5$, Nb filaments were perpendicular to the shear plane

dimple structure (typical for ductile fractures) was observed on the fracture surface of Cu-20vol.%Nb. This indicated that, in addition to shearing, some localized tensile deformation was also produced. The latter required greater energy for deformation leading to the fracture of Cu-20vol.%Nb than that of Cu-10vol.%Nb, as seen in Figure 4. The dimples on the fracture surface did not bear any obvious relationship to the aligned filament morphology depicted in Figure 3. There was no general debonding observed between the Cu matrix and the Nb filaments.

The shear behavior of a material is of significance for friction and wear properties. According to the junction model of adhesion, the shear fracture during sliding between two bodies is said to occur in the weakest location which may be at interface or inside the bulk bodies in contact. With copper surfaces rubbing against steel, the shear strength of copper-steel junctions from friction measurement was estimated to be about 274.4 MPa while the shear strength of pure copper was about 156.8 MPa and that of steel about 882 MPa [22]. Therefore, the shearing in this system occurred mostly in bulk copper. Considering that the shear strengths of Cu-Nb composites, as measured, were 269.7 and 310.0 MPa which are close to 274.4 MPa for copper-steel junctions, the shearing in this system would be expected to occur both in the bulk materials and at the junctions.

Coefficient of Friction

Tests were performed with the sheet composites of Cu-10vol.%Nb, Cu-20vol.%Nb and Cu-30vol.%Nb sliding against tool steel at 0.25 m/s speed and 0.68 MPa normal pressure. Pure Cu was also included in the tests for the sake of comparison. The variation of the coefficient of friction with sliding distance for these composites is

shown in Figure 6. There are two types of transient behaviors seen. For pure Cu and Cu-10vol.%Nb, the coefficient of friction increased with sliding distance up to a maximum value and then it dropped to a steady state value. For the other two materials, the coefficient of friction increased with sliding distance until it reached a steady state value. It is noted that with increased Nb proportion the peak in friction curve in the transient state was suppressed and the steady state coefficient of friction decreased.

The coefficient of friction between sliding surfaces is considered to be the summation of three components which are the asperity deformation component μ_d, a component μ_p from plowing by wear particles and hard surface asperities, and a component μ_a from adhesion between the contacting surfaces [23]. The relative contributions of these components depend on the conditions at the sliding interface, which change with time during the initial stage of sliding. The contribution to friction from asperity deformation is always small in the dry sliding between metals because it is related with hysteresis. In the initial stage, adhesion was not significant because of the presence of adsorbed films on the surfaces, which prevented direct contact between fresh surfaces. The contribution to friction from plowing by hard asperities was relatively significant at this stage. As sliding proceeded, adsorbed films were broken so that a large area of the surfaces was brought into direct contact. This increased the contribution of adhesion to the coefficient of friction. With the generation of wear particles, the plowing component from the wear particles entrapped between sliding surfaces increased drastically. As a result, the coefficient of friction increased with sliding distance. The peak value of the coefficient of friction was reached when the contributions from adhesion and plowing were both maximum. Gradually, the worn

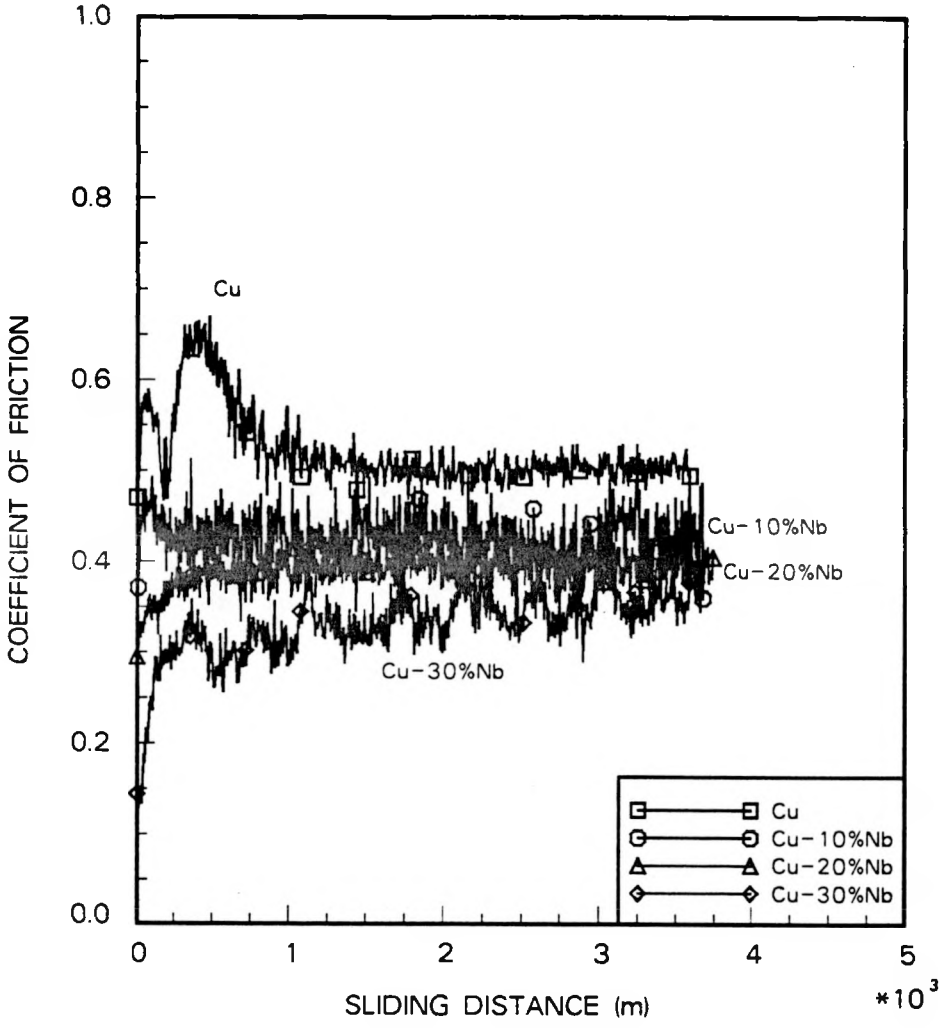

Figure 6: Variation of the coefficient of friction with sliding distance for pure Cu, Cu-10vol.%Nb, Cu-20vol.%Nb and Cu-30vol.%Nb sliding against tool steel disk at the sliding speed of 0.25 m/s and the normal pressure of 0.68 MPa

particles of the softer material filled in the asperity cavities of the harder disk surface thereby developing a layer of transfer film. This produced smoothing of the tool steel disk surface which decreased the plowing contribution to friction. These actions led to the steady state conditions at the interface and so the coefficient of friction also reached a steady state value.

The steady state coefficient of friction is thus governed by the sliding resistance of the pin material against its own transfer film. Because of the multicomponent structure of composites, the adhesion between the composite pin material and its transfer film is expected to be lower than that between pure copper and its transfer film. Thus, the coefficient of friction of composites was lower than that of pure copper. With increasing Nb proportion, there was more incompatibility introduced at the sliding interface thereby resulting in reduced adhesion and so the coefficient of friction was reduced further.

Since the shear strength of tool steel is much higher than that of Cu-Nb alloys, shearing during sliding will occur either in the Cu-Nb substrate or at the sliding interface. As such, the material transfer occurred mainly from the Cu-Nb specimen to the tool steel disk surface. Thus, during steady state sliding, the composite pin material was in contact with its own transfer film. As a first approximation, using the principle of the rule of mixtures, the coefficient of friction may be considered to be comprised of the contributions from Cu-Cu, Nb-Nb and Cu-Nb contacting junctions, the probability of each being dependent upon the volume fraction of the respective constituent. This gives the following expression for the coefficient of friction of the composite

$$\mu = f_{Cu}^2 \cdot \mu_{Cu-Cu} + f_{Nb}^2 \cdot \mu_{Nb-Nb} + f_{Cu} \cdot f_{Nb} \cdot \mu_{Cu-Nb}$$

where f_{Cu} and f_{Nb} are the volume fractions of Cu and Nb, and μ_{Cu-Cu}, μ_{Nb-Nb} and μ_{Cu-Nb} are the coefficients of friction for Cu-Cu, Nb-Nb and Cu-Nb contacts respectively.

Friction tests were also run with pure Cu and pure Nb pins rubbing against pure Nb disks under the same sliding conditions as indicated above. From these tests, it was determined that at steady state μ_{Cu-Nb} was 0.35 and μ_{Nb-Nb} was 0.45. Using $\mu_{Cu-Cu} = 0.50$ from reference [22] and also from our results for the sliding between Cu and tool steel (Figure 6), the variation of the steady state coefficient of friction of Cu-Nb composites with varying Nb proportion was calculated by the above equation. The calculated and the experimental values are plotted in Figure 7. As the composites with more than 30vol.%Nb were not available, their coefficients of friction could not be measured. Based on the limited data, there appears to be a good agreement between the experimental and the calculated values of the coefficient of friction.

Wear

Figure 8 shows the variation of wear volume with sliding distance for Cu and Cu-Nb sheet composites with varying Nb proportions. It is noted that it took very few revolutions for the wear behavior to change from transient state to steady state. This indicates that the transfer film developed on the counterface fairly rapidly. The slopes of the straight lines fitted to the data represent the wear rates in steady state sliding. These are plotted along with hardness in Figure 9 for varying Nb proportions in the composite materials. Whereas hardness increased continuously with increasing Nb proportion, though at a decreasing rate, wear rate decreased to a minimum for

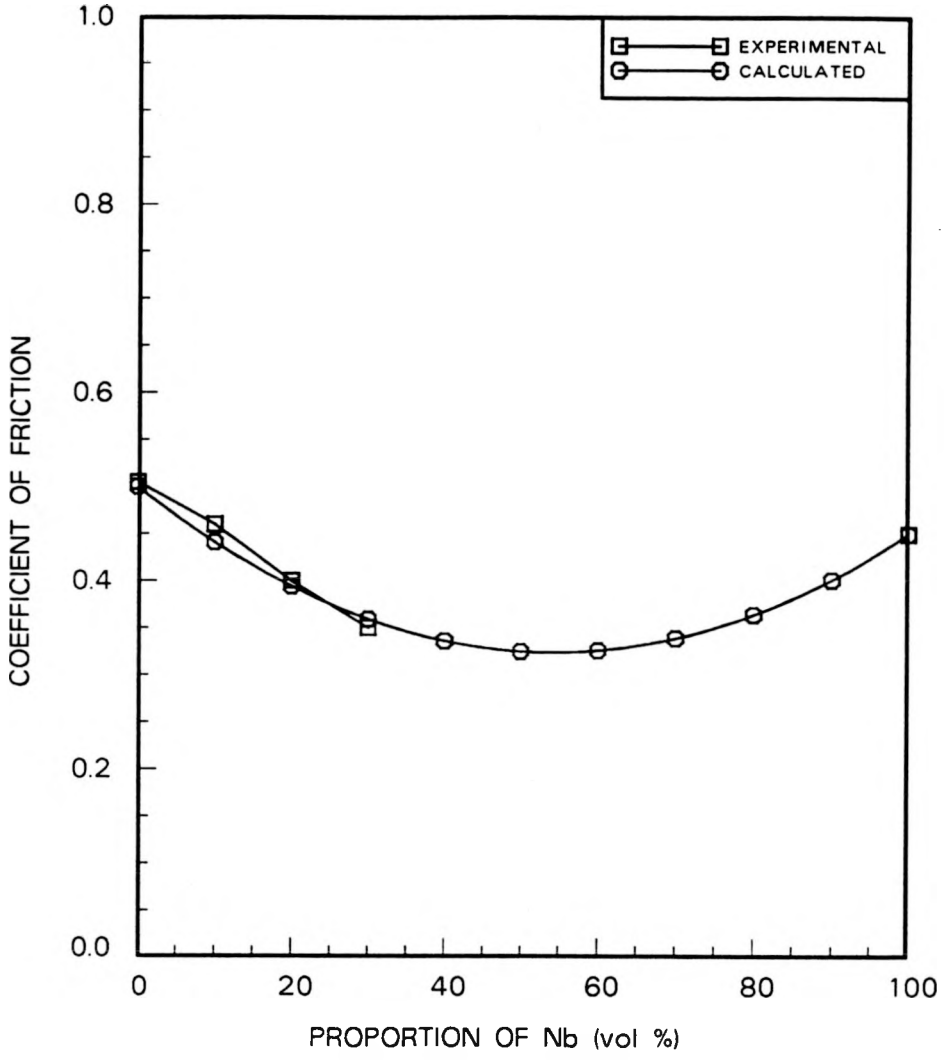

Figure 7: Comparison of the calculated and the experimental values of the coefficient of friction with varying Nb proportion for Cu-Nb composites sliding against tool steel at the sliding speed of 0.25 m/s and the normal pressure of 0.68 MPa

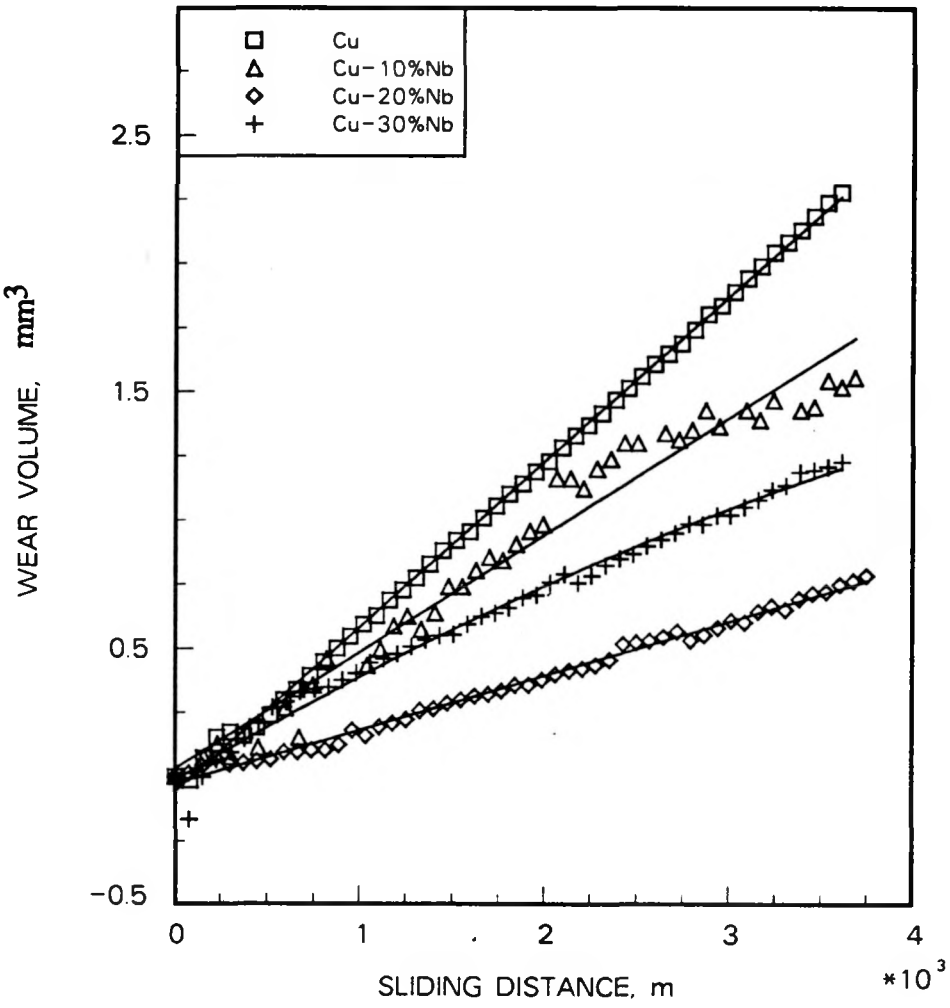

Figure 8: Variation of wear volume with sliding distance for pure Cu, Cu-10vol.%Nb, Cu-20vol.%Nb and Cu-30vol.%Nb sliding against tool steel disk: sliding speed 0.25 m/s, normal pressure 0.68 MPa. All composites had been processed with a true deformation strain of 3.5

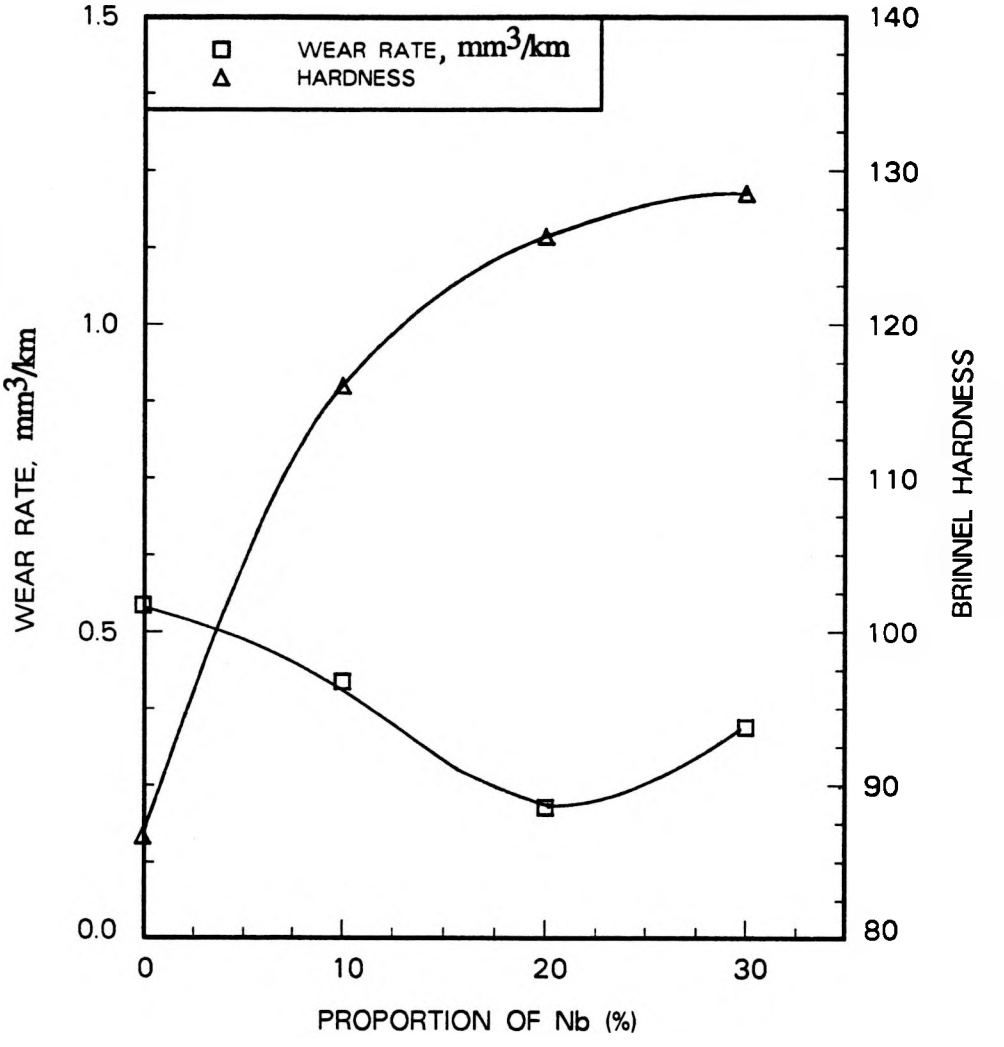

Figure 9: Variation of wear rate and hardness with varying Nb proportions in the Cu-Nb sheet composites

Cu-20vol.%Nb and then increased again. This shows that Archard's law [24], which states that wear rate is inversely proportional to hardness for constant load, was not followed here.

Figure 10 shows the variation of tensile strength with true deformation strain for Cu-15vol.%Nb, Cu-20vol.%Nb and Cu-30vol.%Nb wire composites. Here, the data for Cu-15vol.%Nb and Cu20vol.%Nb were taken from reference [25]. It is noted that the tensile strength of all the composites increased with increasing true deformation strain. At any true deformation strain, the tensile strength of Cu-20vol.%Nb was higher than that of Cu-15vol.%Nb and Cu-30vol.%Nb. The reason for the tensile strength of Cu-30vol.%Nb being lower than that of Cu-20vol.%Nb is presumably its lower workability in deformation processing, as reported earlier [10]. Thus, the Nb filament structure in Cu-30vol.%Nb could not develop as well as it did in Cu-20vol.%Nb. Since filaments provide matrix strengthening and loading support in sliding as well, it could also explain why the wear resistance did not increase and instead decreased when Nb proportion was increased from 20 to 30%.

Effect of True Deformation Strain

In order to study the effect of true deformation strain involved in the processing of Cu-Nb in situ composites on the friction and wear behavior, Cu-15vol.%Nb composites with true deformation strains in the range of 7.2 to 10.0 were prepared by the bundling technique. The true deformation strain here was the sum of the deformation strain in the first extrusion and that of the second extrusion after bundling. The specimens were in the form of rods and the filament orientation was normal to the contact surface. The variation of the coefficient of friction and wear with true

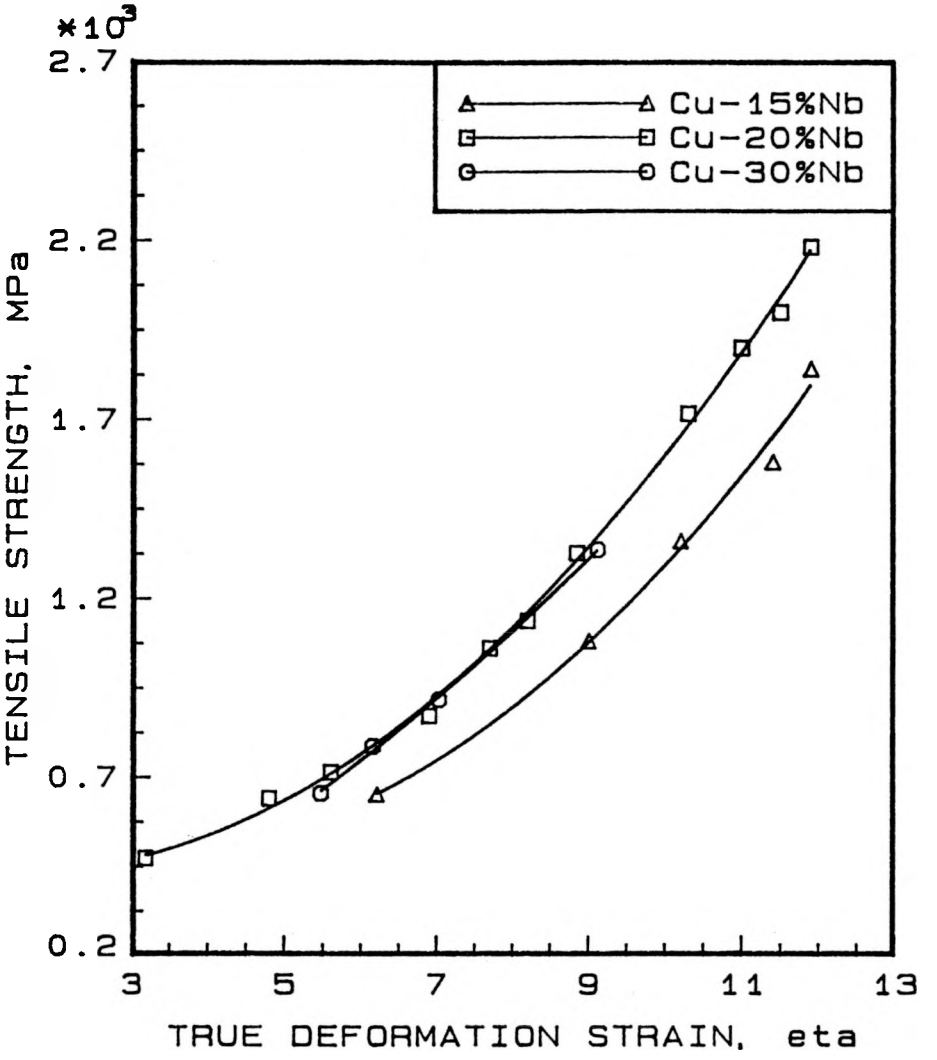

Figure 10: Variation of tensile strength with true deformation strain for Cu-Nb composites

deformation strain for these specimens is show in Figure 11. It is noted that the coefficient of friction increased and wear rate decreased with the increase in true deformation strain. Because of the increase in true deformation strain, the spacing between Nb filaments decreased and so did the size of the filaments. As a result of this, the strength of the composite increased. The number of fibers per unit area resisting wear in the contact zone for the composites with higher true deformation strains was also larger. Because of increased strength and more fibers per unit area in the contact zone, the stress intensity at the contact surface decreased and so the wear rate decreased. Because of the same factors, the force needed for sliding through shearing of the composite material substrate also increased and so the coefficient of friction increased.

In support of the above explanations, Figure 12 shows the cross sections of the wear specimens of Cu-15vol.%Nb in situ bundled composites with two different true deformation strains. These specimens were tested for wear under the same conditions as in Figure 11. It is noted that because of the stresses at the interface, Nb filaments in the subsurface region are oriented along the sliding direction. The thickness of the layer affected by sliding in the composite of lower true deformation strain is larger than that of higher true deformation strain. As a result of this, the shear strain rate in the composite of higher true deformation strain is larger. With the increase in strain rate, shear strength is increased. This means that larger force will be needed to overcome frictional resistance in the sliding of the composite of higher true deformation strain. It is also seen from Figure 12 that the spacing of Nb filaments in the composite of higher true deformation strain is smaller than that of lower true deformation strain. Because of more filaments supporting the load and the increased

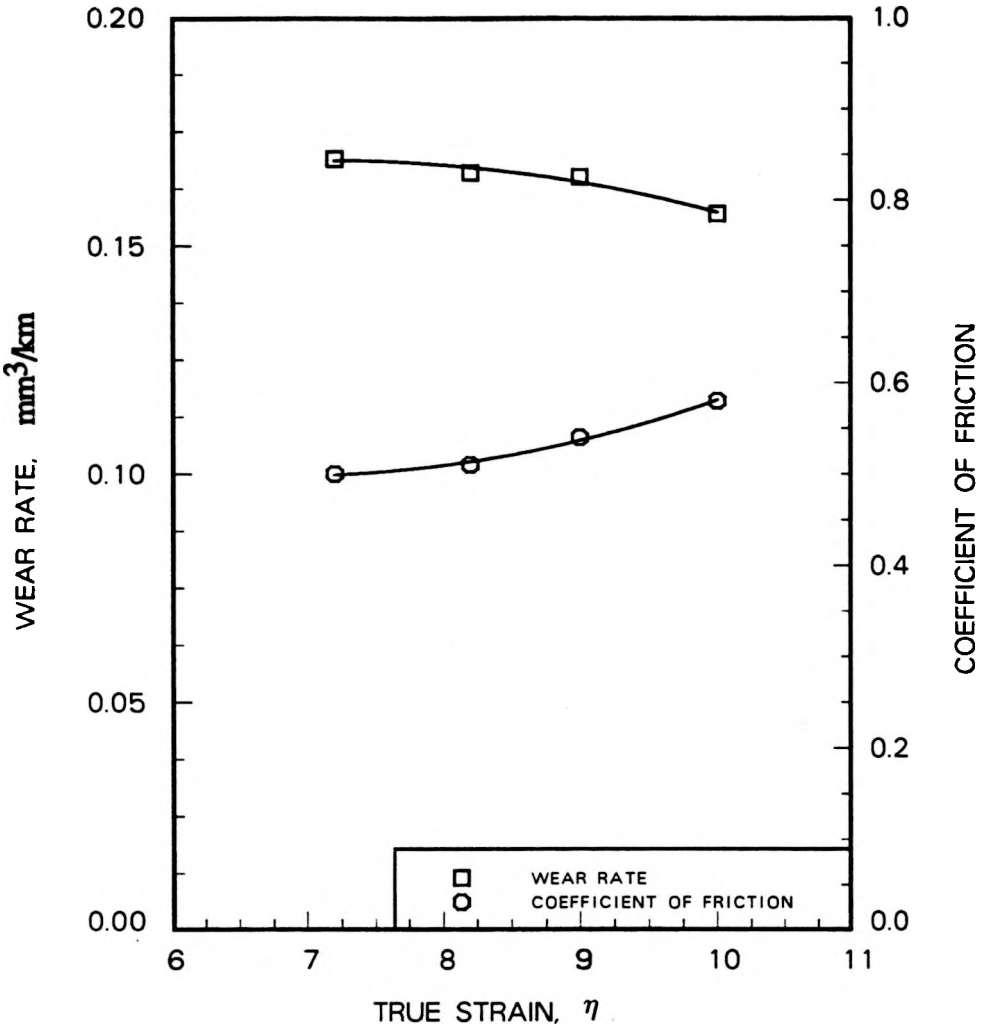

Figure 11: Variation of wear rate and the coefficient of friction with true deformation strain for Cu-15vol.%Nb sliding against tool steel disk at a sliding speed of 1.20 m/s and normal pressure of 0.68 MPa

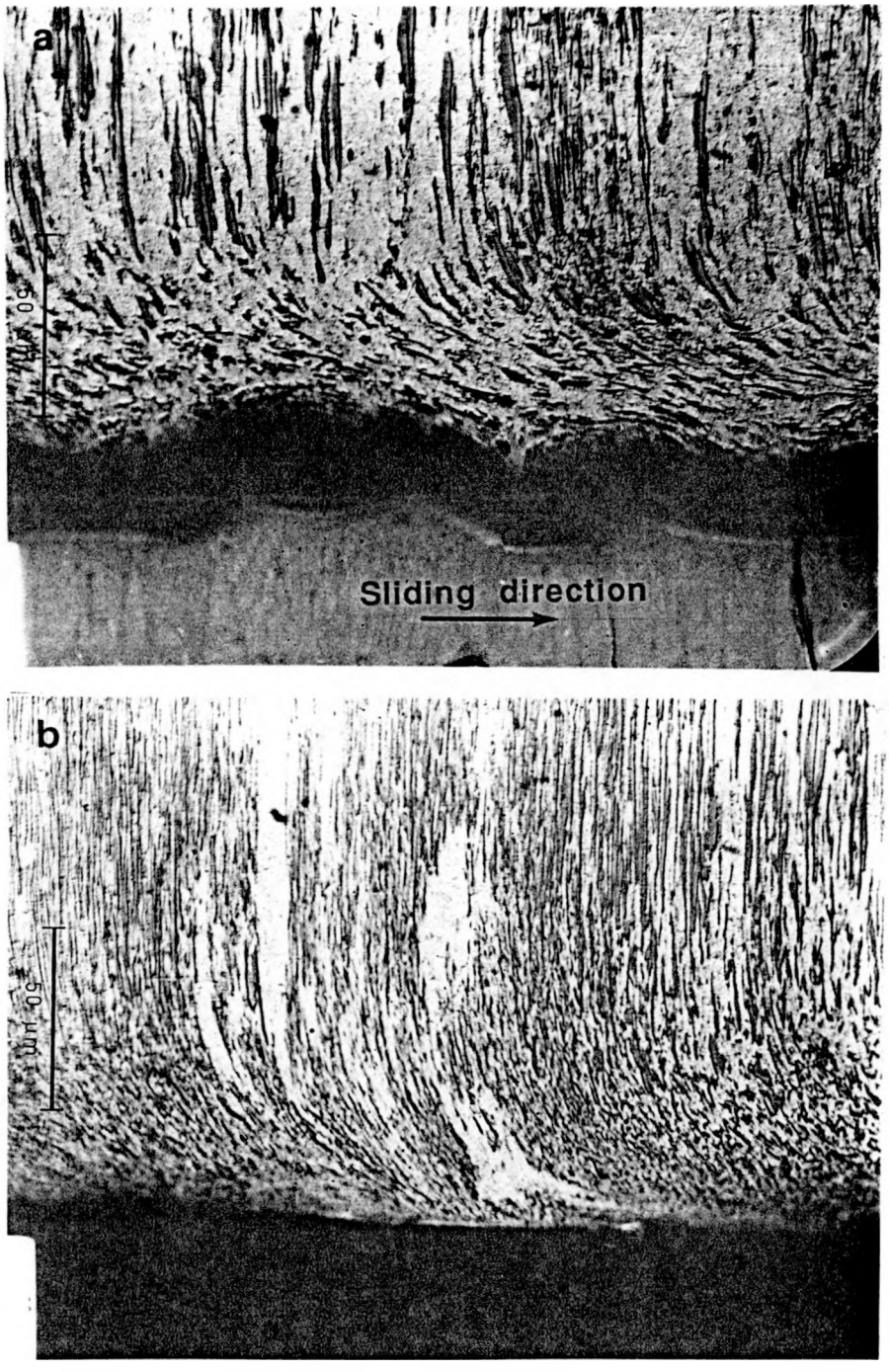

Figure 12: Optical micrographs of the cross sections of Cu-15vol.%Nb in situ bundled composites worn at a sliding speed of 1.20 m/s and normal pressure of 0.68 MPa: (a) $\eta = 7.2$; (b) $\eta = 9.0$

substrate shear strength from higher strain rate, the wear resistance of the composite of higher true deformation strain will be higher.

SEM Studies of Worn Surfaces

In order to understand the mechanism of wear for Cu-Nb in situ composites sliding against tool steel surfaces, the worn surface of a bundled Cu-15vol.%Nb rod composite specimen was studied by scanning electron microscopy. Figure 13 shows that a ripple structure developed on the worn surface of the ductile composite during repetitive sliding. It indicates the overall flow of material in the direction of sliding along with ploughing by discrete asperities on a smaller scale.

Figure 14 shows another typical view of the worn surface of this composite. Here, besides deformation flow, surface cracks and the wear particle separation from deformed layers are also seen. As revealed in the regions marked A and B, wear particles were formed on the extremities of the severely work hardened surface layers. Region A shows the crack initiation and crack propagation phenomena which finally result in the separation of wear particles, as seen in region B. EDS analysis indicated that the wear particle in region B contained Fe in addition to Cu and Nb (Figure 14). The element Fe was obviously back transferred from the tool steel counterface. This suggests that some mechanical alloying also occurred in the contact layers.

From the above observations, it was concluded that the basic wear mechanism in the sliding of Cu-Nb composites against tool steel surfaces was deformation-induced fracture. Because of strong adhesion and high stresses in asperity contacts, the composite material was highly strained in the subsurface layer and was therefore severely work-hardened. As a result of this, cracks were initiated on the extremities of

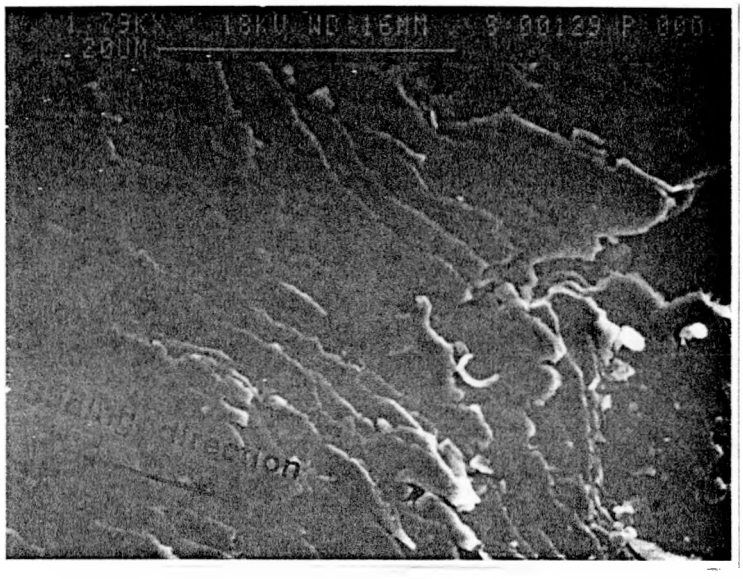

Figure 13: SEM micrograph of the worn surface of Cu-15vol.%Nb bundled rod composite($\eta = 8.2$) sliding against tool steel disk at a sliding speed of 1.20 m/s and normal pressure of 0.68 MPa

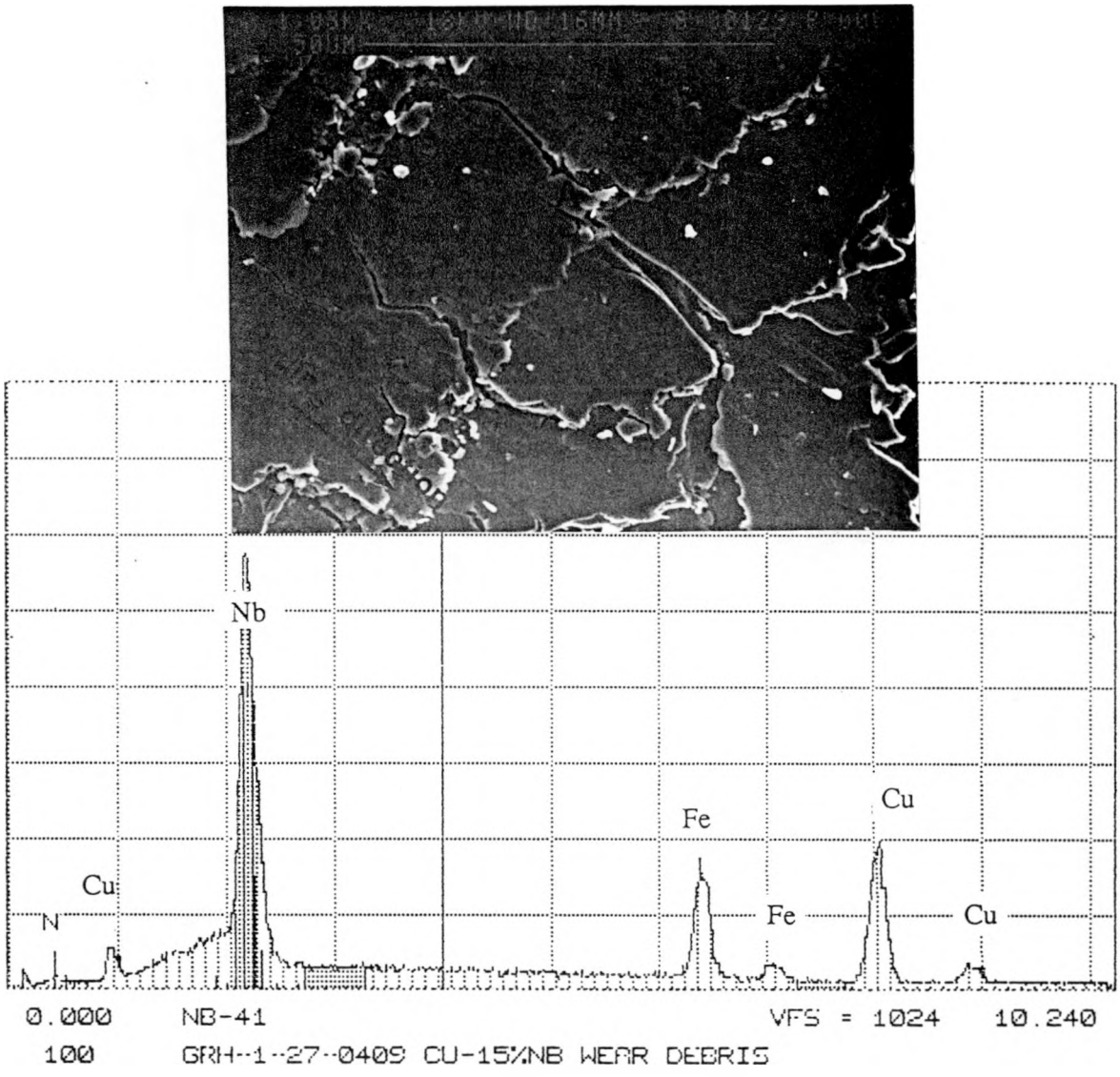

Figure 14: Deformation flow, surface cracks and wear particle formation as seen on the worn surface of Cu-15vol.%Nb rod composite tested under the same conditions as in Figure 12. EDS spectrum shows the composition of wear particle in region B

deformed layers, because these locations were work-hardened the most. The repetitive loading made these cracks grow while other cracks were also initiated. Such events continued and resulted in the generation of wear particles from these deformed layers. The transfer film and its effect on the friction and wear behavior were studied by scanning electron microscopy. The results of these studies will be reported in the second part of this study.

CONCLUSIONS

1. The shear strength of Cu-20vol.%Nb was higher than that of Cu-10vol.%Nb while the shear modulus of elasticity for both was the same. In shear deformation and fracture, the debonding between Cu matrix and Nb filaments was not observed.

2. The Nb filaments in the copper matrix increased the wear resistance of Cu-Nb composites considerably over that of the matrix material.

3. The coefficient of friction of Cu-Nb composites sliding against tool steel surfaces decreased as Nb proportion increased to 30vol.% which was the maximum proportion used in this work.

4. The wear resistance of Cu-20vol.%Nb composite was maximum. It decreased with both the higher and lower percentages of Nb.

5. The wear resistance and the coefficient of friction of Cu-Nb composites increased with increasing true deformation strain.

6. The composite material was transferred to the steel counterface during sliding. There was some transfer of iron from the counterface to the pin surface as well.

7. The major mechanism of wear in the sliding of these composites against tool steel surfaces was deformation-induced fracture.

REFERENCES

[1] Verhoeven, J. D., J. J. Sue, D. K. Finnemore, E. D. Gibson and J. E. Ostenson. "The Morphology and Grain Size of Nb_3Sn Filaments in *in situ* Prepared Multifilamentary Nb_3Sn-Cu Composite Wire." J. Mat. Sci. 15 (1980): 1907-1914.

[2] Metals Handbook (8th edition). vol. 8, ASM, Metals Park, Ohio (1973): 281.

[3] Verhoeven, J. D., F. A. Schmidt, E. D. Gibson and W. A. Spitzig. "Copper-Refractory Metal Alloys." Journal of Metals. Sept. (1986): 20-24.

[4] Bevk, J., J. P. Harbison and J. L. Bell. "Anomalous Increase in Strength of In Situ Formed Cu-Nb Multifilamentary Composites." J. Appl. Phys. 49(12) (1978): 6031-6038.

[5] Brenner, S. S. "Tensile Strength of Whiskers." J. Appl. Phys. 27(12) (1956): 1484-1491.

[6] Spitzig, W. A. and P. D. Krotz. "A Comparison of the Strength and Microstructure of Heavily Cold Worked Cu-20%Nb Formed By Different Melting Procedures." Scripta Metall. vol. 21 (1987): 1143-1146.

[7] Spitzig, W. A., A. R. Peton and F. C. Laabs. "Characterization of the Strength and Microstructure of Heavily Cold Worked Cu-Nb Composites." Acta Metall. vol. 35(10) (1987): 2427-2442.

[8] Trybus, C. L. Microstructure-Strength Relationships of Heavily Deformed Cu-based Composites. Ph. D. dissertation, Iowa State University, Ames (1988).

[9] Downing, H. L., J. D. Verhoeven and E. D. Gibson. "The Emissivity of Etched Cu-Nb in-situ Alloys." J. Appl. Phys. 61(7) (1987): 2621-2625.

[10] Renaud, C. V., E. Gregory and J. Wong. "Development and Application of High Strength, High Conductivity CuNb In Situ Composite Wire and Strip." in Advances in Cryogenic Engineering Materials. vol. 134, edited by A. F. Clark and R. P. Reed (1989): 435-442.

[11] Friedrich, K. Friction and Wear of Polymer Composites. VDI-Verlag, GmbH Düsseldorf (1984): 94-95.

[12] Sung, N. and N. Suh. "Effect of Fiber Orientation on Friction and Wear of Fiber Reinforced Polymeric Composites." Wear 53 (1979): 129-141.

[13] Hawthorne, M. "Wear in Hybrid Carbon/Glass Fiber Epoxy Composite Materials." Wear of Materials-1983. edited by K. C. Ludema, Proceedings of the International Conference on Wear of Materials (1983): 576-582.

[14] Clerico, M. and V. Patierno. "Sliding Wear of Polymeric Composites." Wear 53 (1979): 279-301.

[15] Amateau, M. F., R. H. Flowers and Z. Eliezer. "Tribological Behavior of Metal Matrix Composites." Wear 54 (1979): 175-185.

[16] Das, S. and S. V. Prasad. "Microstructure and Wear Behavior of Cast Aluminum-Silicon Alloy-Graphite Composites." Wear of Materials-1989. edited by K. C. Ludema, Proceedings of International Conference on Wear of Materials (1989): 399-408.

[17] Nath, D., S. K. Biswas and P. K. Rohatgi. "Wear Characteristics and Bearing Performance of Aluminium-Mica Particulate Composite Material." Wear 60 (1980): 61-73.

[18] Tsuya, Y., H. Shimura and K. Umeda. "A Study of the Properties of Copper and Copper-tin Base Self-Lubricating Composites." Wear 22 (1972): 143-162.

[19] Eliezer, Z., C. H. Ramage, H. G. Rylander, R. H. Flowers and M. F. Amateau. "High Speed Tribological Properties of Graphite Fiber/Cu-Sn Matrix Composites." Wear 49 (1978): 119-133.

[20] PRO/Tool Kit Real-Time Interface Library- User's Guide. Digital Equipment Corporation (1984): Ch6.

[21] Bahadur, S. The Correlation of Frictional and Viscoelastic Properties of Polymers. Ph.D. dissertation, University of Michigan, Ann Arbor (1970).

[22] Bowden, F. P. and D. Tabor. The Friction and Lubrication of Solids, I. The Clarendon Press (1950): 33-97.

[23] Suh, N. P. and H. C. Sin. "The Genesis of Friction." Wear 69 (1981): 91-114.

[24] Archard, J. F. "Contact and Rubbing of Flat Surfaces." J. Appl. Phys. 24 (1953): 981-988.

[25] Verhoeven, J. D., W. A. Spitzig, L. L. Jones, H. L. Downing, C. L. Trybus, E. D. Gibson, L. S. Chumbley, L. G. Fritzemeier, and G. D. Schnittgrund. "Development of Deformation Processed Copper-Refractory Metal Composite Alloys." J. Mater. Eng. vol.12(2) (1990): 127-139.

PART II.

FURTHER INVESTIGATIONS ON THE TRIBOLOGICAL BEHAVIOR OF Cu-20%Nb in situ COMPOSITE

ABSTRACT

Sliding friction and wear behaviors of Cu-20vol.%Nb in situ composite sliding against a tool steel disk were studied under dry ambient conditions. Studies were directed towards the understanding of the roles of the filament and the matrix materials during sliding. It was found that Nb filaments underwent reorientation, shearing and refinement. Irrespective of their prior orientation, Nb-filaments close to the contact surface were oriented along the sliding direction. These processes resulted from friction-induced surface deformation and led to the strengthening of the subsurface layer of the composite. There was no separation of Nb-filaments from Cu-matrix observed in the sliding process.

The effects of annealing, sliding speed and filament orientation on the friction and wear behaviors of the composite were also investigated. The micromechanisms of wear were studied by scanning electron microscopy. Surface deformation flow, filament reorientation and refinement, and oxidation seemed to play important roles in the friction and wear processes.

INTRODUCTION

Cu-refractory metal in situ composites have demonstrated a superior combination of thermal/electrical conductivity and strength [1-3]. This attractive blend of properties makes these composites promising for sliding electrical contact applications where high electrical and thermal conductivities, and low friction and wear are required.

Cu and Nb are mutually insoluble at room temperature [4]. Thus, the cast ingot of Cu-Nb has pure Nb dendrites in a nearly pure Cu matrix. The two-phase alloy is so ductile that it may be deformed at room temperature by reduction ratios of greater than 100% [1]. As a consequence of this deformation process, Nb dendrite arms are drawn into ribbon-like filaments. The filaments which are aligned along the deformation axis are refined by further deformation. Thus a Cu-Nb composite with excellent Nb fiber alignment is obtained.

The shear deformation and the tribological behavior of Cu-Nb in situ composites were investigated in our earlier work [5]. It was reported that the shear strengths of these composites increased with increased Nb proportion. The bonding between the fiber and matrix materials was excellent because no debonding between the two components occurred during shear deformation until fracture. The wear resistance of the composites was considerably higher than that of the matrix material while the coefficient of friction was slightly lower. Thus, the filaments of Nb in the copper matrix contributed to both the strengthening and wear resistance. With higher true deformation strains, the wear resistance of Cu-15vol.%Nb composite was found to increase. The investigations with the composites of varying Nb proportions showed that Cu-20vol.%Nb had higher wear resistance than Cu-10vol.%Nb and Cu-30vol.%Nb

composites. In view of these observations, it was decided to study further the tribological behavior of Cu-20vol.%Nb composite with respect to the factors not previously studied, such as sliding speed, filament orientation and annealing behavior. The variations in the tribological behavior have been specially studied in the light of substrate deformation, filament size and orientation, and worn surface features.

EXPERIMENTAL

The details related to the processing of Cu-Nb in situ composites in the form of sheets were reported earlier [1]. Rectangular specimens of Cu-20vol.%Nb composite with a cross-sectional area of 1.6 $mm \times 4.5\ mm$ were machined out of these rolled sheets. The composite had been processed with a true deformation strain (η) of 3.5. The sliding direction in tribological tests was along the dimension of 4.5 mm. The contact surface was finished by polishing with 600 grit emery paper in running water. Sliding friction and wear tests were performed in a pin-on-disk machine with the composite specimen serving as the pin. Sliding occurred between the pin and the hardened O2 tool steel disk (HRC 60) which was finished by mild grinding. The orientation of Nb filaments in the composite was always perpendicular to the sliding plane except when the effect of parallel filament orientation was studied.

Sliding tests were performed under dry ambient conditions ($22^{o}C$, 40% relative humidity) with a contact pressure of 0.68 MPa which required a normal load of 4.9 N. Sliding speed was varied in the range of 0.028 to 2.50 m/s. The coefficient of friction was estimated from strain gage output and the wear volume from linear variable differential transformer output. The details of the experimental set-up and the data acquisition system along with the experimental procedure were reported earlier [5].

RESULTS AND DISCUSSION

Substrate Studies

As mentioned above, our earlier work [5] on Cu-Nb composites revealed that the wear resistance of the composites was much higher than that of the matrix copper. In order to understand the contributions to increased wear resistance from both the matrix and the filaments, the deformation and the structural changes in the substrate were studied. Figure 1 shows the micrograph of the cross-section of the substrate of the worn composite specimen. The specimen was electrolessly plated with Ni, before it was sectioned, in order to preserve the surface layer affected by sliding wear. There is no separation of Nb filaments from Cu matrix observed and both phases seem to have deformed together. The Nb filaments in the thin subsurface layer are refined because the friction-induced tangential flow caused the Nb filaments to undergo further shear deformation. The fiber refinement is a characteristic of the two-phase ductile metal matrix composite. Such a refinement of fibers does not occur in the sliding process of short-fiber reinforced thermoplastics [6] in which fiber cracking and fiber/matrix separation have been reported as the two major mechanisms of wear besides the direct wear of fiber and matrix. This unique behavior observed in the Cu-Nb composite is due to the low flow stresses of both of the constituent materials.

Whereas Nb fibers in the pin were originally perpendicular to the sliding plane, as seen in Figure 1, they have been oriented parallel to the sliding direction in the zone affected by frictional deformation. The thickness of this zone is about 10-12 μm. From the change in the orientation of Nb fibers, it was possible to estimate the

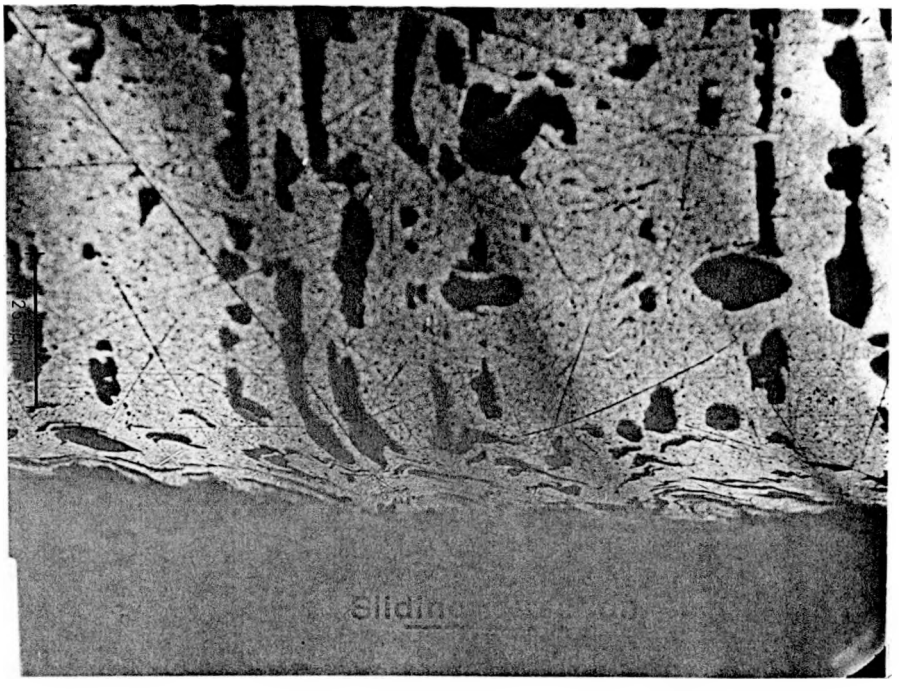

Figure 1: Optical micrograph of the cross-section of Cu-20vol.%Nb ($\eta = 3.5$) in situ sheet composite specimen tested for wear at a sliding velocity of 0.028 m/s and normal pressure of 0.68 MPa

extent of deformation at different depths in the affected subsurface layer. For this purpose, three bent but still continuous Nb fibers which extended close to the sliding interface were located. The measured values of fiber displacement from its original vertical location were plotted against the depth below worn surface and are shown in Figure 2 for the three locations in the X-direction. The three X-locations in the figure represent the distance from the leading edge of the worn composite specimen along the sliding direction. It should be noted that the displacement at any depth in the subsurface layer affected by sliding increased as the distance from the leading edge increased. Since the slope of the tangent at any point on the curve represents strain, it is obvious that the strains induced in the subsurface layer by frictional deformation are very high up to a depth of 5 to 10 μm depending upon the location along the wear specimen.

As a result of the above deformation, the flow of material occurred past the trailing edge of the specimen, as shown in Figure 3. The specimen was here plated again with Ni to preserve the surface from being damaged during sectioning. The displaced material was thus surrounded by plated Ni. The figure shows that Nb filaments have been oriented along the sliding direction and reduced to a much finer size than that before deformation. This kind of filament refinement was possible only because Nb is also a fairly ductile material. The flow pattern shows that material in the contact zone was severely deformed, presumably under hydrostatic conditions, which made the material flow in the tangential direction.

Figure 4 shows the isodisplacement diagram for the subsurface region of the composite wear specimen. Here each curve in the figure represents the same amount of displacement of material in the sliding direction, as marked in μm. Thus, it

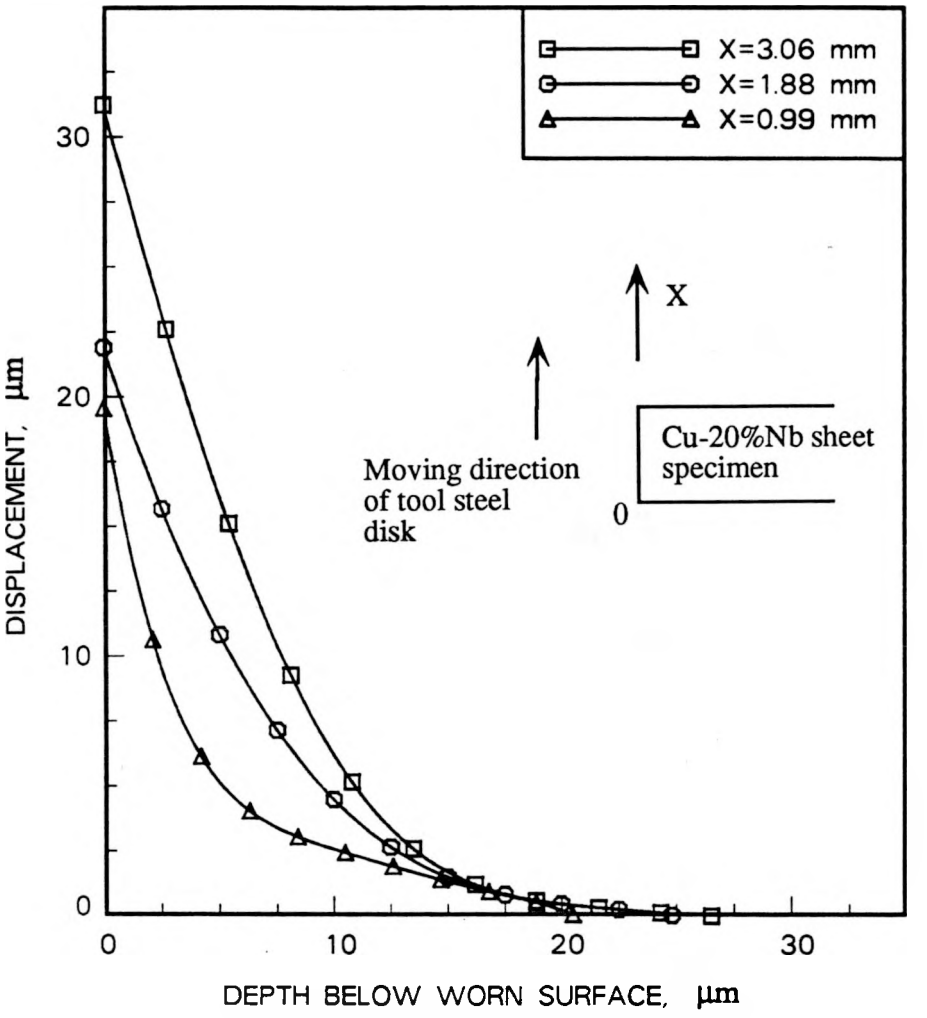

Figure 2: Substrate deformation in terms of the fiber displacement in sliding direction versus the depth below worn surface for three locations (X) of Cu-20vol.%Nb ($\eta = 3.5$) in situ sheet composite specimen tested for wear at a sliding velocity of 0.028 m/s and normal pressure of 0.68 MPa

Figure 3: Optical micrograph of the cross-section of Cu-20vol.%Nb ($\eta = 3.5$) in situ sheet composite specimen tested for wear under the same conditions as in Figure 1. It shows prow formation at the trailing edge of specimen as a result of plastic deformation flow

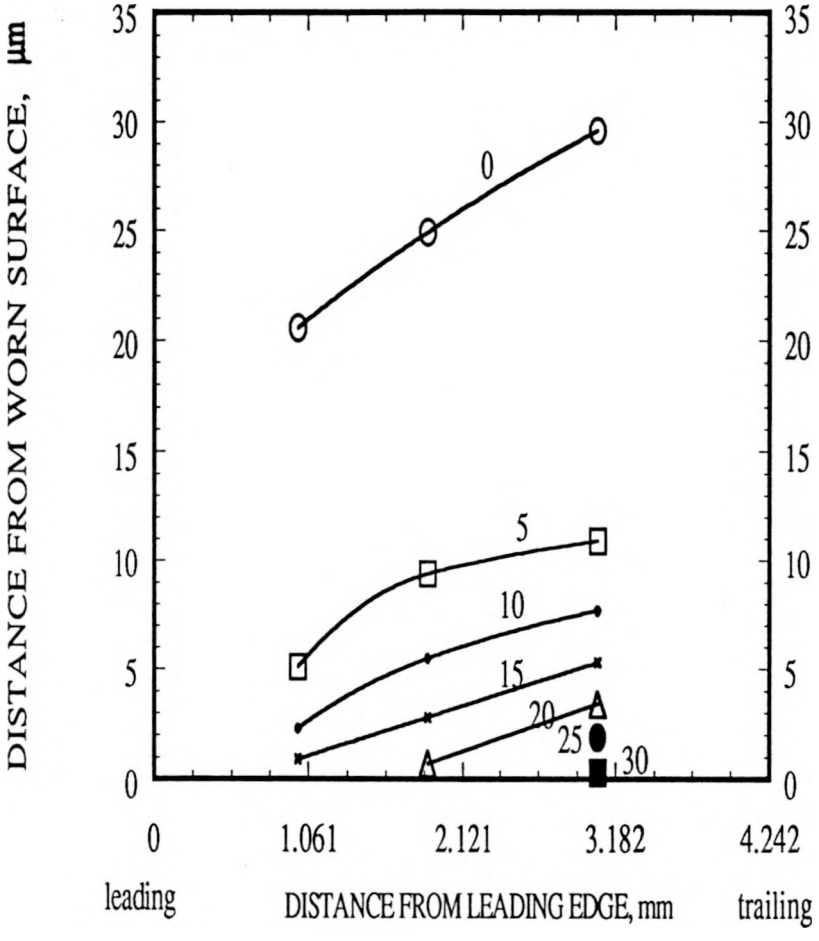

Figure 4: Isodisplacement diagram for the substrate region of wear specimen. The numbers on the curves indicate displacement in μm

provides an indication of the way deformation occurred in the subsurface layer. It is noted that the depth for any deformation increased as the distance from the leading edge of the specimen increased along the sliding direction. The isodisplacement lines get closer toward the sliding surface which means that the deformation gradient increases as the worn surface is approached. The maximum strain occurs at the sliding interface and so yielding will occur there. This observation is in agreement with the analysis by Johnson [7]. He showed that, for the coefficient of friction larger than 0.30, yielding first occurred at the contact surface. On the other hand, yielding occurred below the contact surface when the coefficient of friction was less than 0.25. Since with Cu-20vol.%Nb sliding against tool steel the coefficient of friction was about 0.4, yielding in our case would be expected to occur at the contact surface. Thus, the crack is likely to initiate at the contact surface of the composite material. It would later propagate under the highly stressed conditions in the subsurface zone and would finally give rise to wear particles. This was demonstrated on the worn surface of Cu-Nb composite in our earlier work [5].

The Nb filaments in the composite were subjected to three actions: reorientation, fragmentation and refinement. Because of the first two, the filaments were bent in the sliding direction and broken into smaller segments by the shearing action of frictional force. The fiber segments were also drawn to a finer size because of the flow in the substrate. This in effect produced the refinement of fibers. The wear resistance of the composite was affected by fibers in many ways. The fibers provided direct support to the copper matrix in mechanical loading and those fibers which were exposed to the sliding surface took part directly in resisting wear. Since the presence of fibers resisted deformation of the copper matrix, the wear resistance was

increased because of this strengthening. The fibers also consumed frictional energy through reorientation, fragmentation and fiber refinement so that less energy was available for crack initiation and propagation which are responsible for the formation of wear particles. The refinement action reduced the size and spacing of filaments so that the deformed layer underwent strengthening. It may be pointed out that the strengthening in the rolled Cu-Nb composites correlates with $\lambda^{-1/4}$, where λ is the Nb filament spacing [8]. In addition to strengthening from the above effects, the matrix was also work-hardened. The combined action of the filament and the matrix, as discussed above, was responsible for the increased wear resistance of the composite.

Effect of Sliding Speed

The effect of sliding speed on the friction and wear behavior of a Cu-20vol.%Nb sheet composite was studied by varying speed in the range of 0.028 to 2.5 m/s. The variation of the coefficient of friction and wear rate of this composite with sliding speed for steady state sliding against tool steel is plotted in Figure 5. The fluctuations in the coefficient of friction for any sliding speed were large, as is normally the case in dry sliding. In view of these fluctuations, the variation of the coefficient of friction with sliding speed was not significant. The wear rate decreased with increasing speed and had a considerably larger value at the low speed of 0.028 m/s.

A similar trend of decreasing wear rate with increasing sliding speed was reported by Lancaster [9] for leaded brass sliding against hardened tool steel. The mild wear was accounted for in terms of a protective oxide film that developed because of the temperature rise at the interface [9]. The same appears to be the case with the Cu-Nb

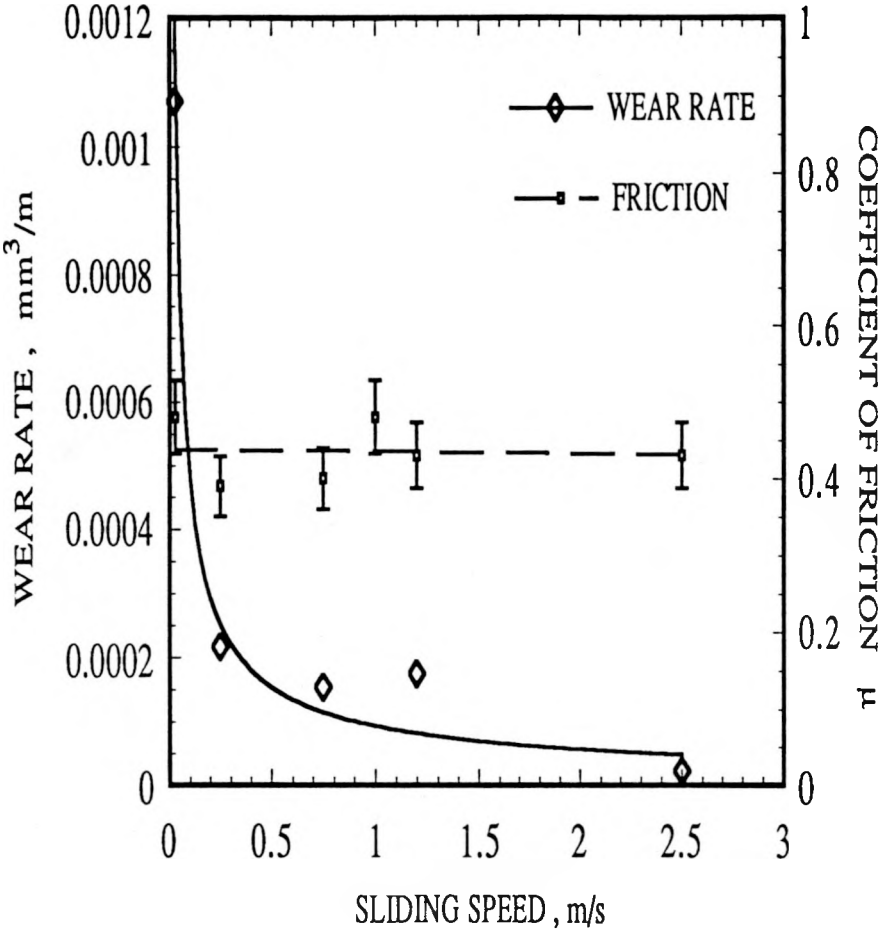

Figure 5: Variation of wear rate and the coefficient of friction with sliding speed for Cu-20vol.%Nb in situ sheet composite with a true deformation strain of 3.5 at a normal pressure of 0.68 MPa

composite as well, because an oxide film could be seen (even by the naked eye) on the sliding surface of the specimen. The film was thicker and darker in the case of sliding at 2.5 m/s than at 0.028 m/s. Obviously, with the increase in sliding speed the temperature at the sliding surface was increased. This increased the oxidation rate which led to the development of an oxide film thick enough to prevent direct metallic contact between the sliding members and thereby reduced the wear rate. Since the thermal conductivity of Cu-Nb is high, the interface temperature was not high enough to produce thermal softening which could increase wear rate.

Figure 6 shows SEM micrographs of the worn surfaces of the composite tested at 0.25 m/s and 1.20 m/s. There are two distinct regions seen on these micrographs—the bright region and the dark region. The bright region exhibits the typical features of adhesion and deformation. The bright and the dark regions were compared, with the help of scanning electron microscopy and energy dispersive spectrometry analysis, with two laboratory specimens, one of which was polished and so had very little oxide, and another had a thick film of oxide deposited on it. This indicated that the dark region was covered by a thicker oxide film than the bright region. The comparison of the two micrographs in Figure 6 shows that the area of the dark region was greater for the higher sliding speed. This implies that the protection from metallic oxide film was also larger at higher speeds.

The effect of sliding speed on the work-hardening of the subsurface was studied by sectioning the wear specimens tested at the sliding speeds of 0.028 m/s and 2.5 m/s and measuring the microhardness in the Cu matrix on the sectional planes. The variation of microhardness with distance from the worn surface for the two sliding speeds is shown in Figure 7. It is seen that the hardness at any distance is higher

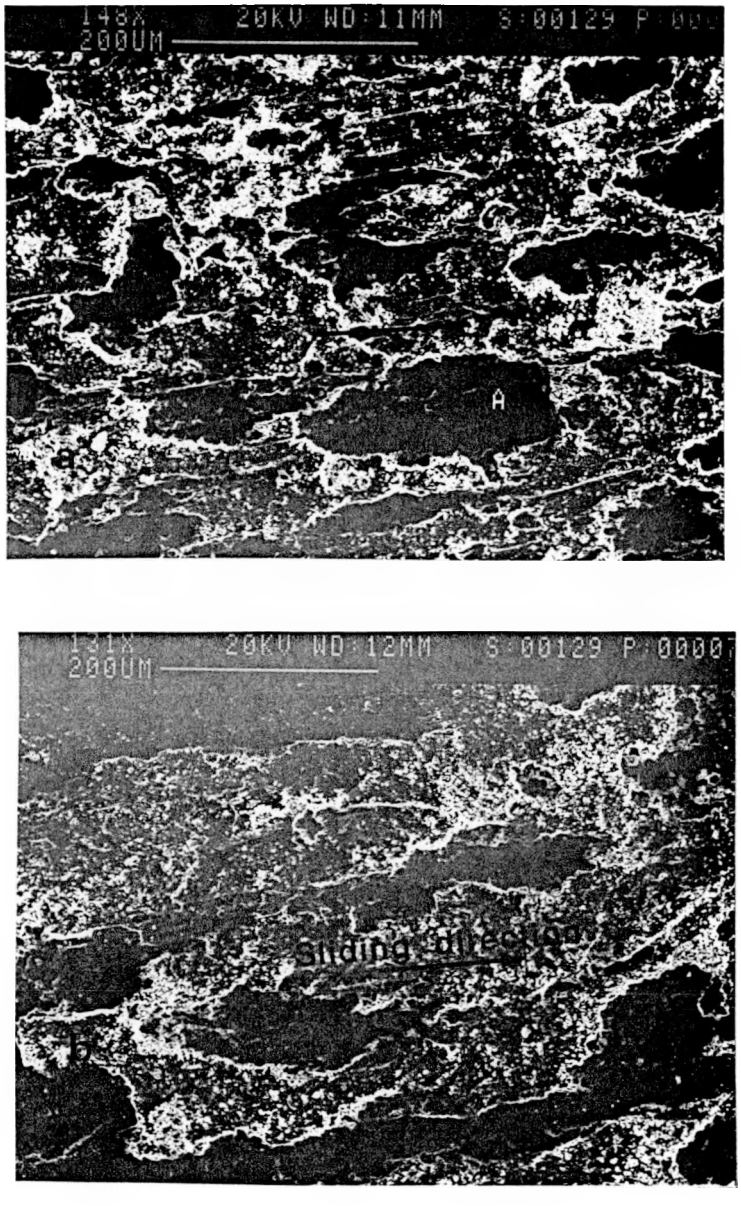

Figure 6: SEM micrographs of the worn surfaces of Cu-20vol.%Nb ($\eta = 3.5$) in situ sheet composite sliding against tool steel at the normal pressure of 0.68 MPa and the sliding speeds of (a) 0.25 m/s; (b) 1.20 m/s

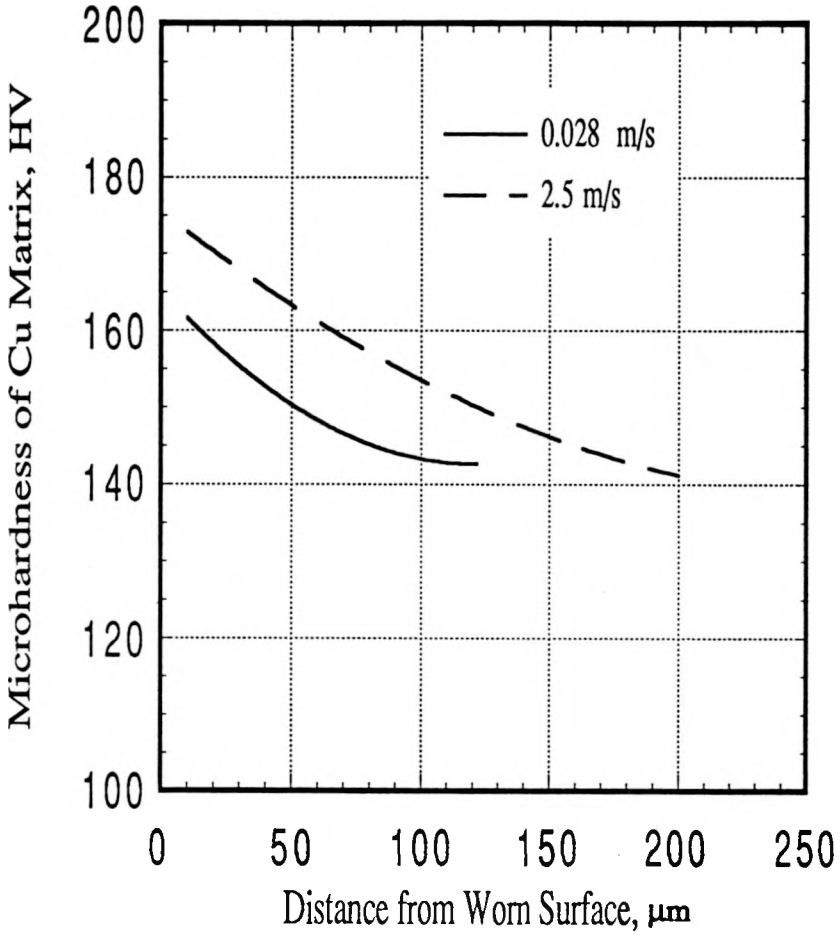

Figure 7: Variation of substrate hardness in Cu matrix in the Cu-20vol.%Nb sheet composite tested for wear at the sliding speeds of 0.028 m/s and 2.50 m/s, normal pressure 0.68 MPa

for the higher sliding speed and the thickness of the hardened depth is also greater. With the increase in sliding speed, the strain rate of deformation in the subsurface layer of the wear specimen is increased. Considering the strain hardening equation [10]

$$\sigma = K \cdot \epsilon^n$$

where σ and ϵ denote the stress and strain, respectively, and K and n are constants, we may write

$$\frac{d\sigma}{d\epsilon} = n \cdot \frac{\sigma}{\epsilon}$$

The dependence between stress and strain rate ($\dot{\epsilon}$) may be expressed as

$$\sigma = C \cdot (\dot{\epsilon})^m$$

where C and m are constants. Combining the above two equations, we get

$$\frac{d\sigma}{d\epsilon} = nC\frac{(\dot{\epsilon})^m}{\epsilon}$$

This equation provides that strain hardening rate is proportional to the mth power of strain rate. Spitzig and Reed [11] also reported that the strengths of heavily cold-drawn copper, niobium and Cu-20%Nb were dependent upon strain rate. It is because of the increased strain rate with increased sliding speed and, therefore, the increased work-hardening rate, that the subsurface hardness at any distance from the worn surface in Figure 7 was higher at higher sliding speed. Thus, in addition to oxidation the greater work-hardening at higher sliding speeds would also account for lower wear with increasing sliding speed.

Effect of Nb Filament Orientation

Figure 8 shows the variation of the coefficient of friction and wear volume with sliding distance for the composites with Nb filaments oriented perpendicular and parallel to the sliding plane. The coefficient of friction of the composite with Nb filaments perpendicular to the sliding plane is higher. The difference in the coefficients of friction for these two orientations may be attributed to greater energy dissipation which is needed for orienting the perpendicular filaments toward the sliding direction. This is so because the filaments in either case are oriented parallel to the sliding plane in the vicinity of the sliding interface. Moreover, the resistance to shearing in the composite is higher with normal filament orientation than that with parallel orientation. This will also account for the higher coefficient of friction for normal filament orientation.

As for wear, it is seen that the composite with a perpendicular filament orientation exhibited higher wear resistance than that with a parallel orientation. As indicated above, the fibers with perpendicular orientation to the sliding plane provide better support to the matrix in terms of loading and so offer more resistance to shearing. The process of fiber refinement in the substrate provides further strengthening. Moreover, any attrition of fibers during the wear process in this case is in bits and pieces. On the other hand, in the case of the composite with parallel filament orientation, the resistance to crack nucleation and propagation is much lower and the filaments may be removed in much greater lengths. Consequently, the wear resistance of the composite with perpendicular filament orientation is greater than that with parallel orientation.

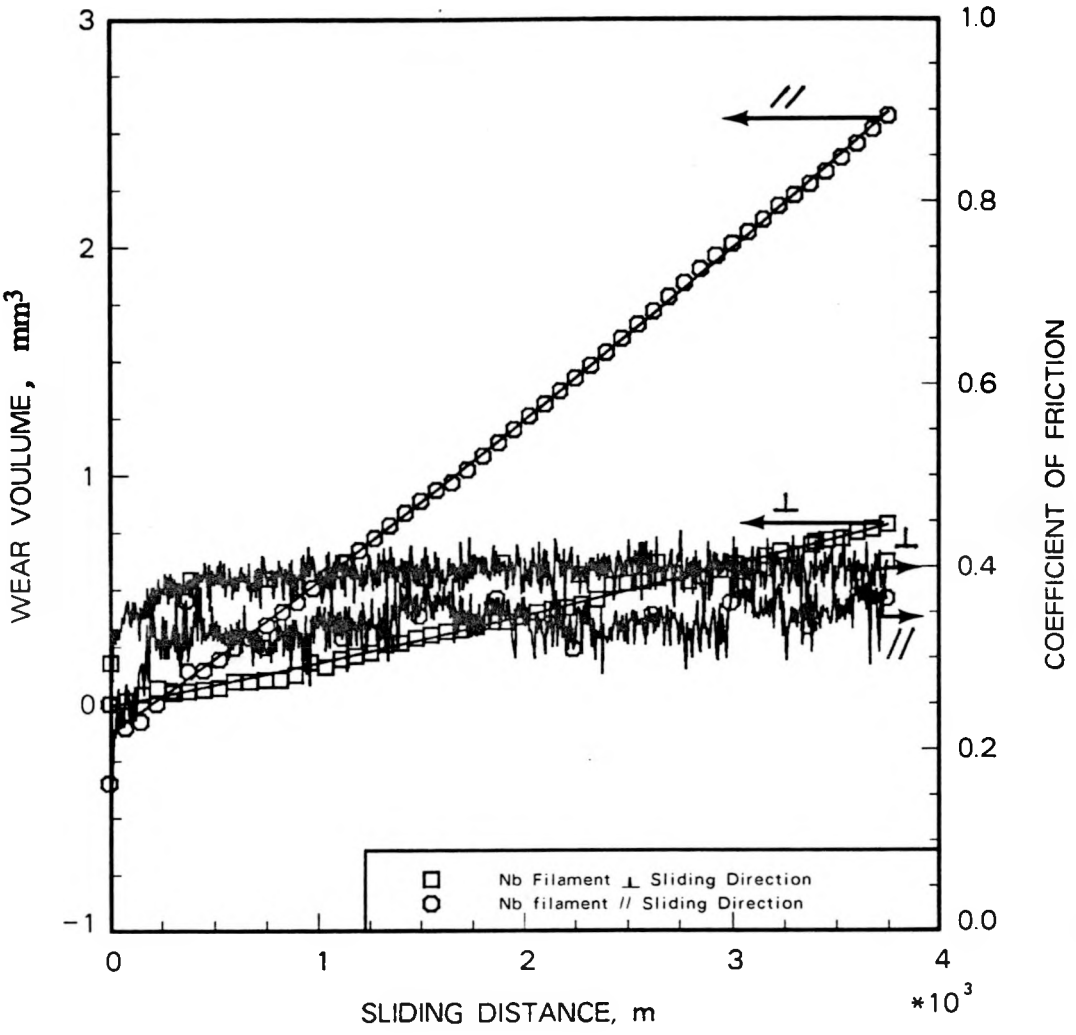

Figure 8: Variation of wear volume and the coefficient of friction with sliding distance for Cu-20vol.%Nb sheet composite ($\eta = 3.5$) with two different Nb filament orientations: sliding velocity 0.25 m/s, normal pressure 0.68 MPa

Effect of Annealing

In order to study the effect of matrix softening and filament coarsening on the friction and wear behavior, the composite specimens were annealed. Annealing was done by holding specimens for 24 hours at four different temperatures up to a maximum of $600^{o}C$ and furnace cooling. The variation of the coefficient of friction with annealing temperature is shown in Figure 9. Due to the large cyclic fluctuations in friction force during dry sliding, there was no significant effect of annealing seen on the coefficient of friction. The changes in hardness and wear rate with annealing temperature are shown in Figure 10. The wear rate increases rapidly with increasing annealing temperature up to $300^{o}C$ but the increase in wear rate above this temperature is minimal. The variation of hardness is opposite to that of wear rate.

The decrease in hardness below $300^{o}C$ was ascribed to matrix softening and above $300^{o}C$ to filament coarsening [12]. The rapid increase in wear rate up to $300^{o}C$ was due to the loss of work-hardening in varying degrees, because the sheet composites were made by cold deformation of the cast ingot. Above $300^{o}C$, the matrix softening was complete and Nb filaments started to grow in size. The coarsening of Nb filaments had a small effect on hardness in the temperature range of 300 to $600^{o}C$ (Figure 10). Therefore, the wear rate was also not affected much with increased annealing temperatures.

Wear Debris and Transfer Film

Figure 11 shows the SEM micrograph of the wear debris formed in sliding at a speed of 0.028 m/s and normal pressure of 0.68 MPa. The wear debris consists

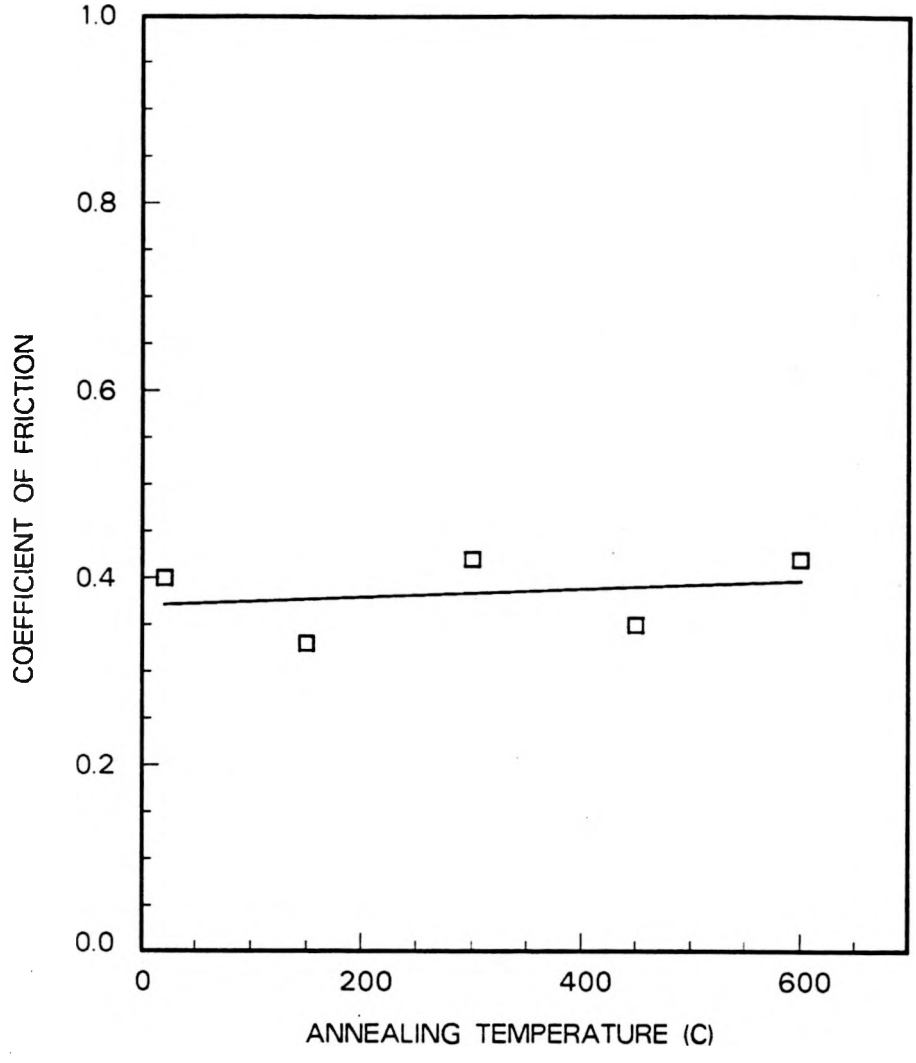

Figure 9: Variation of the coefficient of friction with annealing temperature for Cu-20vol.%Nb sheet composite ($\eta = 3.5$) sliding against tool steel at a sliding speed of 0.25 m/s and normal pressure of 0.68 MPa

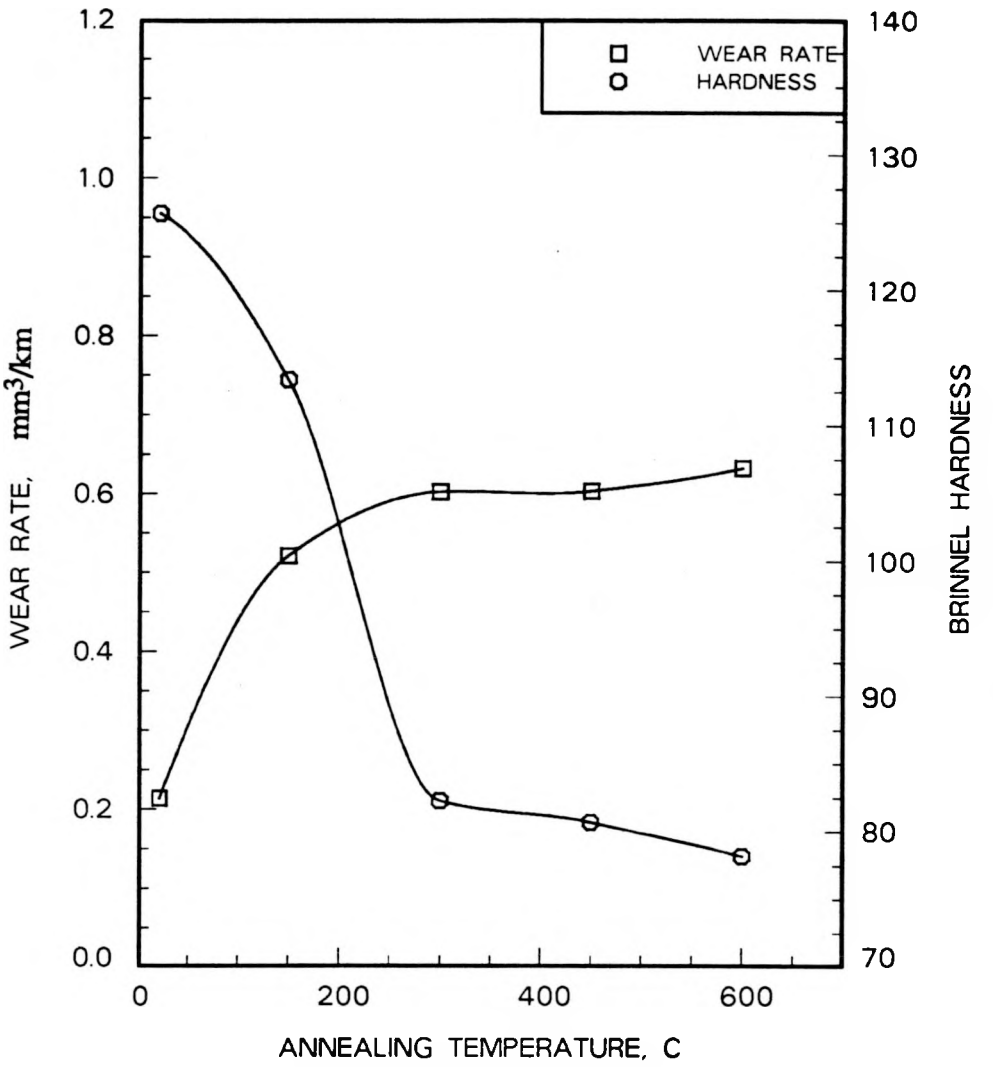

Figure 10: Variation of wear rate and hardness of Cu-20vol.%Nb sheet composite ($\eta = 3.5$) with annealing temperature. Wear tests were performed at 0.25 m/s sliding speed and 0.68 MPa normal pressure

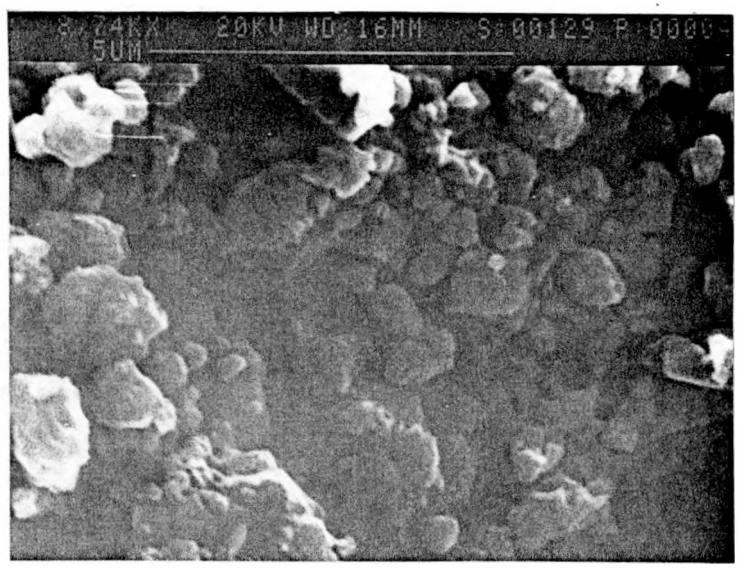

Figure 11: SEM micrograph of wear debris formed in wear test with Cu-20vol.%Nb sheet composite sliding against a tool steel disk at a sliding speed of 0.028 m/s with a normal pressure of 0.68 MPa

of a large number of small particles, typically 0.5 to 1.0 μm in size. Because of the high specific energy, the particles tend to agglomerate. Figure 12 shows an agglomerated particle with a crack in it. The EDS results from the locations A and B indicated nearly the same compositions (Cu-17.8vol.%Nb vs. Cu-20.45vol.%Nb), being essentially the average composition of the bulk material, and there was no trace of Fe found. It thus shows that the composite material maintained its structure even during the fracture process involved in wear, that is, Nb filaments were not separated from Cu matrix.

Figure 13 shows the transfer film formed on the tool steel disk during rubbing at 0.25 m/s. The film is fairly thick and exhibits considerable plastic deformation. Its composition was found by EDS to be the same as that of the composite material. The composition of the film indicated that, during wear, shearing occurred in the composite material. The gradual build-up of wear particles on the tool steel surface resulted in the development of a thick transfer film. Thus, during steady state wear, sliding occurred between the composite and its transfer film.

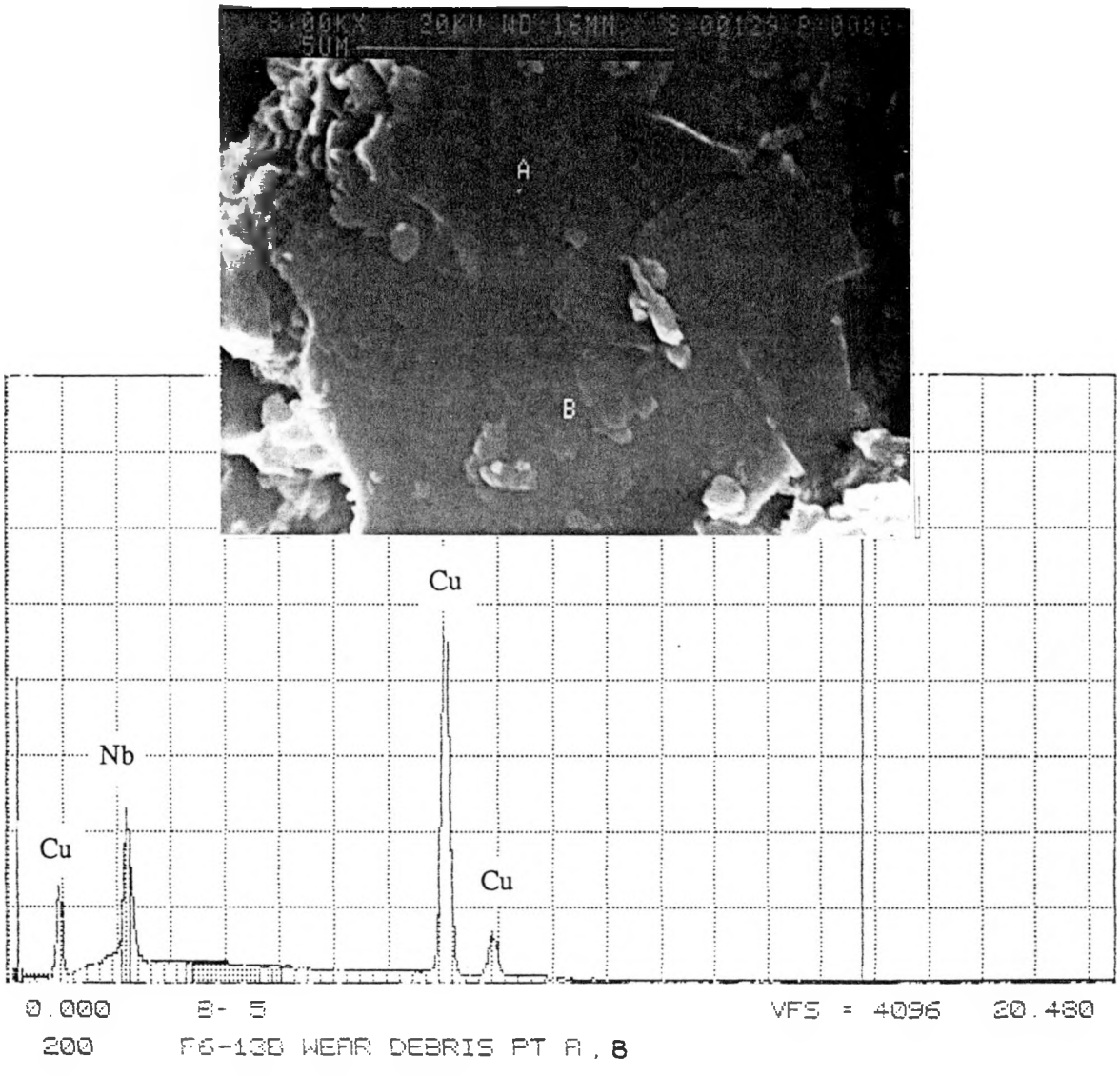

Figure 12: SEM micrograph of an agglomerated mass of wear particles formed in the wear test with Cu-20vol.%Nb sheet composite sliding against tool steel disk under the same conditions as in Figure 11

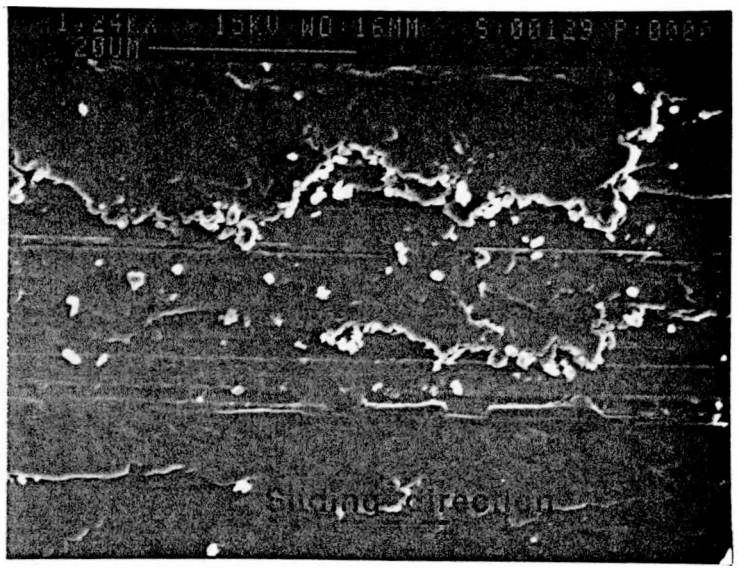

Figure 13: SEM micrograph of the transfer film on tool steel disk rubbing against Cu-20vol.%Nb sheet composite($\eta = 3.5$) at a sliding speed of 0.25 m/s and normal pressure of 0.68 MPa

DISCUSSION

For short-fiber reinforced thermoplastics sliding against smooth steel surfaces, Bahadur [6] proposed a model which accounted for wear in terms of low cycle fatigue, plowing, cutting and oxidative degradation. It was shown that the voids existing at the fiber-matrix interface or those produced by fiber-matrix debonding and fiber pullout contributed to the initiation of cracks. It should be noted that this kind of fiber-matrix debonding did not occur in Cu-Nb in situ composites. There were also no voids generated at the fiber-matrix interface during the processing of the composites. In the subsurface region affected by sliding, Nb filaments were deformed along with the Cu matrix because both Nb and Cu are highly ductile.

As in any composite, Nb filaments in Cu-Nb composite supported the normal load thereby reducing load on the matrix. They also participated directly in sliding. The tangential stress at the interface oriented the fibers in the vicinity of sliding interface in the sliding direction, sheared them to smaller fragments. These actions consumed a part of the energy so that less energy was available for crack initiation and propagation. The filaments provided a barrier for the movement of dislocations in the Cu matrix thereby strengthening the matrix which in effect contributed to increased wear resistance. There was also some work-hardening of Nb material. Due to increased temperature at the sliding interface, the Nb filaments were oxidized. The oxide film reduced adhesion and, therefore, reduced damage on the contact surface.

As for the matrix material, because of sliding action, it was subjected to considerable work-hardening which contributed to strengthening and also to increased wear resistance. The effect of work-hardening on wear resistance was revealed by the experiments on the annealed composite specimens where it was found that annealing

of the initially cold worked composite material decreased its wear resistance significantly. The rate of work-hardening increased with increasing sliding speed because the latter resulted in increased strain rate. In addition, the Cu matrix material was oxidized. This formed a protective film on the surface which reduced wear.

Due to presence of ductile Nb filaments in a ductile Cu matrix, the deformation in the subsurface layer of the wear specimen could be studied by examining its cross-section and noting the change in filament orientation. This kind of study is not possible with non-composites and even with other composites. From this study, it was found that deformation strain was maximum at the sliding interface and so cracks initiated at the sliding surface. This is different from delamination wear where cracks initiate in the substrate. In other words, the composite was worn in the modes of cutting, plowing, adhesion and surface deformation flow.

CONCLUSIONS

Based on the friction and wear studies for sliding between Cu-20vol.%Nb composite and a tool steel disk, the following conclusions were drawn:

1. There was plastic deformation induced by sliding in the subsurface layer of the composite wear specimen. The deformation gradient in this layer increased toward the sliding interface and the thickness of the layer affected by deformation increased toward the trailing edge of the specimen.

2. In the subsurface layer affected by sliding, along with the Cu matrix the Nb filaments were also deformed. As a result of this deformation, filaments were oriented along the sliding direction and were refined.

3. There was no debonding observed between the filament and the matrix and the composition of wear debris was about the same as that of the composite.

4. The coefficient of friction was not affected significantly by sliding speed in the range of 0.028 to 2.50 m/s, but the wear rate decreased with increasing sliding speed.

5. The coefficient of friction and wear resistance of the composites with filament orientation perpendicular to the sliding plane were higher than those with parallel orientation.

6. The wear rate of the composites annealed up to $300^{o}C$ increased rapidly, but the increase in wear rate was minimal for the composites annealed in the range of 300 to $600^{o}C$.

7. As a result of sliding, work-hardening and oxidation occurred in both filament and the matrix materials, and these contributed to the increase in wear resistance.

REFERENCES

[1] Verhoeven, J. D., F. A. Schmidt, E. D. Gibson and W. A. Spitzig. "Copper-Refractory Metal Alloys." Journal of Metals. Sept. (1986): 20-24.

[2] Renaud, C. V., E. Gregory and J. Wong. "Development and Application of High Strength, High Conductivity CuNb in situ Composite Wire and Strip." in Advances in Cryogenic Engineering Materials. vol.24, edited by A. F. Clark and R. P. Reed, Plenum Press: 435-442.

[3] Downing, H. L., J. D. Verhoeven and E. D. Gibson. "The Emissivity of Etched Cu-Nb in-situ Alloys." J. Appl. Phys. 61(7) (1987): 2621-2625.

[4] Metals Handbook (8th edition). vol.8, ASM, Metals Park, Ohio (1973): 281.

[5] Bahadur, S., P. Liu and J. D. Verhoeven. "Cu-Refractory Metal Alloy Application in Sliding Electrical Contacts." Final Report. Center for Advanced Technology Development, Iowa State University, Ames (1990).

[6] Bahadur, S. "Mechanical and Tribological Behavior of Polyester Reinforced with Short Fibers of Carbon and Aramid." Lubrication Engineering. in print.

[7] Johnson, K. L. Contact Mechanics. Cambridge University Press (1985): 207.

[8] Trybus, C. L. Microstructure-Strength Relationships of Heavily Deformed Cu-based Composite. Ph. D. dissertation, Iowa State University, Ames (1988).

[9] Lancaster, J. K. "The Formation of Surface Films at the Transition between Mild and Severe Metallic Wear." Proc. Roy. Soc. A. vol.273 (1962): 466-483.

[10] Dieter, G. E. Mechanical Metallurgy (2nd edition). McGraw-Hill Book Co. (1976): 340-350.

[11] Spitzig, W. A. and L. K. Reed. "Temperature and Strain Rate Dependence of the Strength of Heavily Cold-Drawn Copper, Niobium and Cu-20%Nb." Mat. Sci. Engr. A111 (1989): L13-L17.

[12] Krotz, P. D., W. A. Spitzig and F. C. Laabs. "High Temperature Properties of Heavily Deformed Cu-20%Nb and Cu-20%Ta Composites." Mat. Sci. Engr. A110 (1989): 37-47.

PART III.

SLIDING FRICTION AND WEAR BEHAVIOR OF Cu-Nb in situ COMPOSITES WITH ELECTRICAL LOAD

ABSTRACT

The sliding friction and wear behavior of Cu-Nb in situ composites was studied in the presence of electrical load. The pin-on-disk wear tester was modified for the passage of electrical energy through the sliding interface. Sliding was performed between a Cu-Nb composite pin and the flat surface of a hardened tool steel disk in ambient atmosphere. The effects of varying Nb proportion, electrical current density, sliding speed, and parallel and perpendicular Nb-filament orientation on the friction and wear behavior were investigated. It was found that with the application of electrical load in excess of 0.287 MA/m^2, the coefficient of friction and wear rate decreased. Both of these decreased with increasing Nb proportion as well. These changes along with those caused by other variables have been explained in terms of oxidation caused by the temperature rise produced by both the sliding and arcing actions. The worn surfaces as well as the subsurface deformation have been analyzed. The studies indicated rapid oxidation in electrical sliding and also revealed melting and crater formation by arc erosion.

INTRODUCTION

Cu-Nb in situ composites have demonstrated a superior combination of thermal/electrical conductivity and strength [1-3]. This attractive blend of properties makes these composites promising for applications in which both high electrical conductivity and superior mechanical strength are needed. In terms of such applications, sliding electrical contacts are possibly the best example where both electrical conduction and mechanical motion are involved. Therefore, it was decided to study the sliding friction and wear behavior of these composites in the presence of electrical load.

Previous electrical sliding research has been basically directed to the studies of friction, wear, electrical contact resistance, and material transfer in the sliding systems involving carbon brush and different slip-ring materials [4, 5]. It was shown [4] that the wear of carbon brushes was significantly increased when they were mated against steel and high-zinc brass rings. Shobert [6] showed that, excluding high friction situations caused by light load running, the wear rates of graphite or metal graphite brushes sliding against copper or copper alloy commutators were usually higher with electrical current than without it. Konchits [7] studied the influence of the magnitude and the direction of electrical current on the wear of carbon brushes. It was shown that, in the absence of sparking, the basic cause of increased brush wear under electrical current was the Joule heat released in the friction zone. The general pattern observed was the rapid increase in wear intensity with the increase in electrical current density.

Garshasb and Vook [8] studied the electrical contact system involving a copper brush sliding on a silver slip-ring in humidified CO_2. They found that with the

increase in electrical current, the metal transfer across the interface increased and so did the number of wear particles. At higher currents, the magnitude of metal transfer varied linearly with the square of current. Reichner [9] studied the sliding friction and wear of metal fiber brushes against silver-plated copper slip-rings in humidified CO_2 atmosphere. He observed very low wear rates for fiber brushes at high current densities. Burton and Burton [10] studied the friction, wear and resistivity of the specimens made of copper fibers in vitreous or glassy carbon matrix sliding against 303 stainless steel. The resistivity and friction observed in this case were comparable to those reported for typical copper graphite specimens, and the wear was exceptionally low. There is no research work reported on the sliding friction and wear of Cu-Nb in situ composites under electrical load.

In our previous studies, the mechanical and tribological behaviors of Cu-Nb in situ composites under dry, non-electrical sliding conditions were investigated [11]. It was found that the coefficient of friction decreased slightly with increasing Nb proportion and the wear resistance of Cu-20vol.%Nb was the highest. With the increase in true deformation strain, its wear resistance increased and there was a slight increase in the coefficient of friction as well. Further studies [11] on Cu-20vol.%Nb composite revealed that during sliding Nb filaments were reoriented in the sliding direction and refined in the subsurface layer. The mechanisms involved in the wear of composite were adhesion, cutting, plowing, deformation flow and microfracture.

The objective of this work was to study the sliding friction and wear behavior of Cu-Nb in situ composites under electrical load. These aspects have been investigated with the variations in Nb proportion, electrical current density, sliding speed, and Nb filament orientation in the composite.

EXPERIMENTAL

The fabrication process of Cu-Nb in situ composites was described elsewhere [1]. For sliding tests, the pin-on-disk wear test machine [11] was modified as shown in Figure 1 so as to make electrical current flow across the sliding interface. A DC power supply was connected across the specimen and the copper disk which supported the tool steel disk and was insulated from the drive system. The power supply worked in a constant current output mode where the current range was 0 to 50 A. The drop in voltage between the specimen and the pick-up member was measured. It was used in calculating the contact resistance. The contact resistance measured here was the sum of the two contact resistances across the two sliding interfaces and the bulk resistance of the tool steel disk in series. Since all other conditions were kept the same, the variation of this resistance provided a measure of the change in real contact resistance.

Sliding friction and wear tests were performed in this modified pin-on-disk wear machine with the composite specimen rubbing under dry atmospheric conditions against a hardened and ground O2 tool steel disk. The contact size of the pin specimen was 1.6 $mm \times 4.5$ mm where 4.5 mm dimension was parallel to the sliding direction. This pin was loaded with 4.9 N so that the nominal contact pressure was 0.68 MPa. The track diameter was 45 mm and the sliding speed was varied in the range of 0.25 to 2.5 m/s. The orientation of Nb filaments in the composite pin was perpendicular to the sliding plane except when the effect of Nb filament orientation on friction and wear was studied.

In view of the difficulty in measuring the flash temperature at the sliding interface, the temperature rise in the specimen was measured by a thermocouple inserted

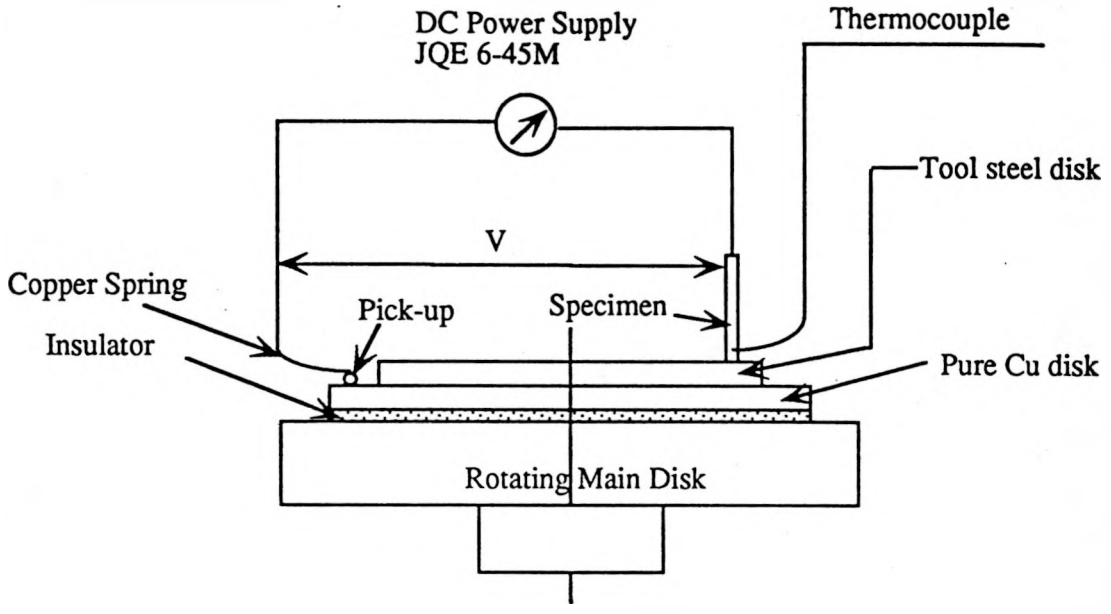

Figure 1: Schematic of electrical circuit for the supply of electrical current across sliding interface

as close to the interface as possible. For this purpose, a type-T miniature thermocouple was inserted into the specimen through a hole of 1.59 *mm* diameter and to a depth of about 0.76 *mm* from the sliding interface, and soldered in position. A digital voltmeter was added to the data acquisition system [11] in order to read the output of the thermocouple. The thermocouple was compensated to room temperature. The coefficient of friction, wear volume and temperature rise were recorded in a data file by the data acquisition system. The data were later processed in a digital computer.

RESULTS AND DISCUSSION

Effect of Nb Proportion

Figure 2 shows the variation of wear rate and the coefficient of friction for Cu-Nb sheet composites with varying Nb proportion by volume. Here, sliding occurred between the composite and the tool steel disk at a speed of 0.25 m/s and normal pressure of 0.68 MPa. The wear rate was calculated from the slope of the curve of volume loss versus sliding distance. The coefficient of friction decreased with increasing Nb proportion and it was lower with electrical load than without it for any composition. Furthermore, the difference between the two coefficients of friction increased with increasing Nb proportion. The wear rate of the composites with and without electrical load also decreased initially with increasing Nb proportion, reached a minimum value for 20vol.%Nb, and increased afterwards. The application of electrical load increased the wear rate of pure Cu but decreased the wear rate of Cu-Nb composites (with Nb proportion from 10 to 30vol.%).

The above variations in the friction and wear behavior appear to be related to the temperature rise at sliding interface. Holm [12] showed that the coefficient of friction for graphite/graphite and graphite/metal pairs sliding in air, with or without electrical load, decreased with increasing temperature from ambient to 200^oC. Johnson [4] also observed that the coefficient of friction decreased with increasing current density or the bulk temperature of the brush in the case of Ag-graphite brushes sliding on copper rings in a humidified CO_2 environment. Since the thermal/electrical conductivity of Cu-Nb in situ composites decreases with increasing Nb proportion [13] and the surface temperature rise varies inversely as the square root

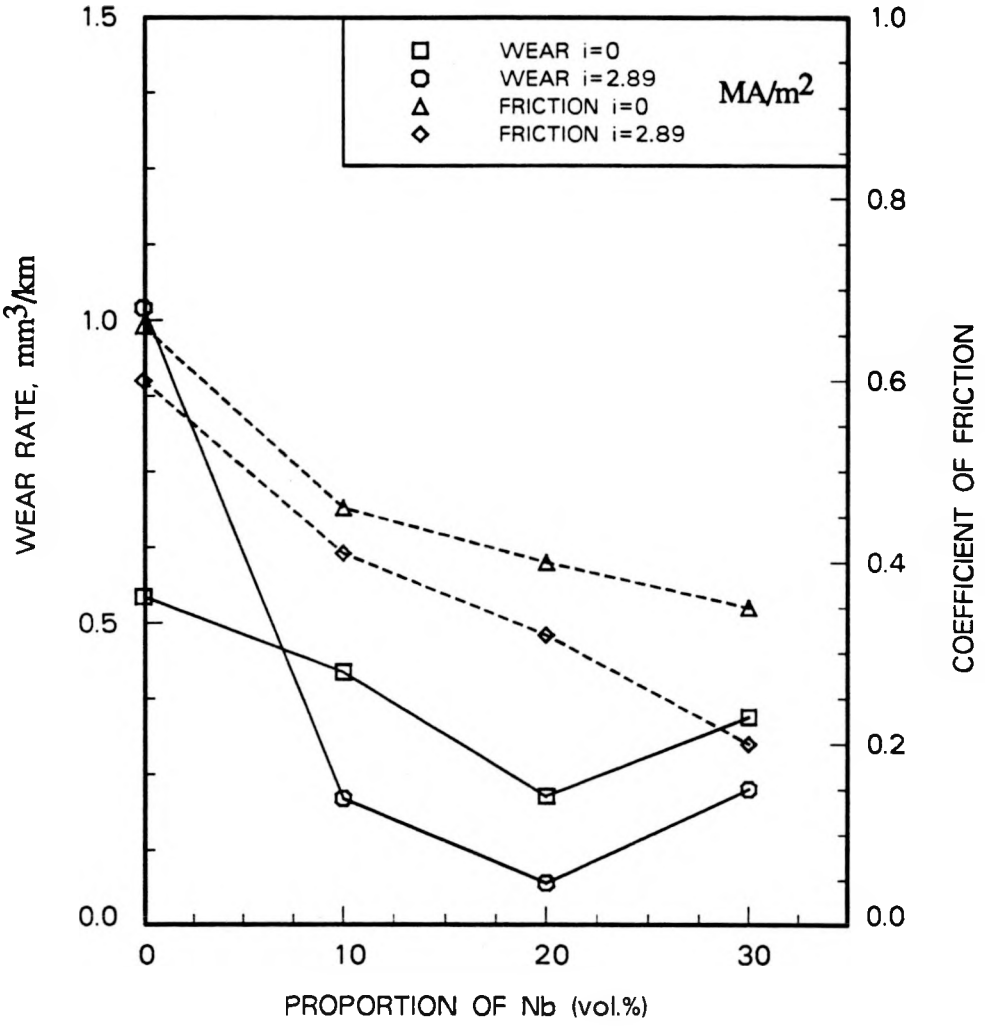

Figure 2: Variation of wear rate and the coefficient of friction with volume proportion of Nb in Cu-Nb in situ composites ($\eta = 3.5$) sliding against a tool steel disk at a sliding speed of 0.25 m/s, normal pressure of 0.68 MPa

of the thermal conductivity [14], the temperature rise at the sliding interface will be higher in the case of composites with higher Nb percentages. With increased temperature rise, the adhesion between the sliding surfaces decreased because of increased surface oxidation, and so the coefficient of friction decreased and the magnitude of the decrease increased with increasing Nb proportion. Since the passage of electrical current through the interface increased the temperature rise because of contact resistance and so also the oxidation rate, the coefficient of friction for any Nb proportion was lower with electrical load than without it.

The increased oxidation rate of the contacting surfaces also contributed to the decrease in wear rate of Cu-Nb composites with electrical current. A black oxide surface film was seen on the surfaces of Cu-Nb specimens. It prevented metallic contact between the surfaces and so reduced adhesive wear. In some materials, high temperature may contribute to increased wear rate but that was not the case here because Cu-Nb in situ composites have been reported to have good mechanical strength at elevated temperatures [15]. Thus, the oxide film had a strong subsurface support. On the other hand, the subsurface support in the case of pure Cu deteriorated with increased temperature rise because of the application of electrical load, and so the wear rate was higher than that in the absence of electrical load. This is further supported by the reported arc erosion resistance of Cu-Nb composites which was found to be much better than that of pure Cu [16].

Temperature Rise in Electrical Sliding

In view of the above explanations, it was considered desirable to verify if temperature rise was indeed a prominent factor in sliding with electrical load. The

temperature was measured in the pin specimen at a distance of 0.76 mm from the contact surface. Figure 3 gives the variation of temperature with time. The lower two curves represent the temperature variation for stationary electrical contact and non-electrical sliding. It is seen that the temperature rise in both of these cases is fairly low, a maximum of $12^{o}C$ for stationary electrical contact and $21^{o}C$ for non-electrical sliding. However, the temperature in the case of electrical sliding increased rapidly as soon as sliding commenced. Thereafter, it increased erratically reaching a maximum of $276^{o}C$. The erratic behavior may have to do with the random nature of the events related to the formation and disruption of oxide film during sliding.

In order to probe into the temperature rise variation for electrical sliding, the contact resistances of both the stationary and sliding contacts in the presence of electrical load were measured as a function of time and are plotted in Figure 4. It is seen that the contact resistance of stationary contact was very low and basically constant. The resistance in electrical sliding was high and irregular. This indicated the build-up of thick oxide film during sliding. As such, the temperature rise at the contact surface was much higher in electrical sliding than that in stationary contact.

Effect of Current Density

The variation of wear rate and the coefficient of friction with electrical current density is shown in Figure 5 for Cu-20vol.%Nb sheet composite sliding against a tool steel disk at a sliding speed of 0.25 m/s and a normal pressure of 0.68 MPa. The wear rate and the coefficient of friction both increased initially with the increase in current density to 0.287 MA/m^2 but then decreased with further increase in current

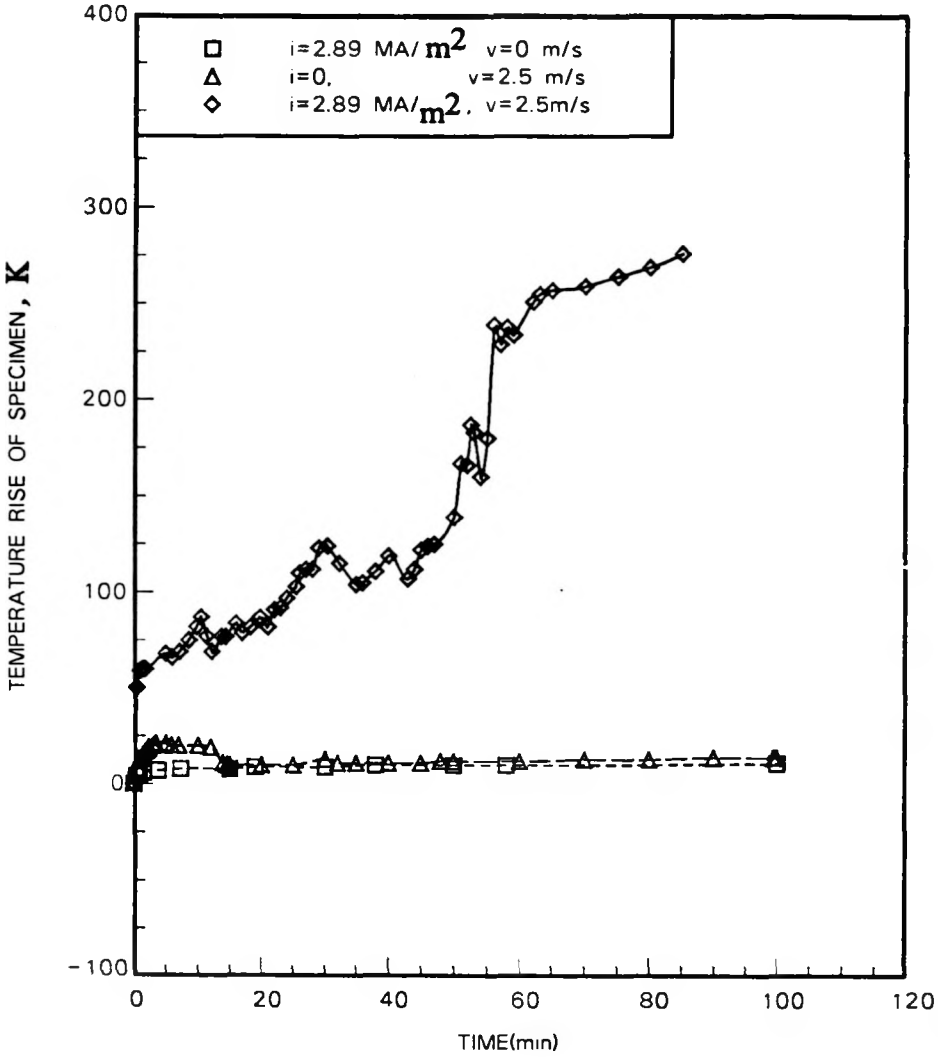

Figure 3: Variation of specimen temperature rise with time for: (a) stationary contact and (b) dry sliding with and without electrical current for Cu-20%Nb ($\eta = 3.5$) sheet composite sliding against a tool steel disk at a normal pressure of 0.68 MPa and an electrical current density of 2.89 MA/m^2

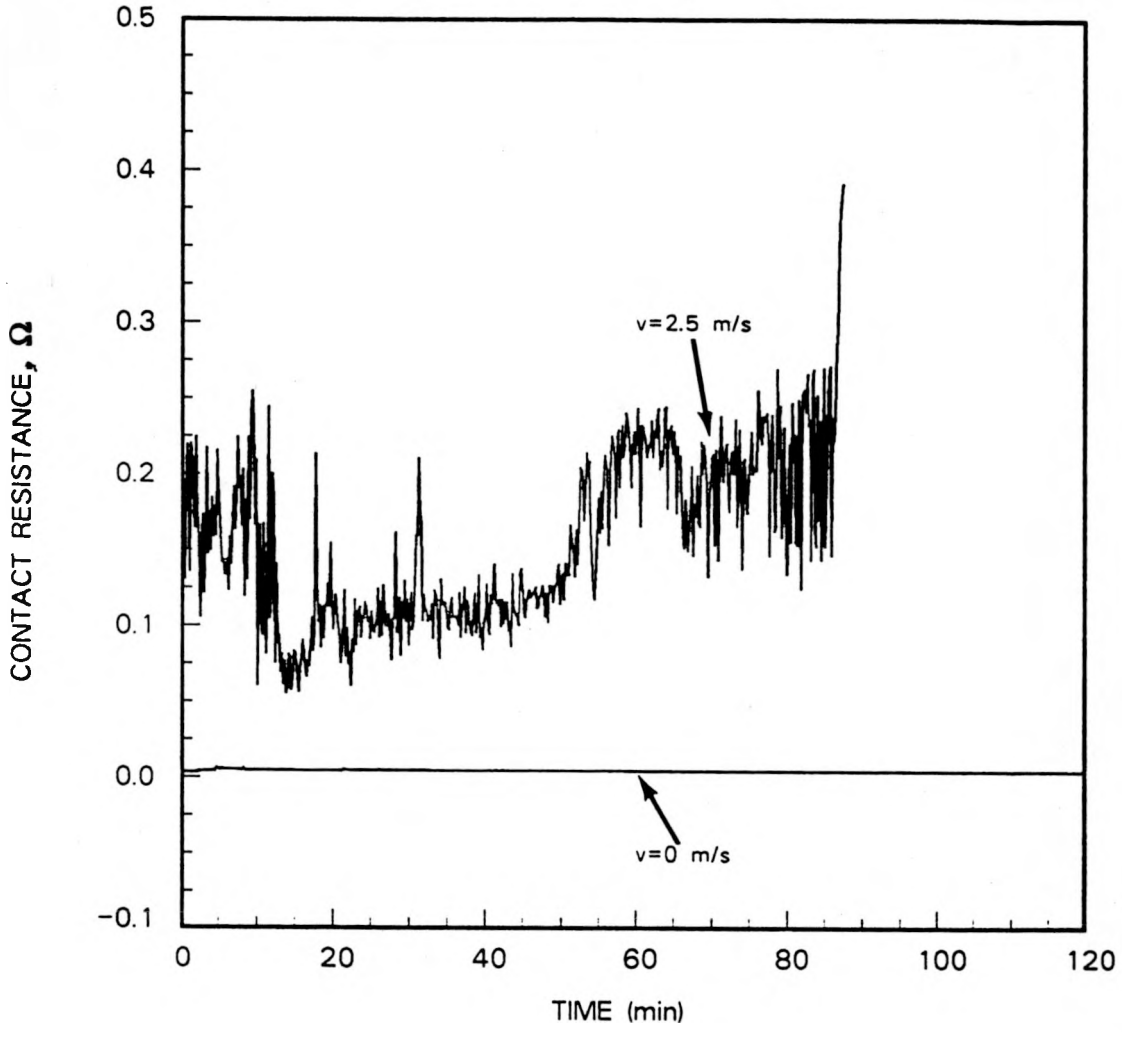

Figure 4: Variation of contact resistance with contact time for (a) stationary contact and (b) sliding contact (sliding speed 2.5 m/s) for Cu-20%Nb ($\eta = 3.5$) sheet composite sliding against a tool steel disk at a normal pressure of 0.68 MPa and an electrical current density of 2.89 MA/m^2

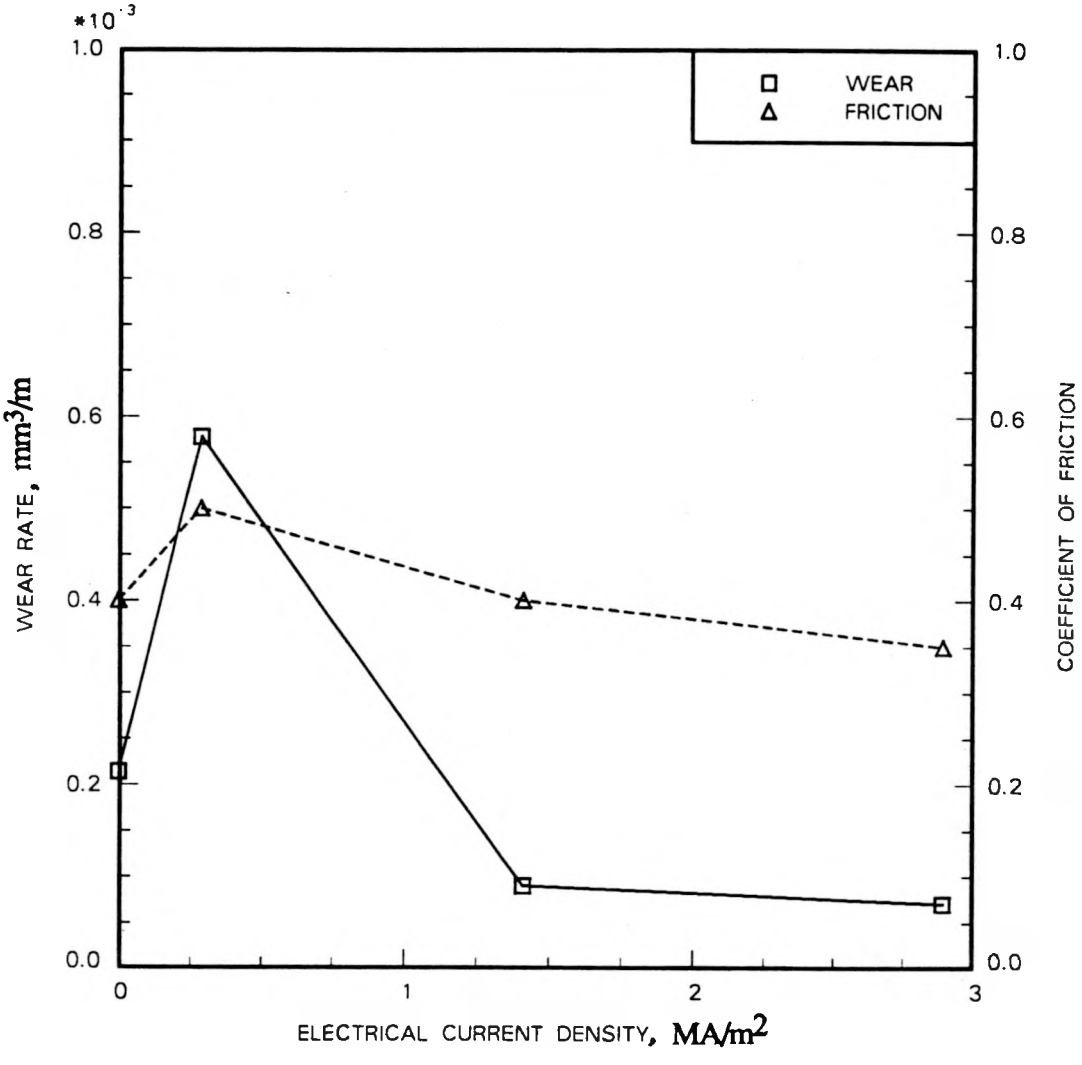

Figure 5: Variation of friction and wear with electrical current density for Cu-20vol.%Nb in situ sheet composite ($\eta = 3.5$) sliding against tool steel at a sliding speed of 0.25 m/s and normal pressure of 0.68 MPa

density. Similar results were also reported by Rabinowicz and Chan [5] for silver-graphite brushes sliding on various ring materials at high current densities. The initial increase in the wear rate and the coefficient of friction with the application of electrical load may be due to the microwelding of asperities on the contacting surfaces because the temperature rise promoted diffusion but was not high enough to increase oxidation to the extent that it could prevent metallic contact. As the current density increased, the temperature rose and so the oxidation rate increased. This resulted in developing a thicker oxide film on the surfaces so that adhesion was considerably reduced. Thus, shearing now occurred at the interface as opposed to the bulk material in the earlier case. Consequently, both wear rate and the coefficient of friction decreased with the higher levels of current density.

Effect of Sliding Speed

The mean value of the coefficient of friction of Cu-20vol.%Nb sheet composite ($\eta = 3.5$) sliding against tool steel with and without electrical current is given for two different sliding speeds in Figure 6. The coefficient of friction in the absence of electrical current was about the same at both speeds. With the application of electrical load, the coefficient of friction decreased at both speeds, and the decrease was larger at the higher sliding speed. The decrease in the coefficient of friction with the application of electrical current and its decrease with increased sliding speed are again attributed to higher temperature rise. The higher temperature increased oxidation rate and thereby promoted rapid film formation on the contact surface. The surface film prevented the direct contact between surfaces and so adhesion was reduced. This led to the reduction in the coefficient of friction.

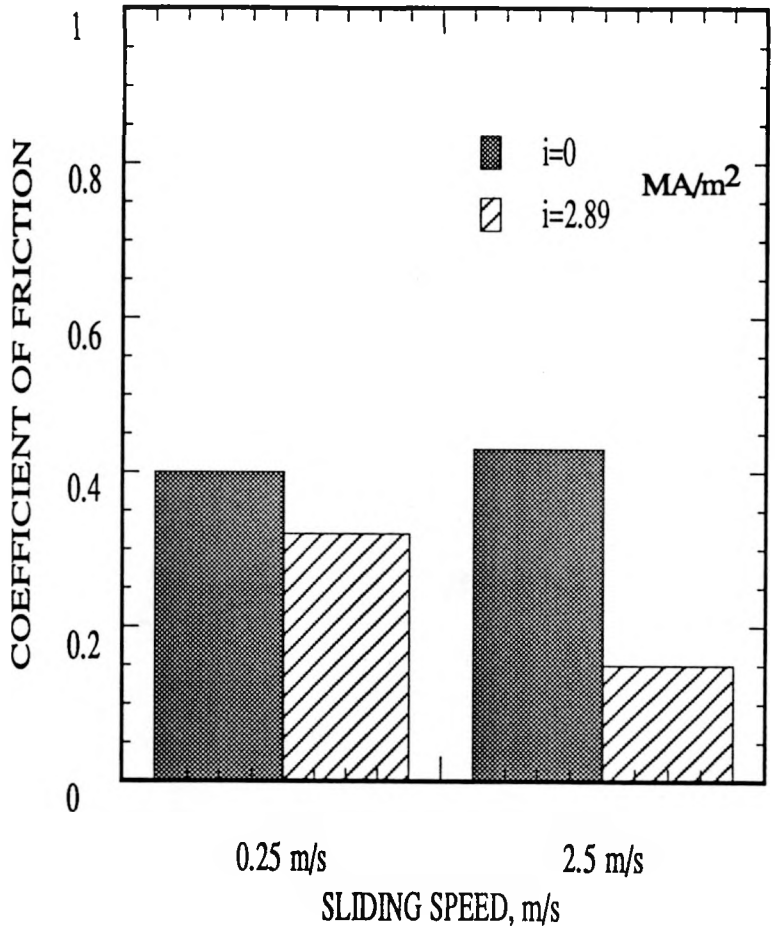

Figure 6: Effect of sliding speed on the coefficient of friction for Cu-20%Nb sheet composite ($\eta = 3.5$) sliding against tool steel with and without electrical load at the normal pressure of 0.68 MPa

Figure 7 gives the wear rate of Cu-20%Nb at two sliding speeds. In both the cases, with and without electrical load, the wear rate at 2.5 m/s was much lower than at 0.25 m/s. This is again because of the higher temperature rise that occurred at the higher sliding speed which increased the formation of oxide on the contact surface. Since the Cu-Nb composite maintains high strength at high temperatures, the substrate was capable of providing good support to the oxide film even at these temperatures and so the wear rate was reduced with the increased sliding speed.

Effect of Nb Filament Orientation

The variation of the coefficient of friction with sliding distance for Cu-20vol.%Nb composite ($\eta = 3.5$) with Nb filaments parallel and perpendicular to the sliding plane is shown in Figure 8. For sliding in the absence of electrical load, the coefficient of friction did not show any significant variation for the two orientations. With the application of electrical load, the coefficient of friction for both Nb filament orientations was reduced because of increased oxidation at the contact surface, as explained earlier. Because of the large fluctuations in the kinetic coefficient of friction, it is reasonable to conclude that there was no significant change in the coefficient of friction for these two Nb filament orientations here as well.

Figure 9 provides the comparison between the wear rates of Cu-20vol.%Nb sheet composites ($\eta = 3.5$) for the parallel and perpendicular Nb filament orientations. It is seen that in both the cases, with and without electrical load, the composite with perpendicular filament orientation had better wear resistance than that with parallel orientation. This is so because the Nb filaments perpendicular to the sliding plane provided strengthening to the composite in shear parallel to the sliding plane. On

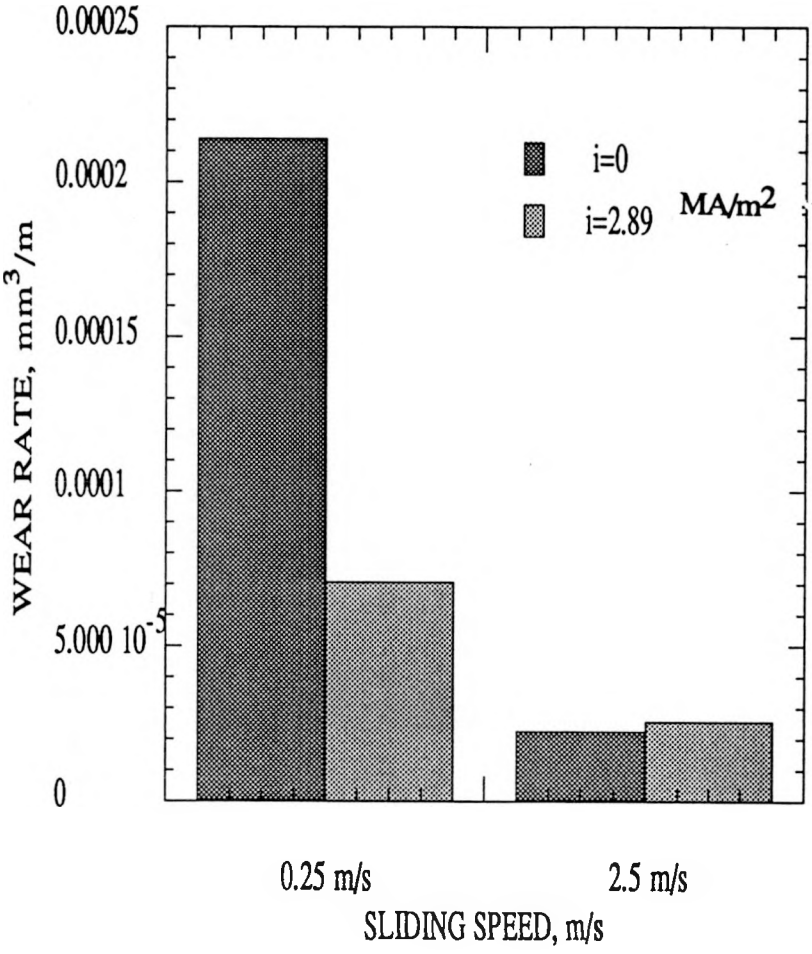

Figure 7: Effect of sliding speed on wear rate for Cu-20%Nb sheet composite (η = 3.5) sliding against tool steel with and without electrical load at the normal pressure of 0.68 MPa

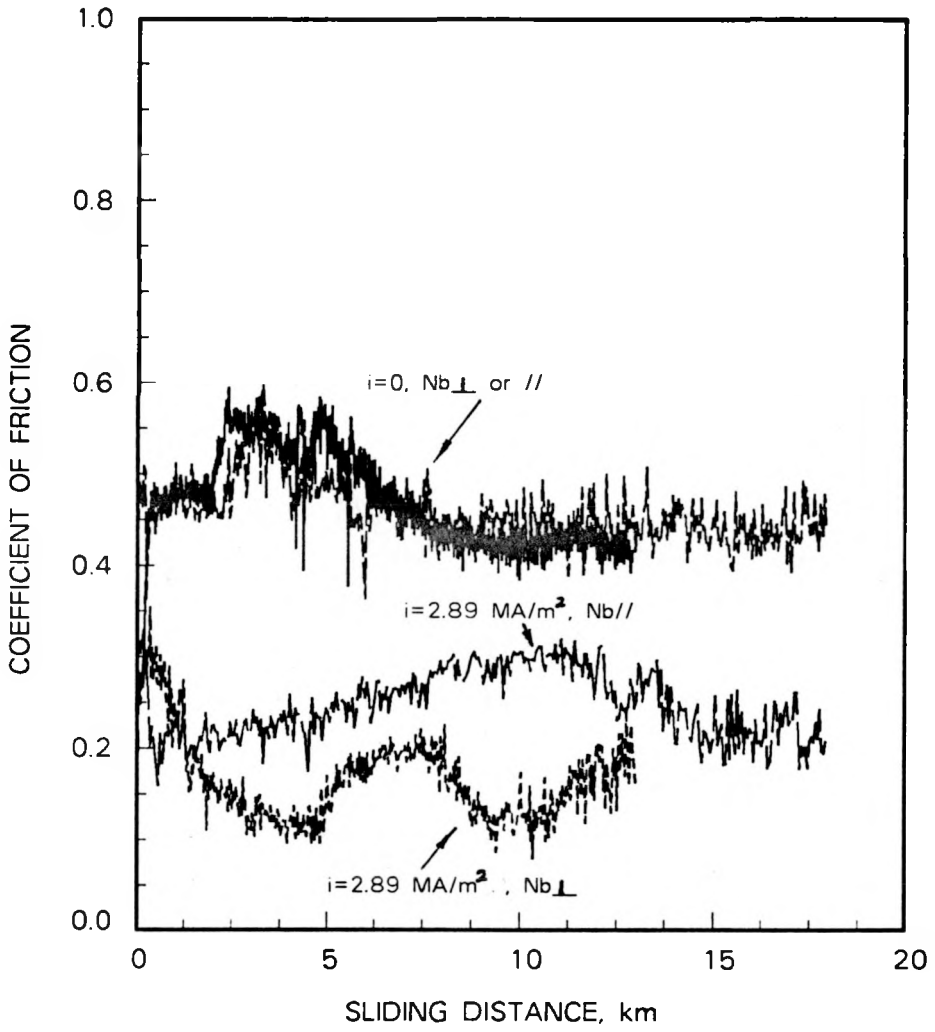

Figure 8: Variation of the coefficient of friction with sliding distance for Cu-20%Nb composite, with Nb filaments parallel and perpendicular to sliding plane, both in the absence and presence of electrical load, at the sliding speed of 2.5 m/s and normal pressure of 0.68 MPa

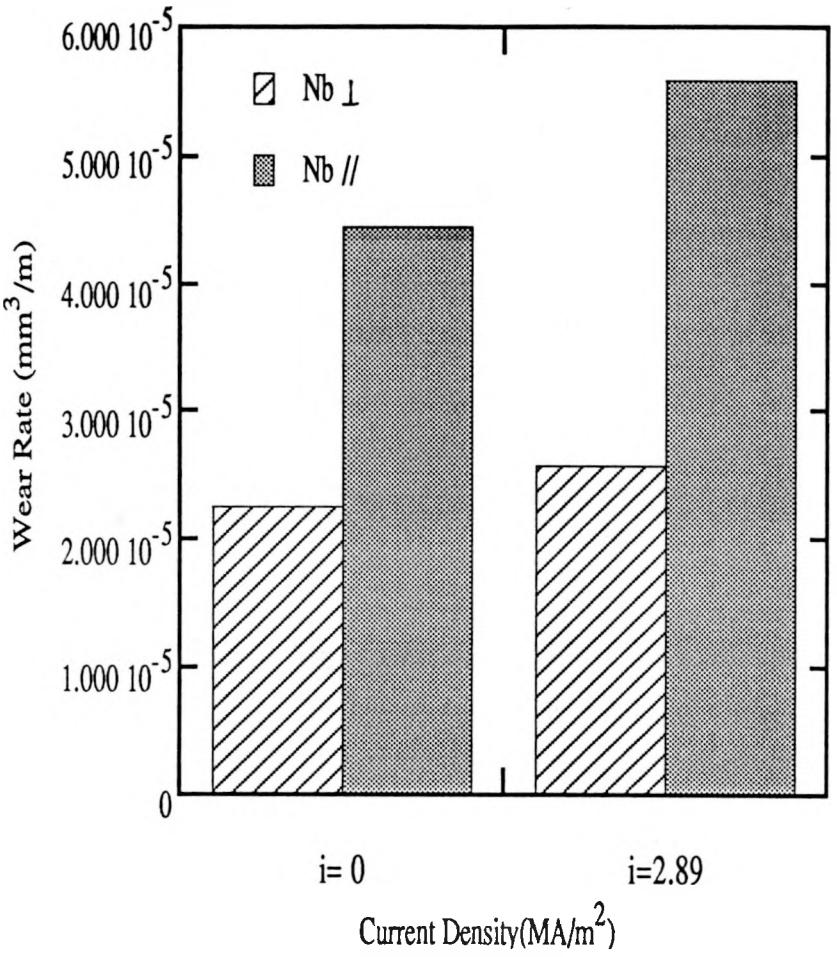

Figure 9: Comparison of the wear rates for Cu-20%Nb sheet composite with Nb filaments parallel and perpendicular to sliding plane, sliding against tool steel, with and without electrical current, at the sliding speed of 2.5 m/s and normal pressure of 0.68 MPa

the other hand, because of the uniaxial orientation of fibers, the shear strength in the sliding direction of the composite with parallel filament orientation may be equal to or less than that of the matrix material.

Deformation and Wear Studies

Figure 10 shows the cross-sections of wear specimens of Cu-20vol.%Nb for both the non-electrical and electrical sliding. The subsurface layer deformation of the composite in electrical sliding has basically the same characteristics as that for non-electrical sliding. In both cases, Nb filaments have been reoriented along the sliding direction and refined in size in the subsurface layer. There is, however, a marked difference between the thicknesses of the oxide films formed on the two surfaces. The oxide film on the specimen surface involved in electrical sliding is about 10–15 μm thick compared to 2–3 μm in non-electrical sliding. Because of the protective role of oxide film, both the coefficient of friction and wear rate decreased when electrical current was added in the sliding process. The bend in the filaments indicates that a considerable depth of the material is affected in terms of deformation during sliding.

There are three typical zones noticed on the composite pin wear surface involved in sliding with electrical load. These are marked in Figure 11 (a) while Figure 11 (b), (c) and (d) show their characteristic features. Zone 1, where the tool steel disk came in contact first with the pin surface, exhibits extensive plowing along with smearing of grooves by the plastic flow of material (Figure 11 (b)). The plowing on the composite surface was caused mainly by the action of asperities on the hardened tool steel disk. There are very few wear particles seen in this area. The wear particles, if created in

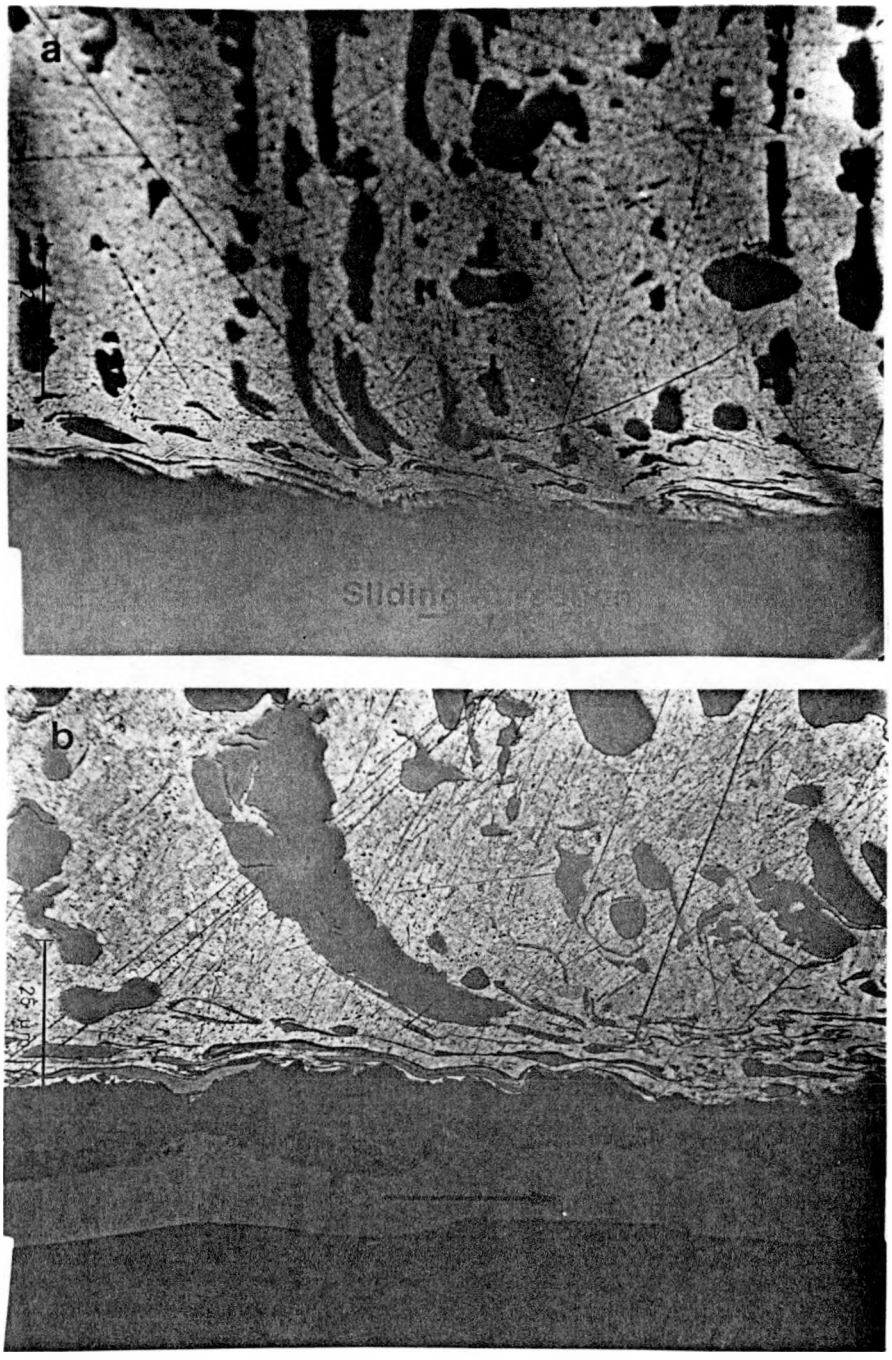

Figure 10: Cross-sections of Cu-20%Nb sheet composites tested at the sliding speed of 0.25 m/s and normal pressure of 0.68 MPa: (a) non-electrical sliding; (b) sliding with electrical load of current density 2.89 MA/m^2

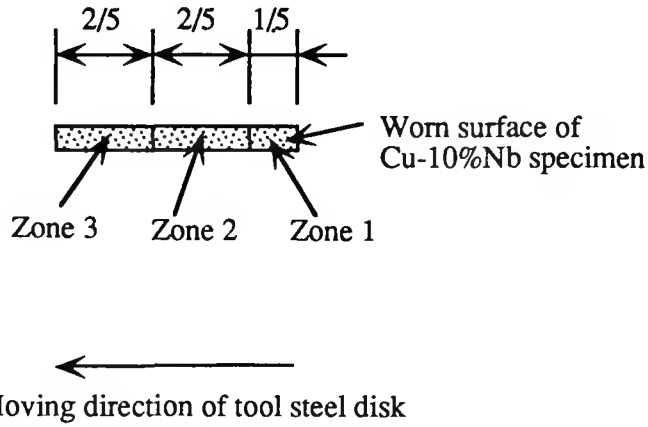

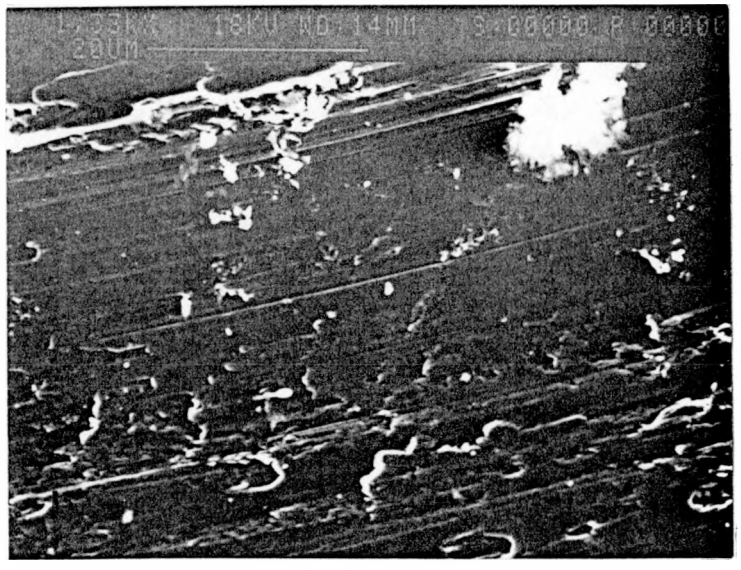

Figure 11: Three zones on the worn surface of Cu-10%Nb sheet composite sliding against tool steel at a speed of 0.25 m/s, normal pressure of 0.68 MPa and electrical current density of 2.89 MA/m^2: (a) Schematic representation of zones; (b) Zone 1; (c) Zone 2; (d) Zone 3

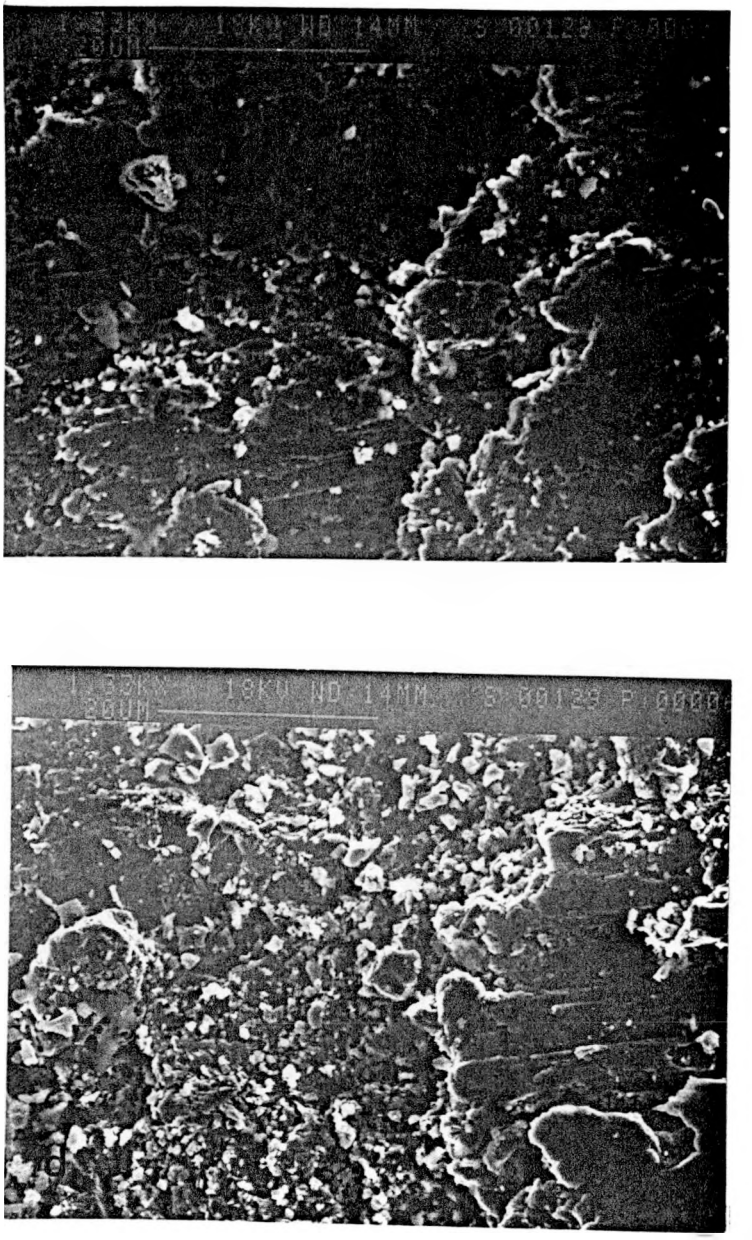

Figure 11 (Continued)

this early stage of contact, were presumably displaced toward the outgoing edge of the specimen. Figure 11 (c) shows zone 2 where grooving along the sliding direction can still be seen but the grooves are not as sharp as in zone 1. There are also more wear particles seen on this surface. In zone 3 considerable plastic deformation and wear debris accumulation but with much less grooving was observed. It so appears that most of the wear particles were created by microfracture in the preceding zones and were relocated by deformation flow in zone 3. Some of these particles were later thrown out of the contact region in the form of loose wear debris or else transferred to the steel disk surface. Some material transfer presumably occurred in zones 1 and 2 as well.

The characteristics of arc erosion and surface melting were also seen in zone 3. Figure 12 shows the evidence of arc erosion. It exhibits surface melting and the formation of craters. The latter were formed by arcing action which was necessitated for the flow of electrical current by the everchanging gap between the asperities on contacting surfaces. The intermittent arcing action melted the material in discrete locations and thereby produced a profusion of craters. There is also an indication of cracking which initiated from dimples and this could be seen much better at higher magnifications.

Figure 13 shows droplets on the surface of Cu-Nb in zone 3. These provided the proof of surface melting due to high temperature arcing. These droplets may actually be in either the rheological or liquid state. These appear to be capable of being deformed easily by the relative motion of sliding members because some of these are worm-shaped or elongated. The energy dispersive spectrometry (EDS) analysis of the droplet in the upper-right corner of the picture showed that it was

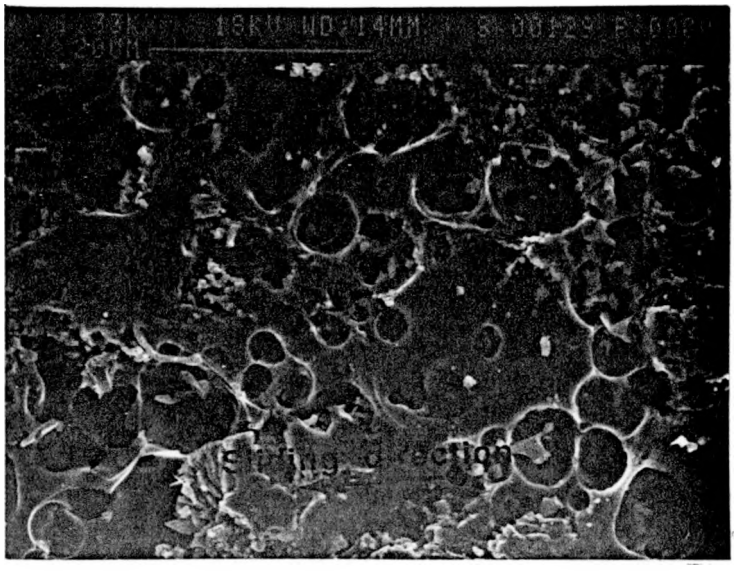

Figure 12: Arc eroded surface of Cu-Nb in zone 3 of Figure 11

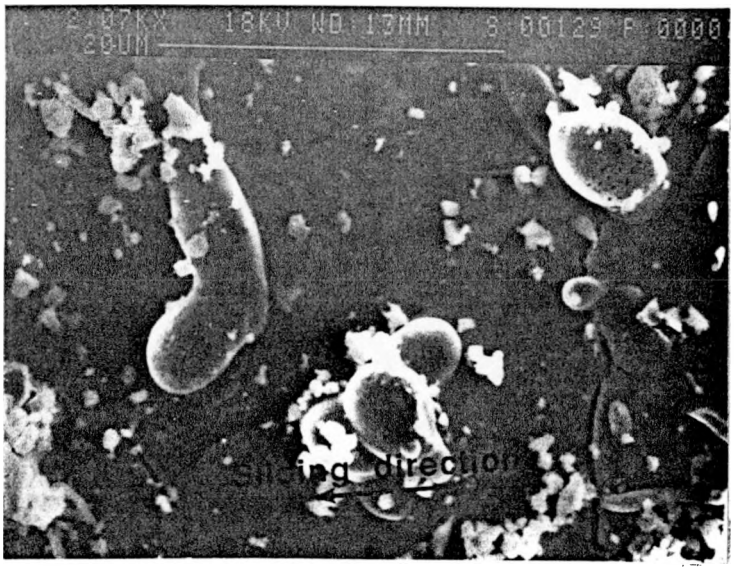

Figure 13: Evidence of molten droplets found on the worn surface of Cu-20%Nb in zone 3 of Figure 11

Cu-rich and had Nb, Fe and Si as constituents. The proportion of Cu in the droplet was greater than its average composition in Cu-Nb composite. Two major points could be made according to this observation. First, melting occurred preferentially in the lower melting point Cu phase so that more Cu than Nb was eroded away from the parent Cu-Nb composite. This implies that the refractory Nb phase was able to escape melting so that it could have helped the Cu matrix against further melting or erosion. Second, the constituents of Fe and Si in the droplet are from the tool steel disk. It indicates that material was transferred not only from Cu-Nb pin to tool steel disk but also from the disk back to the pin surface.

Figure 14 shows a wear particle randomly selected in zone 2 of Figure 11. EDS analysis of that particle indicated that it contained 73.7%Cu, 17.7%Fe and 8.6%Nb. Even though EDS could not show here the composition accurately, it depicted the presence of a large quantity of Fe in Cu-Nb specimen. The Fe constituent here was obviously from the contacting tool steel disk. Since the diffusion coefficient of Fe is fairly low at this temperature and the contact time for any contact spot is very limited, the back transfer of tool steel is believed to occur in the form of tool steel fragments and not by atomic diffusion. Most probably it originated from the microfracture of asperity in the parent material and the small fragments so formed were pressed onto the opposite surface. This produced in effect mechanical alloying [17]. The Fe transfer to liquid droplet might be from a different mechanism. When arc caused melting on the surface of the composite specimen, the liquid phase was pressured against the tool steel disk. This pressed molten layer had a very good contact with iron oxide film on the tool steel surface. As the molten layer was forced to roll over the surface, the Fe could be transferred to the molten layer either by

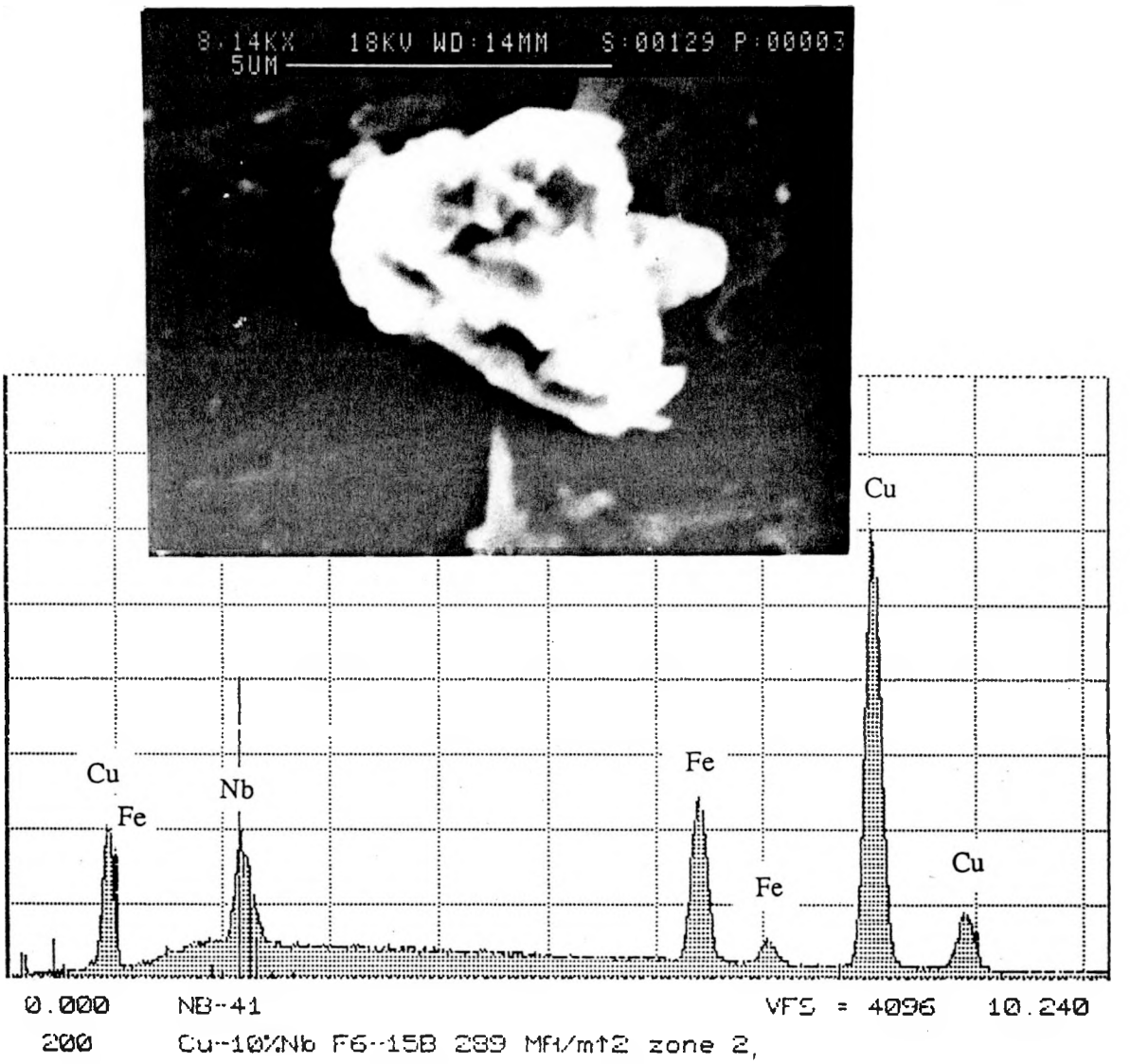

Figure 14: SEM micrograph of a wear particle in zone 2 of Figure 11 and EDS analysis of that particle

means of diffusion or oxide cracking. This resulted in the transfer of material from tool steel to liquid droplet formed on the composite surface.

The sliding track on the hardened tool steel disk was severely damaged in the case of electrical sliding. The wear track turned dark gray and it had very little Cu color in it. This was in contrast to the sliding track for non-electrical sliding which was shining mostly with Cu color. There were plenty of grooves seen on the track which was again not the case in non-electrical sliding. These grooves were created in the transferred material at the high surface temperatures generated in electrical sliding. The transfer of tool steel segments to the Cu-Nb surface and the mechanical mixing of the constituent elements from both surfaces (Fe, Cu, Nb, Si and Cr) produced a much stronger material that was presumably able to produce grooving on the tool steel disk surface. In addition to surface oxidation, this could be another reason why the wear of Cu-Nb composite pin decreased on application of the electrical load.

The wear track on the tool steel disk was featureless, as shown in Figure 15. This was so because of severe oxidation. The black region in the photograph was covered by a thick oxide film and adhesive deformation and plowing occurred mostly in the bright region. EDS analysis of the wear particles in the bright region indicated that wear debris was composed of Fe, Cu, Nb, Mn and Si which were the elements present in both the tool steel and the Cu-Nb composite.

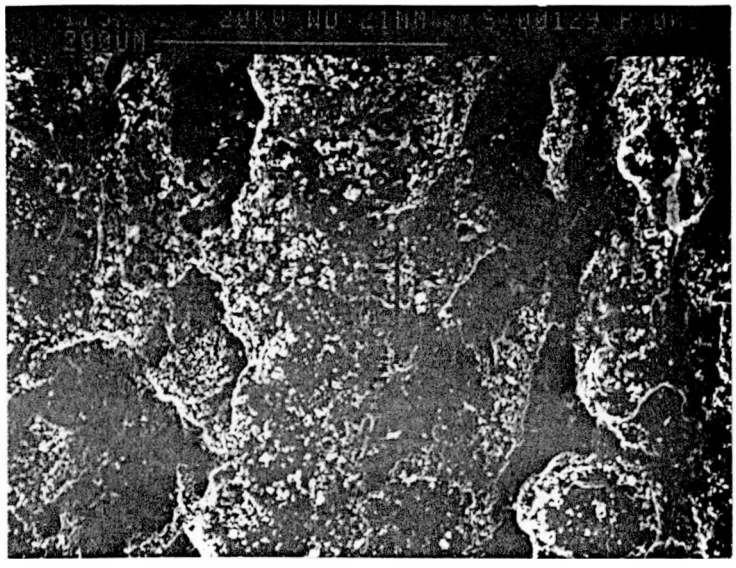

Figure 15: SEM micrograph of the wear track on tool steel disk sliding against Cu-20%Nb composite at a speed of 0.25 m/s, normal pressure of 0.68 MPa and electrical current density of 2.89 MA/m^2

CONCLUSIONS

From sliding studies between Cu-Nb in situ composite pins and tool steel disks, the following conclusions were drawn:

1. The coefficient of friction increased on the application of electrical load but decreased with higher current densities. It also decreased with increasing Nb proportion in both the electrical and non-electrical sliding.

2. Of all the composites tested, the wear resistance of Cu-20vol.%Nb composite was the highest in both electrical and non-electrical sliding, and it was higher in the presence of electrical load than without it.

3. The temperature rise in sliding contact was very significant from electrical Joule heating which was proportional to contact resistance.

4. With the increase in sliding speed from 0.25 to 2.5 m/s, the coefficient of friction did not change in the absence of electrical load, but the wear rate decreased considerably. When an electrical load was applied, both the coefficient of friction and wear rate decreased at the higher sliding speed.

5. The composite with Nb filaments perpendicular to sliding direction had higher wear resistance than that with parallel orientation in both the electrical and non-electrical sliding, but the orientation did not have any significant effect on the coefficient of friction.

6. The subsurface deformation features in sliding with electrical current were similar to those for non-electrical sliding except that the thickness of oxide film was much larger in the presence of electrical current. There was evidence of melting and crater formation by arc erosion which seemed to occur preferentially in the Cu matrix.

7. The material transfer occurred mainly from the composite pin to the tool

steel disk surface but some tool steel was also transferred to the pin surface. The wear track on the tool steel disk was severely damaged and oxidized in sliding with electrical load.

8. Oxidation and material transfer were the governing factors affecting the friction and wear behavior of Cu-Nb composites.

REFERENCES

[1] Verhoeven, J. D., F. A. Schmidt, E. D. Gibson and W. A. Spitzig. "Copper-Refractory Metal Alloys." Journal of Metals. Sept. 1986: 20-24.

[2] Renaud, C. V., E. Gregory and J. Wong. "Development and Application of High Strength, High Conductivity CuNb In Situ Composite Wire and Strip." in Advances in Cryogenic Engineering Materials. vol. 34, edited by A. F. Clark and R. P. Reed, Plenum Press: 435-442.

[3] Downing, H. L., J. D. Verhoeven and E. D. Gibson. "The Emissivity of Etched Cu-Nb in-situ Alloys." J. Appl. Phys. 61(7), 1987: 2621-2625.

[4] Johnson, J. L. "Sliding Monolithic Brush Systems for Large Currents." Electrical Contacts-1986. Proceedings of the 32nd IEEE Holm Conference on Electrical Contacts, Oct. 1986: 3-17.

[5] Rabinowicz, E. and P. Chan. "Wear of Silver-Graphite Brushes against Various Ring Materials at High-Current Densities." IEEE Trans. vol. CHMT-3(2), 1980: 288-291.

[6] Shobert II, E. I. Carbon Brushes: The Physics and Chemistry of Sliding Contacts. Chemical Publishing Company, Inc. 1965: 11-12.

[7] Konchits, V. V. "Wear in the Sliding Contact of Electrical Machines, I." Soviet Journal of Friction and Wear. vol.7(1), 1986: 90-96.

[8] Garshasb, M. and R. W. Vook. "Fundamental Analysis of Cu Brush-Ag Slip Ring Sliding Electrical Contacts." IEEE Trans. vol. CHMT-9(1), 1986: 23-29.

[9] Reichner, P. "High Current Tests of Metal Fiber Brushes" IEEE Trans. vol. CHMT-4 (4), 1981: 1-4.

[10] Burton, R. A. and R. G. Burton. "Vitreous Carbon Matrix for Low Wear Carbon/Metal Current Collectors." Electrical Contacts-1988. Proceedings of the 34th IEEE Holm Conference on Electrical Contacts, Sept. 1988: 223-228.

[11] Bahadur, S., P. Liu and J. D. Verhoeven. "Cu-Refractory Metal Alloy Application in Sliding Electrical Contacts." Final Report. Center for Advanced Technology Development, Iowa State University, Ames, 1990.

[12] Holm, E. "Specific Friction Force in a Graphite Brush Contact as a Function of the Temperature in the Contact Spots." J. Appl. Phys. vol. 33(1), 1962: 156-163.

[13] Verhoeven, J. D. W. A. Spitzig, L. L. Jones, H. L. Downing, C. L. Trybus, E. D. Gibson, L. S. Chumbly, L. G. Fritzemeier and G. D. Schnittgrund. "Development of Deformation Processed Copper-Refractory Metal Composite Alloys." J. Mat. Engr. vol.12(2), 1990: 127-139.

[14] Bowden, F. P. and D. Tabor. The Friction and Lubrication of Solids, I. The Clarendon Press, 1950: 33-42.

[15] Krotz, P. D., W. A. Spitzig and F. C. Laabs. "High Temperature Properties of Heavily Deformed Cu-20%Nb and Cu-20%Ta Composites." Mat. Sci. Engr. A110, 1989: 37-47.

[16] Donaldson, A. L., T. G. Engel and M. Kristiansen. "State-of-the-art Insulator and Electrode Materials for Use in High Current, High Energy Switching." IEEE Trans. of Magnets. vol.25(1), 1989: 138-141.

[17] Rigney, D. A., M. G. S. Naylor and R. Divakar. "Low Energy Dislocation Structure Caused by Sliding and by Particle Impact." Mat. Sci. Engr. (81), 1986: 409-425.

PART IV.

ELECTRICAL SLIDING CONTACT BEHAVIOR OF Cu-Nb in situ COMPOSITES

ABSTRACT

The contact behavior of Cu-Nb in situ composites sliding against tool steel surfaces was studied in terms of the contact resistance and temperature rise. The effects of sliding speed, current density, Nb proportion, filament orientation, and true deformation strain of the composite were investigated. It was found that the contact resistance and temperature rise were much higher for sliding than for stationary contact. The contact resistance in sliding was affected by surface films, wear particles, and the bouncing action between sliding surfaces. It increased with lower electrical current density and increased with Nb proportion in the composite. The surface films formed on the composite and the tool steel disk surfaces were studied by optical and scanning electron microscopy of the specimen surfaces and their cross-sections and analyzed by X-ray diffraction. The oxides of the constituent elements such as NbO, CuO and Fe_2O_3 were found in the surface films and the material transfer from the tool steel to the composite specimen occurred by way of migration of these oxides.

INTRODUCTION

The purpose of an electrical sliding contact such as brush-slip ring assembly is to transfer electrical current from moving metal surfaces to stationary conductors. Such contacts are essential to many electrical rotating machines and their uses range from very large industrial machines, traction and automobile applications to fractional horse power applications of the type often found in households, even down to electrical toothbrushes. A considerable amount of effort has been expended in the research and development of these contacts, primarily those with increasing electrical currents and speeds to fulfill rather demanding requirements [1]. The contact behavior is crucial to all of these applications.

Contact resistance is composed of the bulk resistance of the contacting material (R_b), the constriction resistance (R_c), and the film resistance (R_f). The contributions to all these resistance components are affected by the sliding interface conditions such as wear particle accumulation, temperature rise and surface film structure. Walls [2] developed the high-speed, high-current copper finger brushes for pulsed homopolar generator service. He found that the effective contact resistance decreased with increasing current and leveled off at a very high current, and the contact resistance was higher at higher sliding speeds. Garshasb and Vook [3] also noted that the contact resistance tended to be lower at higher contact currents for Cu brush-Ag slip ring sliding electrical contacts. They attributed the decrease in contact resistance to the softening of the materials at the interface due to the increased heating at higher currents. Johnson and Schreurs [4] studied the effect of polarity on contact resistance and found that the resistance increased with contact time at the anode and decreased at the cathode. McNab [5] indicated that the contact resistance could

be reduced by subdividing the contact into a large number of independently loaded units. This led to the concept of multi-element brushes. Saka et al. [6] investigated the mechanism of electrical contact resistance between lightly-loaded fretting surfaces. They found that the increase in contact resistance of base metal contacts was due to the oxidation of metallic wear debris that was entrapped between sliding members. A base metal contact with modulated contact surface was shown to have a low electrical contact resistance. Reichner [7] proposed the pressure-wear theory for sliding electrical contacts in which the effects of nonuniform velocity, rotor eccentricity, multi-material brushes, and composite materials were considered. He proposed that in sliding electrical contact, nonuniform velocity, nonuniform material wear coefficient, or geometrically imposed nonuniform wear would produce a nonuniform contact pressure. The higher pressure regions of the interface would have lower electrical contact resistance and, therefore, would carry an increased current density.

Because of the superior combination of mechanical strength and conductivity [8, 9], deformation processed Cu-Nb in situ composites seem to be promising materials for sliding electrical contacts. The friction and wear studies on these composites sliding against O2 tool steel revealed [10] that their coefficients of friction decreased with increasing Nb proportion, and that the Cu-20%Nb composition had the best wear resistance, irrespective of whether the electrical current was passing or not through the sliding interface. The wear resistance of the composite with Nb filaments perpendicular to sliding plane was higher than that with parallel filaments and there was no significant effect of orientation on the coefficient of friction. In view of the above observations, it was decided to study in this work the contact behavior of Cu-Nb composites so as to evaluate them for sliding electrical contact applications.

The variables considered were sliding speed, current density, Nb proportion, filament orientation, and deformation processing strain. Surface and subsurface studies have also been made.

EXPERIMENTAL

The pin-on-disk wear tester was modified to supply electrical current through the sliding interface. The details related to this modification and the data acquisition system were reported earlier [10]. Using a DC power supply, a constant current was supplied across the sliding interface where the test specimen served as anode. The voltage drop between the test specimen and the pick-up member was measured. This voltage drop was used to calculate the contact resistance by Ohm's law. The contact resistance so calculated was actually the sum of the contact resistances of the two sliding surfaces and the bulk resistance of the steel disk.

The materials processing and specimen preparation were described earlier [10]. The test involved sliding between a composite pin and an O2 tool steel disk. The contact area of the pin was 1.6 $mm \times 4.5$ mm where 4.5 mm dimension was parallel to the sliding direction. The pin rode on the tool steel disk, 4 mm thick and 70 mm in diameter, in a track of 45 mm diameter. The Nb filaments in the pin were always oriented perpendicular to the sliding plane except for the case when the effect of Nb filament orientation was studied.

The temperature close to the sliding surface was measured. For this purpose, a type-T miniature thermocouple was inserted in a hole of 1.59 mm diameter to a distance of about 0.76 mm from the sliding interface and soft soldered in position. A digital voltmeter was used to measure the thermocouple electrical potential which was stored in the microcomputer. The temperature was calculated from the measured potential using the calibration data. A number of data such as the contact time, sliding distance, contact resistance, the coefficient of friction and temperature, were recorded in a data file and were later processed in a digital computer.

RESULTS AND DISCUSSION

Stationary Contact

In order to investigate the difference in contact resistance introduced by sliding, initially the contact resistance in a stationary contact was measured as a function of time and is shown in Figure 1. Here a Cu-20vol.%Nb pin specimen rested on the tool steel disk with a normal pressure of 0.68 MPa and an electrical current density of 2.89 MA/m^2. The contact resistance increased initially with increasing contact time and then decreased to a steady state value. Its magnitude was very low (on the order of 10^{-3} Ω) and the total change in contact resistance during 2 hour contact time was of the order of 10^{-4} Ω. The temperature also increased by about 11^oC in the initial 10 minutes but afterwards the change in temperature with time was very small. The initial increase in contact resistance occurred because of the growth of a surface film, which was caused by increased temperature. The presence of the surface film reduced the adhesion between asperities and so increased the constriction resistance R_C. It also increased the surface film resistance R_f and so the contact resistance was increased. Because of temperature rise in the initial stage, the asperities in contact were presumably softened slightly so that the real area of contact increased. This decreased the constriction resistance and so also the total contact resistance because the film resistance in this stage was practically unchanged.

Effect of Sliding Velocity

Figure 2 shows the variation in contact resistance for sliding between Cu-20vol.%-Nb sheet composite and a tool steel disk. The contact resistance was much higher

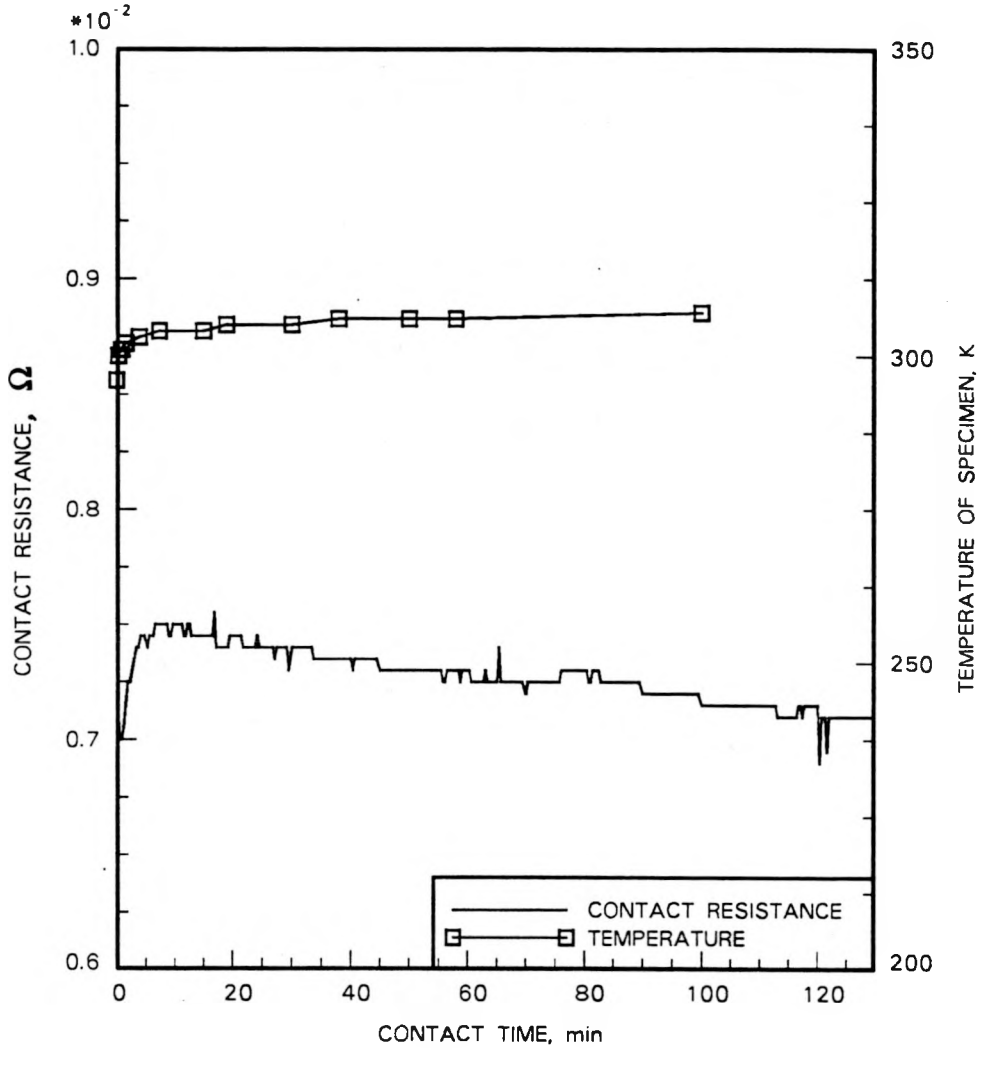

Figure 1: Variation of contact resistance and temperature for the stationary contact between Cu-20vol.%Nb pin and tool steel disk at a normal pressure of 0.68 MPa and electrical current density of 2.89 MA/m^2

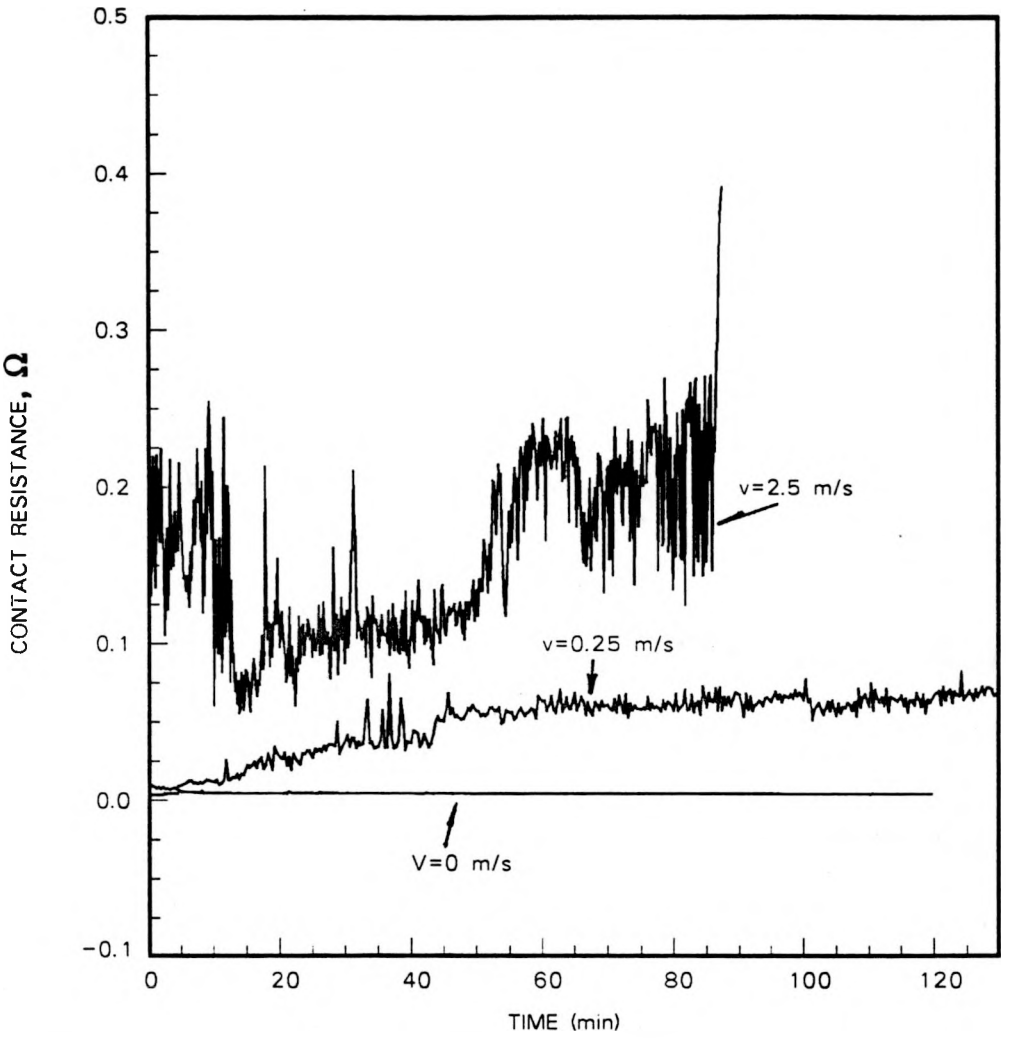

Figure 2: Variation in contact resistance with contact time and at different sliding speeds for the contact between Cu-20vol.%Nb pin and tool steel disk: normal pressure 0.68 MPa, electrical current density 2.89 MA/m^2

and it fluctuated much more during sliding than in stationary contact. At the sliding speed of 0.25 m/s, the contact resistance increased gradually with time and finally reached a steady state value after about 50 minutes. The sliding here was relatively smooth with no significant jumping between the contacting surfaces. The temperature in the contact area increased because of the frictional and electrical Joule heat so that the growth in the surface film occurred. This increased the contact resistance. During sliding, wear particles were generated so that the sliding surfaces were pushed apart. This reduced the contact area drastically and caused voltage flashes. These events accelerated the temperature rise and thereby increased the contact resistance significantly because of a rapid growth in film thickness. The steady state situation is reached when the growth in surface film thickness becomes negligibly small and the number of wear particles generated per unit time stays constant. At the higher sliding speed of 2.5 m/s, the contribution of wear particles to contact resistance was about the same as at the lower sliding speed of 0.25 m/s because there was no significant change in the wear rates at these two speeds [10]. There was a marked difference in temperature rise as the temperature measured at 2.5 m/s was $276^{o}C$ as opposed to $117^{o}C$ at 0.25 m/s. Because of the increased temperature rise at the higher sliding speed, the rate of oxidation increased and so the contribution of the oxide film to contact resistance increased. Moreover, there was more bouncing action between the sliding surfaces at the higher sliding speed so that the frequency and the intensity of voltage flashes increased. This contributed to the increase in temperature further and so also to the increase in contact resistance. The initial higher contact resistance at the higher sliding speed was due to jumpy contact and the larger fluctuations were due to intermittent contacts and occasional rupture of oxide film.

Effect of Current Density

The variation of contact resistance with sliding distance for two current densities is shown in Figure 3. As sliding distance increased, the contact resistance increased rapidly but then stabilized after sliding over a distance of about 0.5 km. The contact resistance at the higher current density was lower than that at the lower current density. Since the energy transferred across the contact interface is proportional to current, the temperature rise at the specimen surface was higher at the higher current density. This temperature rise accelerated the film formation and so increased the film resistance. It also softened the contact asperities so that the contact area increased and the constriction resistance decreased. In addition, the film resistance was also affected by the energy level transferred across the interface. Holm [11] studied the tunnel effect of a thin film in metallic contact and observed that tunnel resistivity decreased as the voltage across the film increased. Thus, with increased current density, the tunnel resistance and the constriction resistance decreased and so also the contact resistance decreased even though the surface film thickness increased.

Effect of Nb Proportion

The variation of contact resistance with sliding distance for three Cu-Nb composites along with pure Cu is shown in Figure 4. The contact resistance of pure copper was lower than that of Cu-Nb composites throughout the entire period of sliding. As for Cu-Nb composites, the contact resistance increased with increasing sliding distance and stabilized after sliding over a distance of about 1 km. The contact resistance of Cu-30%Nb was much higher than for both Cu-10%Nb and Cu-20%Nb, whereas the contact resistance of Cu-20%Nb was fairly close to that of the

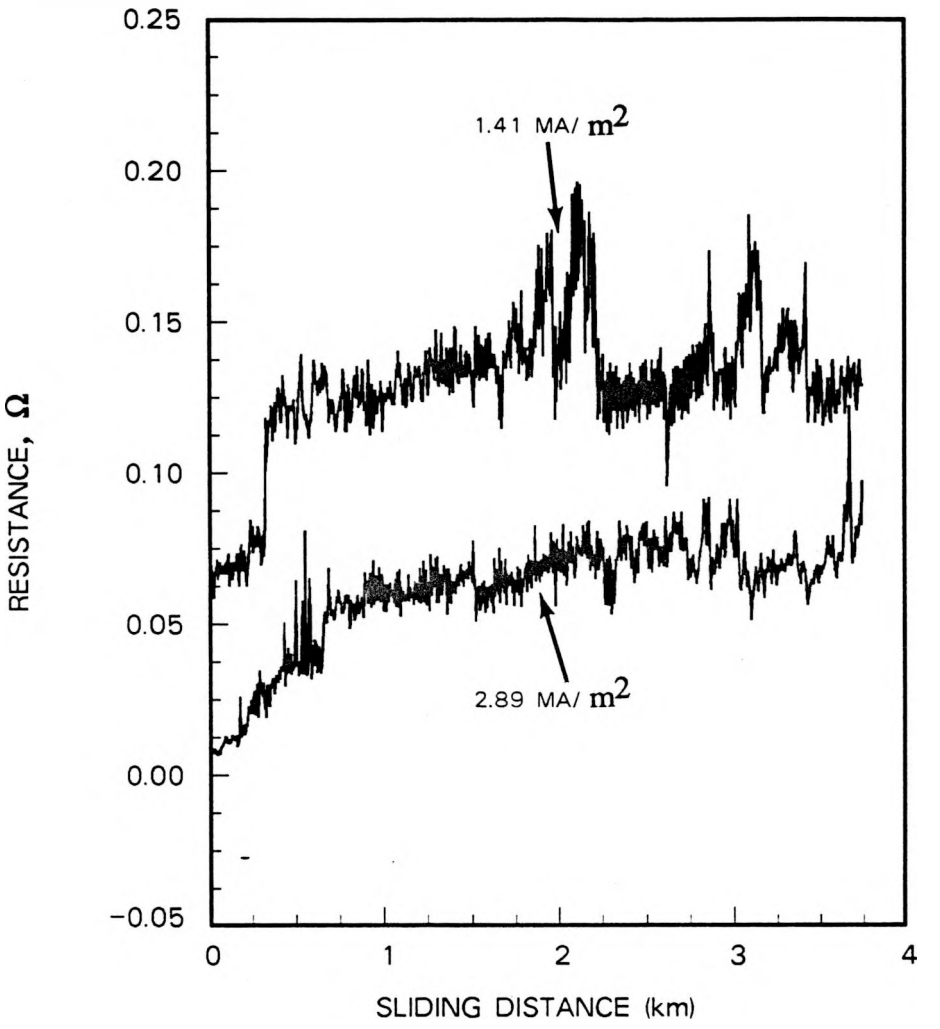

Figure 3: Contact resistance versus sliding distance for Cu-20vol.%Nb sheet composite sliding against a tool steel disk at two current densities: sliding speed 0.25 m/s, normal pressure 0.68 MPa

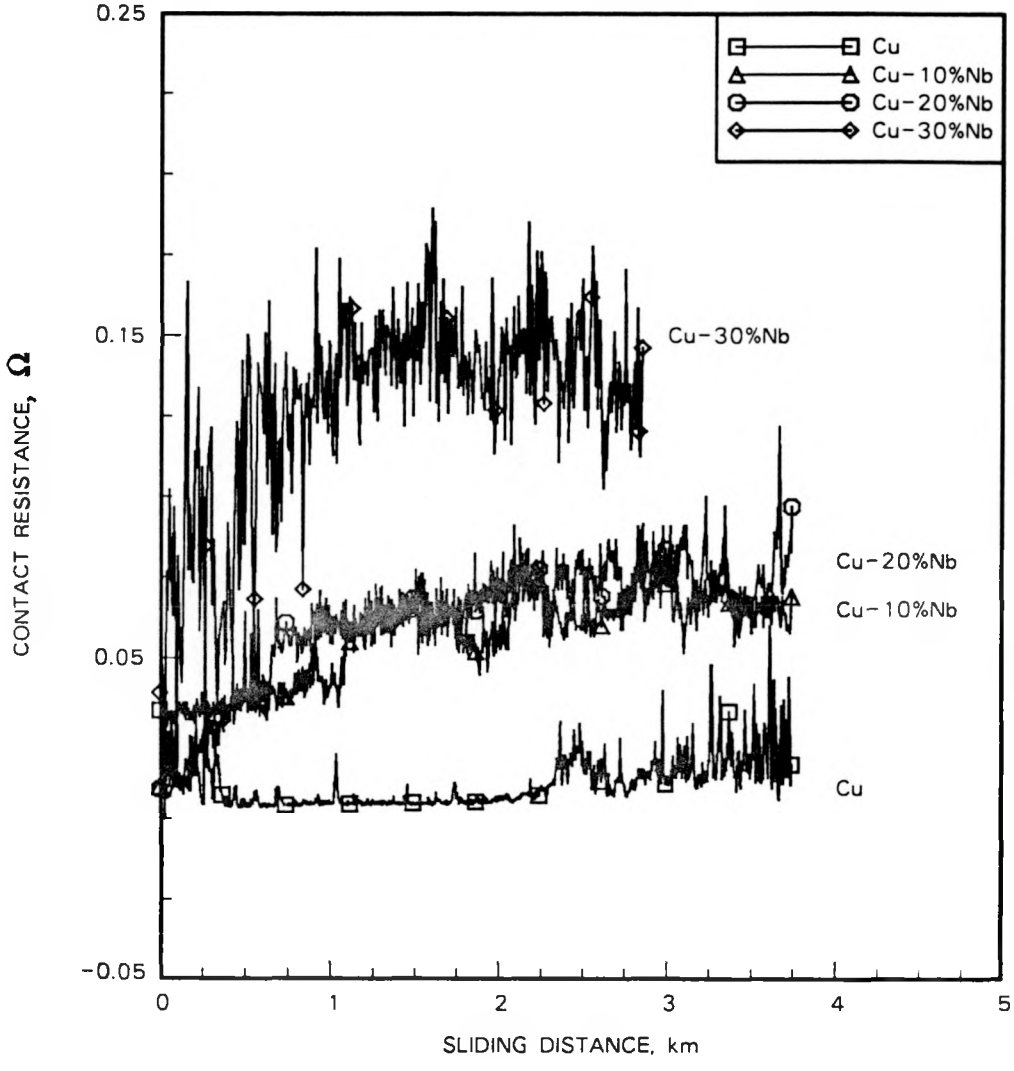

Figure 4: Variation of contact resistance with sliding distance for Cu and three Cu-Nb composites sliding against tool steel disk: sliding speed 0.25 m/s, normal pressure 0.68 MPa, and electrical current density 2.89 MA/m^2

Cu-10%Nb. The fluctuations in the contact resistance of Cu-30%Nb were also greater. These variations in contact resistance may be explained in terms of the changes in the conductivities of contacting composites, and the film and the constriction resistances. Based on the International Annealed Copper Standard (IACS), the conductivity of pure copper is $102\%IACS$ and that of niobium is only about $13.2\%IACS$ [12]. Thus, with increasing amounts of Nb, the resistivity of the composites was increased. Therefore, the contribution to contact resistance from the resistance of bulk materials was much higher in the case of Cu-Nb composites. With increasing Nb proportion, the temperature rise as measured in the specimen was also higher. This produced a thicker surface film which increased the film resistance. Since the hardness of the composites increased with increasing Nb proportion, the contact area decreased and so the constriction resistance increased. Thus, all of the above factors contributed to the increase in contact resistance with increasing Nb proportion.

Ordinarily, Cu-20%Nb would be expected to have higher contact resistance than that of Cu-10%Nb. That was not the case here because of the role of wear particles. Cu-20%Nb had the best wear resistance among the three composites with and without electrical current, as shown in Figure 5. Thus, the number of wear particles entrapped between the sliding surfaces for Cu-20%Nb was less than for the other two. It seems therefore reasonable to assume that the effect of wear particles in increasing the contact resistance of Cu-20%Nb was less than for Cu-10%Nb and Cu-30%Nb. This in effect helped in reducing the contact resistance of Cu-20%Nb to the level of Cu-10%Nb.

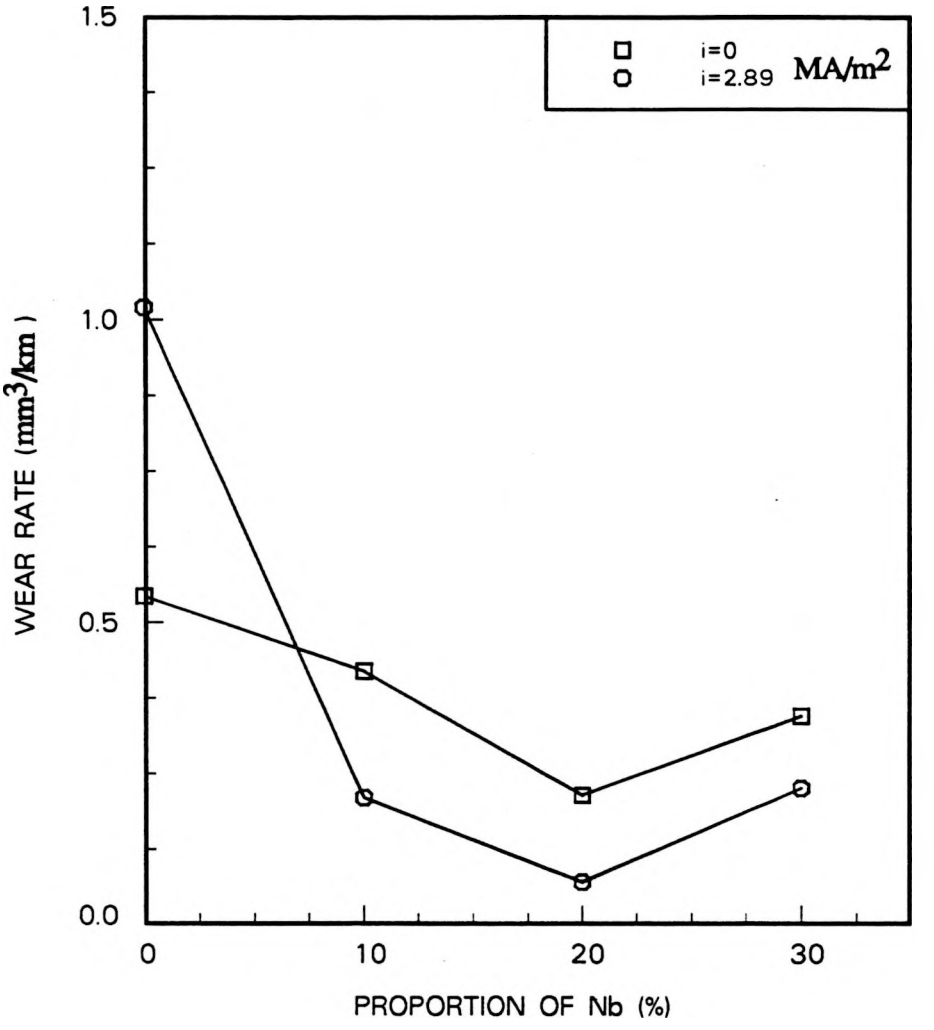

Figure 5: Variation of wear rate with volume proportion of Nb in Cu-Nb composites with and without electrical current

Effect of Nb Orientation

Figure 6 shows the variation in contact resistance and temperature rise with contact time for stationary and sliding contacts between Cu-20%Nb composites and tool steel disks and for two filament orientations in the composites. In the case of stationary contacts, the contact resistance and the temperature rise were very small and the difference between the two orientations was minimal. In the case of sliding, the contact resistance and the temperature rise for the perpendicular filament orientation were higher than for the parallel orientation.

In the initial stage, the contact resistance of the composite with Nb filaments perpendicular to the sliding plane was higher than that for the parallel orientation. This suggests that constriction resistance may be a dominant factor affecting contact resistance, since at this stage the wear particles and surface film were not fully developed yet. Because of the load-supporting function of Nb filaments, the composite with the perpendicular filament orientation had smaller real contact area than that with parallel orientation. Therefore, the contribution of constriction to contact resistance was larger for the perpendicular orientation. There should not be expected significant differences from filament orientation in the surface film growth rate and the bulk conductivity. In view of these factors, since the composite with perpendicular filament orientation had higher constriction resistance, it also had higher contact resistance than that with parallel orientation.

Effect of True Deformation Strain

Figure 7 shows the variation of contact resistance and specimen temperature with sliding distance for Cu-20%Nb composites with true deformation strains of 3.47

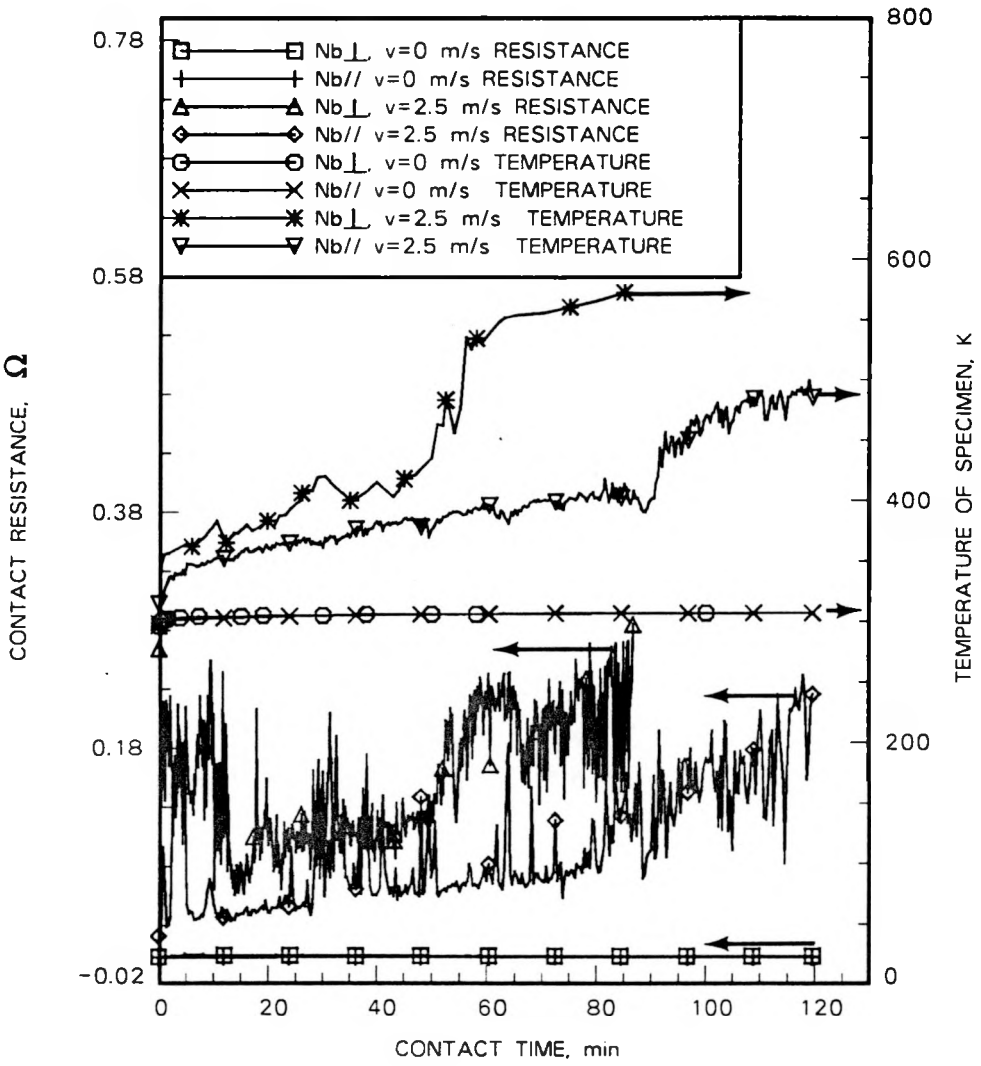

Figure 6: Variation of contact resistance and specimen temperature with contact time for stationary and sliding contacts and for perpendicular and parallel filament orientation in Cu-20%Nb sheet composites: normal pressure 0.68 MPa, electrical current density 2.89 MA/m^2

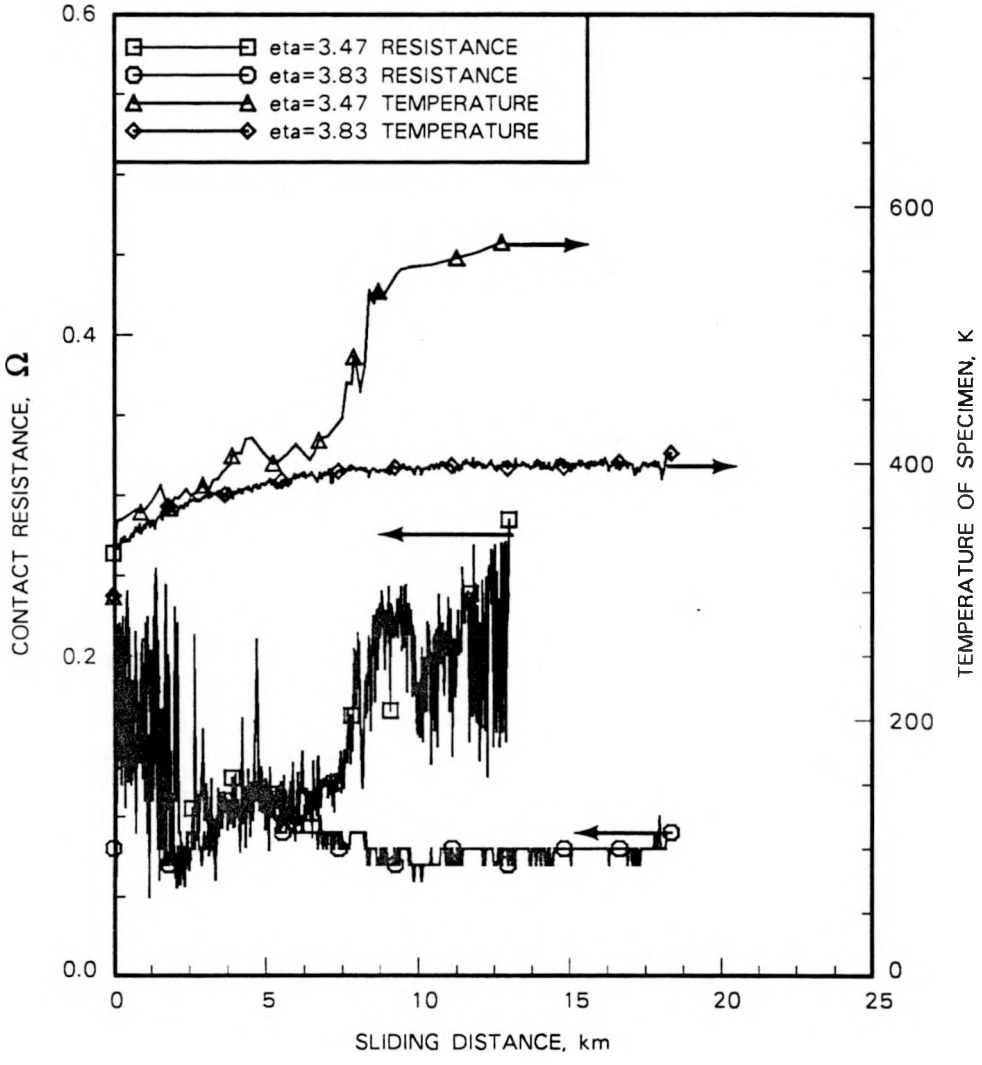

Figure 7: Variation of contact resistance and specimen temperature with sliding distance for Cu-20vol.%Nb sheet composites with true deformation strains of 3.47 and 3.83, sliding against tool steel at a sliding speed of 2.5 m/s, normal pressure of 0.68 MPa and electrical current density of 2.89 MA/m^2

and 3.83 for the sliding conditions described in the figure. The contact resistance for the two true deformation strains did not deviate until the sliding distance of 6 km. After that, the composite with the true strain of 3.47 had higher contact resistance than the other composite and the fluctuation in its contact resistance was also much larger. This difference in contact resistance is believed to be related to "dust wear" [1] in which entrapped foreign dust particles or the wear particles created at sliding interface drastically reduce the real area of contact and cause severe voltage flashes. As reported earlier [10], the composite with $\eta = 3.47$ had a lower wear resistance than that with $\eta = 3.83$ in the presence of electrical current. This implies that the rate of generation of wear particles in the lower strain composite was higher. This increased the possibility of the entrapment of more wear particles. As a result, both the contact resistance and the temperature rise were higher in the composite with lower deformation strain.

Surface Analysis

In order to study the structure of the surface film formed during the sliding process, the worn specimens were sectioned after the worn surface was plated with nickel to prevent damage of the surface features. As seen in Figure 8, the presence of electrical current promoted the formation of a much thicker surface film. The oxide film on the specimen surface involved in electrical sliding was about 10-15 μm thick compared to 2-3 μm in non-electrical sliding. The contact resistance increased as the thickness of the surface film increased during sliding. In some subsurface regions affected by sliding, the surface film was broken into pieces and the fragments were pressed into the deformed subsurface layer (Figure 9). This led to an additional

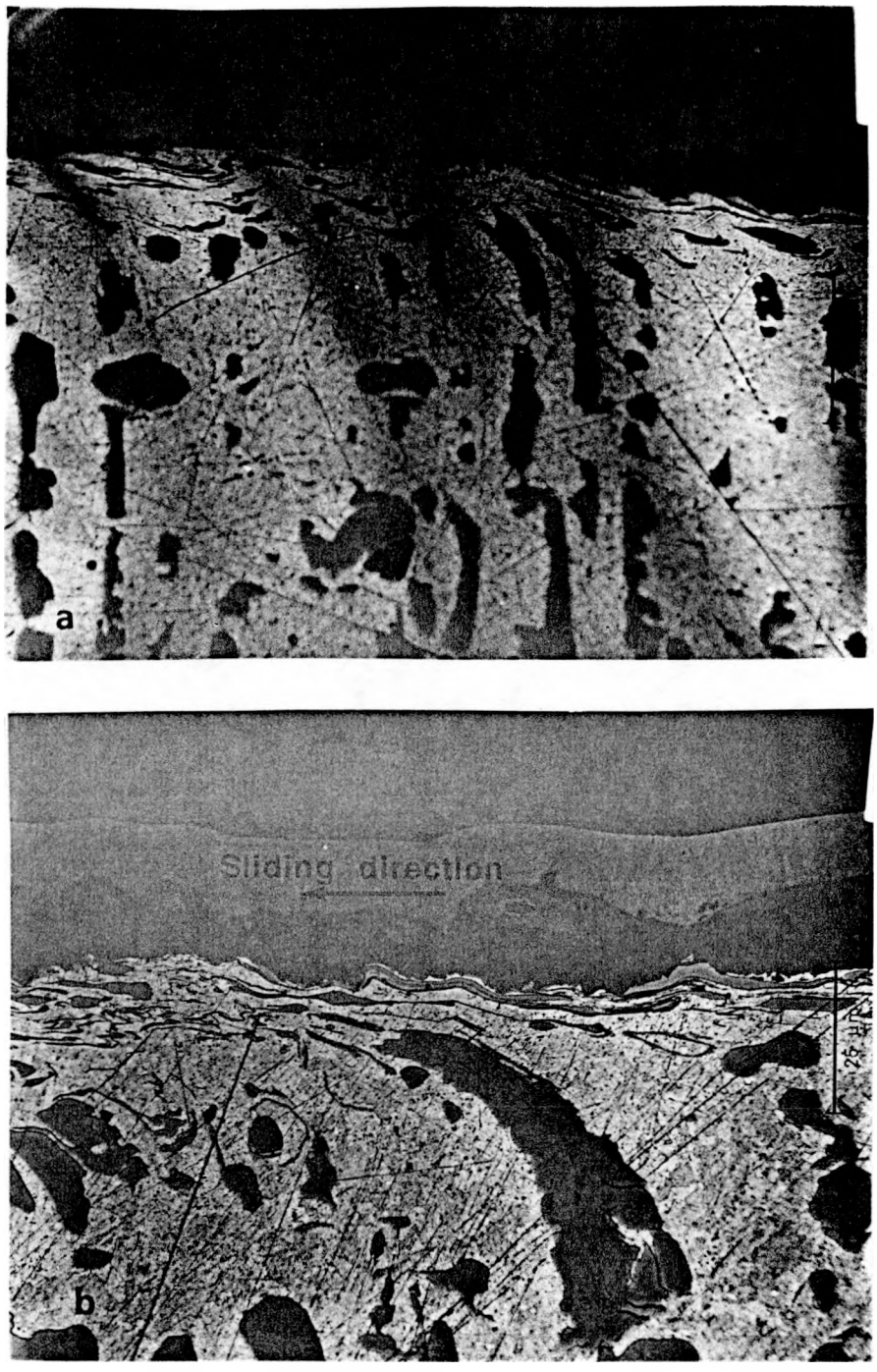

Figure 8: Cross-sections of Cu-20vol.%Nb sheet composites tested in wear: (a) non-electrical sliding; (b) sliding with the electrical current density of 2.89 MA/m^2

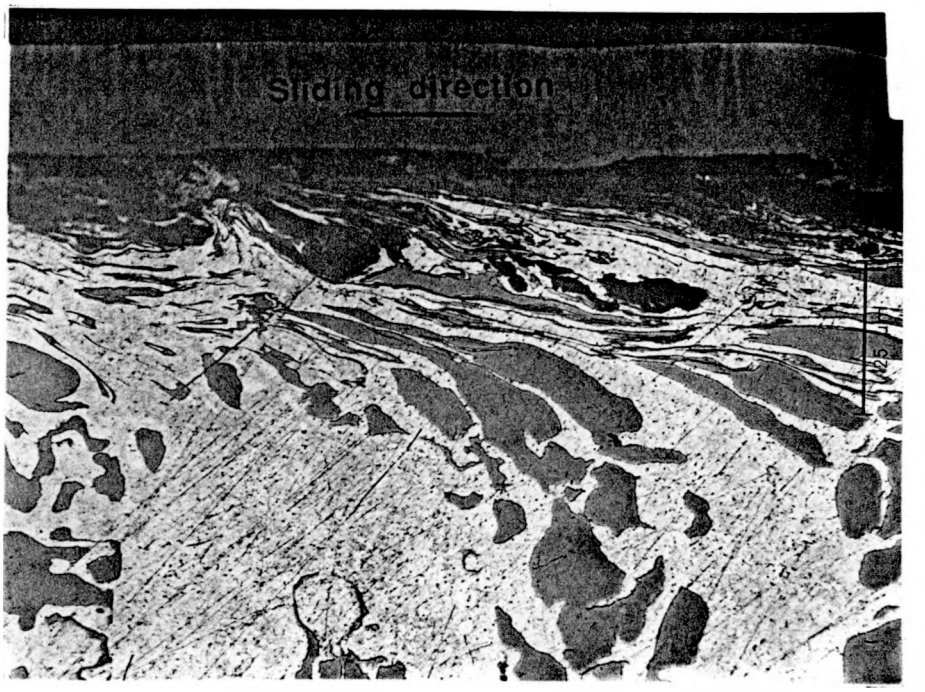

Figure 9: Cross-section of Cu-20vol.%Nb slid against tool steel in the presence of electrical current

decrease in the conductivity of the subsurface layer of the composite and therefore increased the electrical contact resistance during sliding.

The chemical structure of the surface film was analyzed using an X-ray diffraction. Figure 10 shows the X-ray diffraction spectra of the surface films formed on the Cu-20%Nb composite during sliding on the tool steel disk both with and without electrical current. It is seen that both surface films are composed of Cu, Nb, CuO, NbO and Fe_2O_3. The electrical resistivity data for these film constituents are given in Table 1. It should be noted that the resistivity of metal elements is very low, being of the order of 10^{-8} Ωm. NbO is also metallic because it has a low resistivity which is linearly temperature dependent [14]. Copper monoxide (CuO) is a semiconductor ($\rho = 6000$ Ωm) and Fe_2O_3 is resistive in nature with resistivity up to 10^6 Ωm. Therefore, among these oxides formed on the sliding surface, Fe_2O_3 contributed the most to the increase in contact resistance.

Table 1: Electrical Resistivity of Film Constituents

Substance	Resistivity, $\rho(\Omega m)$
Cu	1.534×10^{-8} [13]
Nb	12.5×10^{-8} [13]
NbO	10^{-7} [14]
CuO (Melaconite)	6000 [15]
Fe_2O_3 (Hematite)	$10^2 - 10^6$ [16]

The relative amount of Fe_2O_3 in the surface film was much larger in electrical sliding than in non-electrical sliding. That is, the application of electrical current helped material transfer from tool steel disk to the Cu-Nb composite specimen surface. It also contributed to the increased contact resistance of the surface film on the Cu-Nb surface where Fe_2O_3 increased the film resistance directly and also by

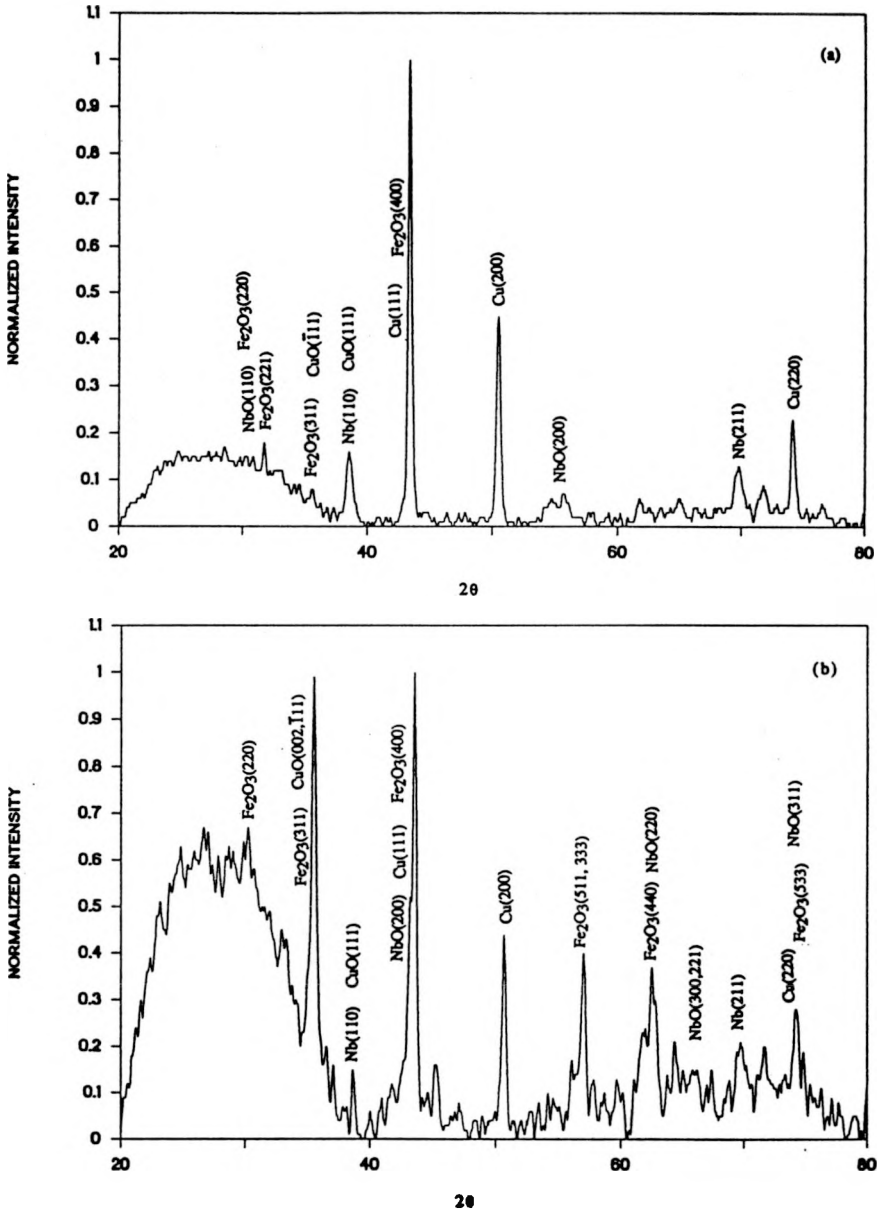

Figure 10: X-ray diffraction spectra of worn surface of Cu-20vol.%Nb slid against tool steel: (a) non-electrical sliding; (b) electrical sliding with a current density of 2.89 MA/m^2

alloying with the Cu-Nb composite subsurface layer. Because of increased contact resistance, the passage of electrical current during sliding increased the temperature rise and caused voltage flashes and arcing on the sliding surfaces. All of these factors increased the rate of oxide film formation on the sliding surfaces.

Another interesting finding from the X-ray diffraction spectra is that no diffraction peak was observed for elemental Fe and only Fe_2O_3 was detected. It suggests that oxide film was formed quickly on the tool steel surface before any material transfer occurred. In other words, materials transfer occurred presumably by the movement of oxides between the mating materials. Wear debris was presumably formed from the oxides on surfaces. Because of the continuous supply of oxygen from surrounding air, the surfaces were always covered with oxide films which contributed to increased contact resistance.

The worn surface of the Cu-20%Nb composite was studied by scanning electron microscopy. Figure 11 shows a SEM micrograph of the worn surface and an energy dispersive spectrum of a wear particle on the surface. It shows that, in addition to oxidation, electrical arcing caused melting or softening of the surface. Because of craters, the surface became more irregular. This increased the gap in discrete spots between mating surfaces and thereby resulted in voltage flashes and more arcing. The EDS spectrum showed that the wear particle surface contained Fe, Si, Mn and Cr in addition to Cu and Nb. These elements obviously came from the tool steel surface.

The sliding track on the tool steel disk was also studied. The track was severely burnt or oxidized and had a black oxide layer on the surface. Very little Cu color could be seen on the track formed with electrical sliding in contrast to the copper-

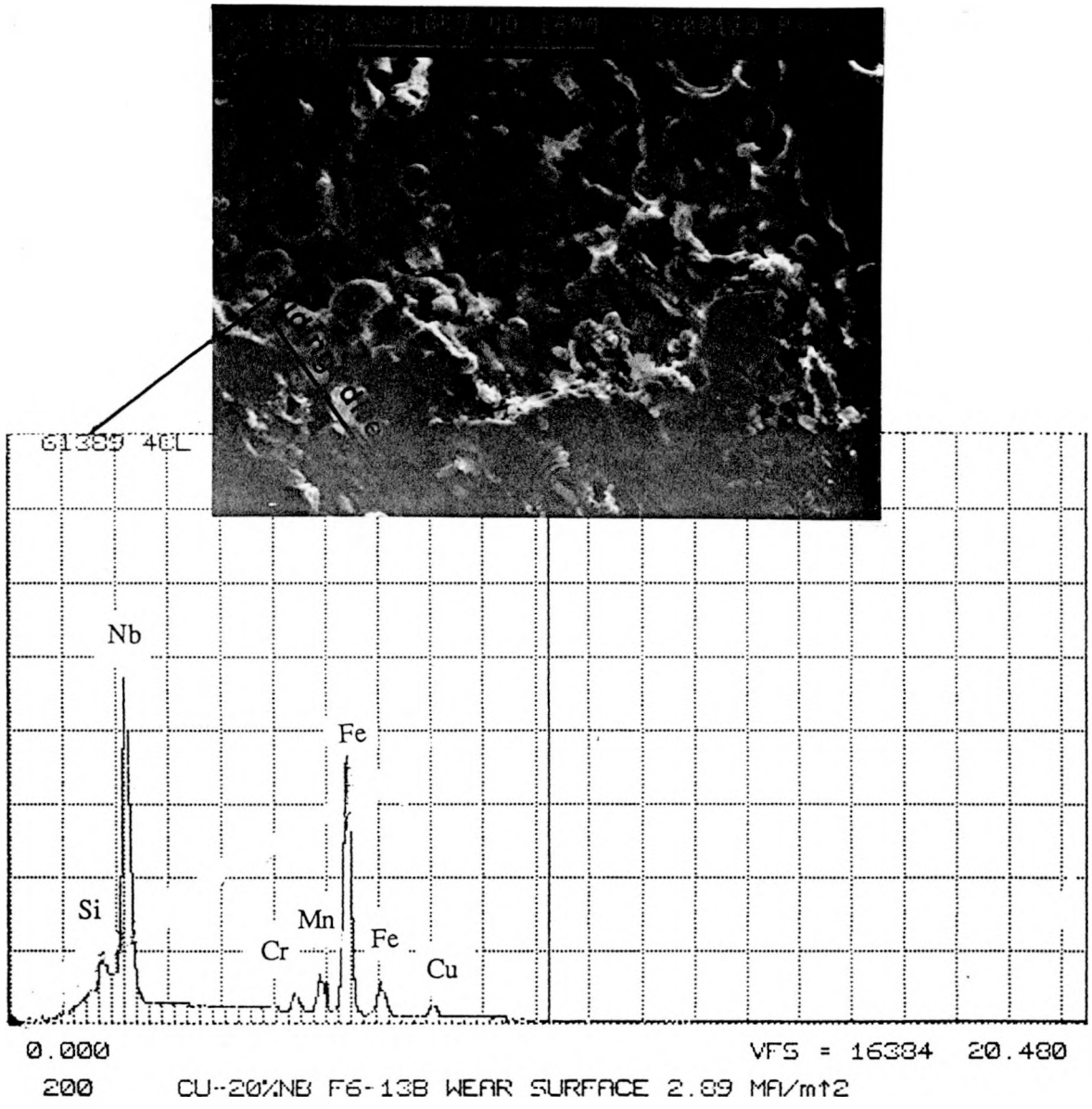

Figure 11: SEM micrograph of the worn surface of Cu-20%Nb pin involved during sliding against a tool steel disk in the presence of electrical current, and EDS spectrum of the wear particle marked on the diagram

colored sliding track for non-electrical sliding. The track for electrical sliding had also lot more grooves than could be seen on the track for non-electrical sliding. Figure 12 shows the SEM micrograph of the sliding track on the tool steel disk surface for electrical sliding and the EDS spectrum of the particles in the surface film. Only the trace amounts of Cu and Nb are seen in the spectrum. During transfer of electrical current across the sliding interface, the temperature on the tool steel disk surface increased much more than on the Cu-Nb surface because of the considerable difference in the conductivities of the two materials. The material transfer from tool steel to the composite made the composite surface layer stronger. As a result of these two factors, the transfer layer on the steel disk was worn out as revealed by the presence of grooves on the disk surface. Consequently, the transfer film from Cu-Nb composite specimen was not able to stay permanently on the sliding track on the disk surface. This was different from the case of non-electrical sliding where the transfer film was not subjected to this kind of abrasion. The surface of tool steel track was ragged and covered basically by the oxides of the elements in the tool steel. This kind of surface structure provided a highly resistive film for the contact system because all the oxides had higher electrical resistivities than that of the elements. In other words, the oxide films on both the mating surfaces contributed to the increase in contact resistance of the electrical sliding system.

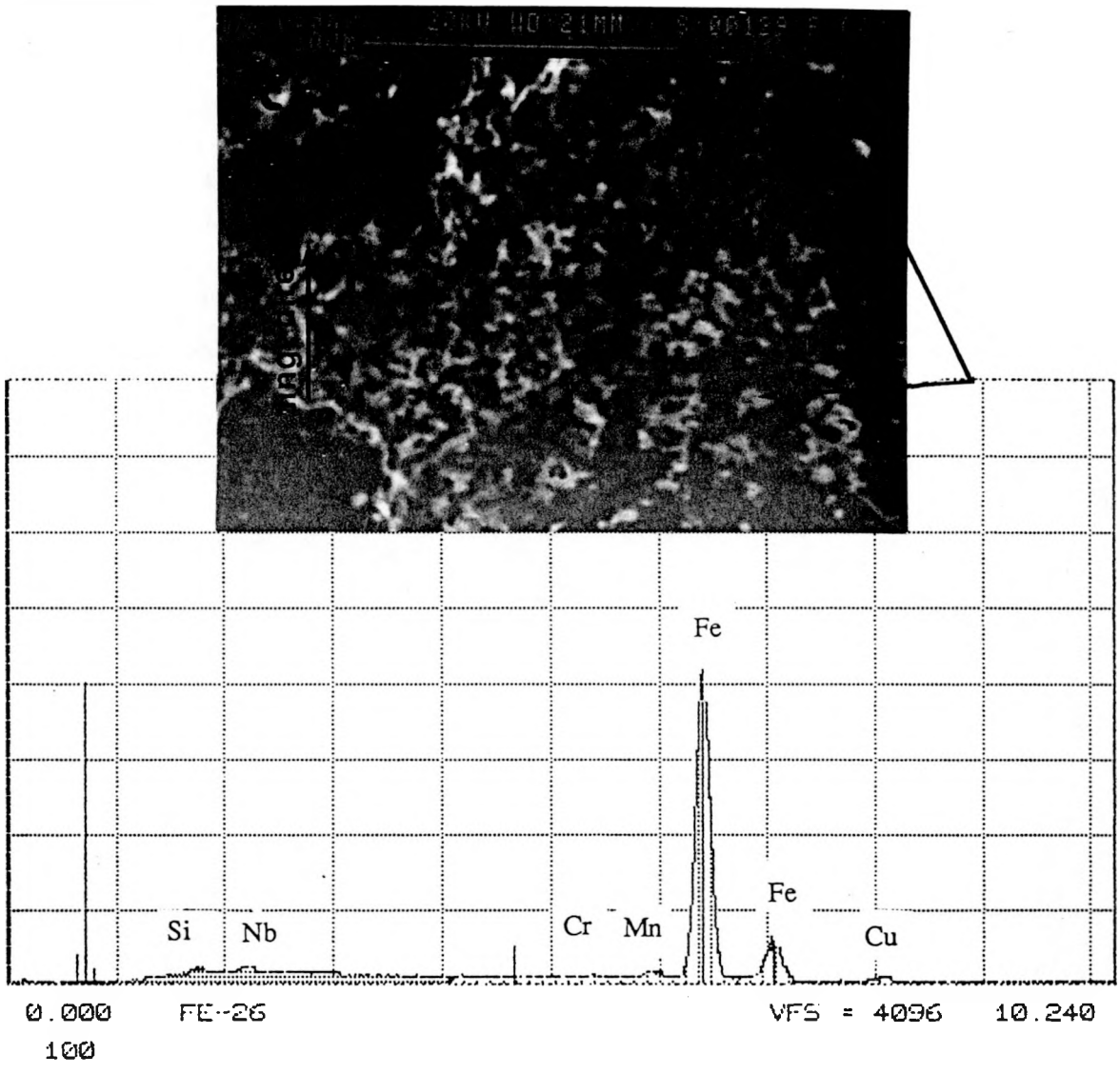

Figure 12: SEM micrograph of the sliding track on tool steel disk generated in electrical sliding, and the EDS spectrum of surface film

CONCLUSIONS

The investigations of the contact between Cu-Nb composite and tool steel disk led to the following conclusions:

1. The contact resistance in sliding was much higher than that in stationary contact.

2. At the lower sliding speed of 0.25 m/s, the contact resistance was basically controlled by the growth of a surface film and wear particle accumulation. At the high sliding speed of 2.5 m/s, the bouncing action between the sliding surfaces which generated more voltage flashes became the additional governing factor.

3. The contact resistance was lower for higher current density.

4. With Nb filaments in the composite being perpendicular to the contact plane, the contact resistance and the temperature rise were higher than when the filaments were parallel.

5. The contact resistance and the temperature rise were higher for the composite of lower true deformation strain.

6. Oxidation was a dominant factor affecting the contact resistance in electrical sliding. The thickness of the oxide film was much higher in electrical sliding than in non-electrical sliding.

7. There was evidence of melting on the Cu-Nb surface involved in electrical sliding.

8. The wear particles were formed by mechanical alloying of the elements, namely Fe, Si, Mn, Cr, Cu and Nb, which were present in the mating members.

9. The contact resistance was affected by surface oxide films, materials transfer, wear particles, and the bouncing action between the surfaces.

REFERENCES

[1] Johnson, J. L. "Sliding Monolithic Brush System for Large Currents." Electrical Contacts-1986. IEEE Holm Conference on Electric Contact Phenomena, Oct. 1986, Boston: 3-17.

[2] Walls, W. A. "High-Speed High-Current Copper Finger Brushes for Pulsed Homopolar Generator Service." IEEE Trans. vol. CHMT-9(1), 1986: 117-123.

[3] Garshasb, M. and R. W. Vook. "Fundamental Analysis of Cu Brush-Ag Slip Ring Sliding Electrical Contacts." IEEE Trans. vol. CHMT-9(1), 1986: 23-29.

[4] Johnson, J. L. and J. Schreurs. "High Current Brushes VIII: Effect of Electrical Load." Wear 78, 1982: 219-232.

[5] McNab, I. R. "Recent Advances in Electrical Current Collections." Wear 59, 1980: 259-276.

[6] Saka, N., M. J. Liou and N. P. Suh. "The Role of Tribology in Electrical Contact Phenomena." Wear 100, 1984: 77-105.

[7] Reichner, P. "Pressure-Wear Theory for Sliding Electrical Contacts." IEEE Trans. vol.CHMT-4(1), 1981: 45-51.

[8] Bevk, J., J. P. Harbison and J. L. Bell. "Anomalous Increase in Strength of In Situ Formed Cu-Nb Multifilamentary Composites." J. Appl. Phys. 49(12), 1979: 6031-6038.

[9] Spitzig, W. A., A. R. Pelton and F. C. Laabs. "Characterization of the Strength and Microstructure of Heavily Cold Worked Cu-Nb Composites." Acta Metall. vol. 35(10), 1987: 2427-2442.

[10] Bahadur, S., P. Liu and J. D. Verhoeven. "Application of Cu Refractory Metal in situ Composite Alloys for Electrical Sliding Contacts." Final Report. Center for Advanced Technology Development, Iowa State University, Ames (1990): 61-143.

[11] Holm, R. Electric Contact, Theory and Applications (4th edition). Springer-Verlag, 1967: 118-134.

[12] Metals Handbook (9th Edition). vol.2, ASM, Metals Park, Ohio (1978): 778.

[13] Weast, R. C., D. R. Lide, M. J. Astle and W. H. Beyer. CRC Handbook of Chemistry and Physics (70th edition). CRC Press, Inc., Boca Raton, Florida, 1990: F-146-147.

[14] Tallal, N. M. (editor) Electrical Conductivity in Ceramics and Glass. Marcel Dekker, Inc., New York, 1974: 380-384.

[15] Carmichael, R. S. CRC Handbook of Physical Properties of Rocks. CRC Press, Inc., Boca Raton, Florida, 1982: 231.

[16] Shuey, R. T. Semiconducting Ore Minerals. Elsevier Scientific Publishing Company, New York, 1975, pp357-358.

PART V.

ARC EROSION BEHAVIOR OF Cu-15%Nb and Cu-15%Cr in situ COMPOSITES

ABSTRACT

The arc erosion behaviors of Cu-15%Nb and Cu-15%Cr in situ composites were studied for both the low-energy make-and-break contact and the high-energy stationary arcing gap configuration. For low-energy make-and-break contacts, a computerized test set-up was developed, while the high-energy pulsed power stationary arcing tests were performed in the Mark VI facility at Texas Tech University, Lubbock. The items studied included the variation in contact resistance for make-and-break contacts, arc erosion at both energy levels, and materials response to arc erosion. The surface films formed in the make-and-break operation were analyzed by X-ray diffraction techniques, and the eroded surfaces and arc mechanisms were studied by scanning electron microscopy. It was inferred that in low-energy contacts, oxidation was the major cause for the deterioration of electrical contacts while melting was the major failure mode in high-energy contacts. The contact resistance of Cu-15%Nb was much lower than that of Cu-15%Cr. The arc erosion resistance of Cu-15%Nb and Cu-15%Cr was higher than that of the commercially used Cu-W composite in stationary arc erosion tests.

INTRODUCTION

There are two types of electrical contacts: make-and-break contact in which one contact member moves perpendicularly to and from another contact surface, and sliding contact in which tangential motion between the contact surfaces is involved. In both electrical contacts, arcing is a significant factor in governing the life of contacts. For make-and-break contacts, arcing takes place when contacts are in the process of establishing a current flow (i.e., making) or interrupting the flow of current (i.e., breaking). In sliding electrical contacts, arcing occurs because of unsteady contact which reduces the normal load and contact area and even causes the contact members to separate. The arc is actually a gaseous discharge involving electrons, metal vapors and ions. It is characterized by a high current density in the arc column and high temperature [1]. Because of the high temperature and mass flow, the contact surface is severely corroded and eroded, which results in erratic contact resistance, higher temperature and material loss. Therefore, a contact material should have high electrical/thermal conductivity, high melting point, and high resistance to environmental reaction, as well as high arc erosion resistance to maintain contact integrity.

Arcing erosion in contacts has been known for a long time, but the understanding of the erosion mechanisms and the erosion behavior of different materials is far from being satisfactory. Michal and Saeger [2] documented that the contacts of $AgCdO, AgNi$ and $AgSnO_2$ in DC load gained material at the cathode and lost at the anode. A continuous arc duration generally consists of two parts: the metallic phase arc for low current and the gaseous phase arc for high current [3]. Sone and Takagi [4] studied the influence of metallic phase arc discharge on contact performance and showed that the contact resistance increased when the arc duration in the

metallic phase arc region grew, and it remained high and almost constant after the arc reached the transition border to the gaseous state. They proposed that the material loss and transfer were log-proportional to the arc duration and this relationship was good irrespective of the air pressure condition. Shen and Gould [5] studied the contact surface, cross-section and debris, in order to understand the erosion modes of $AgCdO$ and $Ag\text{-}(Sn, In)O$ materials made by the internal oxidation method. They observed that the internally oxidized $Ag\text{-}(Sn, In)O$ material was more brittle than $AgCdO$ made by the same method and that the fabrication method of the contact material was one of the important factors influencing the erosion mode. Donaldson et al. [6] studied the arc erosion behavior of Cu-Nb composite of low true deformation strain at high currents and high energy transient arcs and indicated that the Cu-Nb composite had lower erosion rates than the commercially used Cu-W composite.

The sliding contact behavior, as well as the friction and wear behaviors of Cu-Nb composites in electrical sliding were studied by the authors earlier [7]. It was shown that the Nb filaments in the composite increased the wear resistance of Cu-based composites in both the electrical and non-electrical sliding. The refractory Nb filaments kept the adjacent Cu matrix from being further melted and eroded. The arc erosion characteristics of these composites were studied by scanning electron microscopy of the surfaces worn in electrical sliding as bouncing and unsteady contacts always occurred during sliding thereby producing arcing. As an extension of the above work, it is intended in this work to study the arc erosion behavior of Cu-15%Nb and Cu-15%Cr composite materials. The study involved the investigation of electrical contact resistance and the material response to arc erosion in view of the changes in surface structure.

EXPERIMENTAL

Materials

Based on our earlier work [7] which revealed that the sliding wear resistance in an electrical field increased with deformation strain, it was decided to study the arc erosion behaviors of Cu-15%Nb and Cu-15%Cr also at a high deformation strain. In order to achieve a high true strain, the bundling technique as described below was used. Initially, the material was cast into an ingot of 70.6 *mm* diameter by consumable electrode arc melting [8]. The ingot was put in a pure Cu can which was evacuated and sealed under vacuum. It was then extruded in the form of a hexagonal wire. The copper jacket was later etched away by using a $50\% HNO_3$ aqueous solution. A total of 72 hexagonal wires were bundled and placed in another pure Cu can. This can was further extruded to provide rods of smaller sizes. The outside pure copper jacket was either machined off or etched away. These rods were used for electrode specimens. A pair of electrodes were made of identical materials. The cylindrical contacts with a diameter of 6.35 *mm* were used for low-energy arcing contact tests and the hemispherical electrodes of 12.7 *mm* diameter for high-energy stationary arc tests. The Nb or Cr filaments in all of these specimens were oriented parallel to the direction of electrical current flow.

Test Facility

Low-energy arcing contact test set-up In order to measure the contact resistance variation and arc erosion rate during make-and-break operation, the test set-up as shown in Figure 1 was developed. Here, a cylindrical specimen, 6.35 *mm*

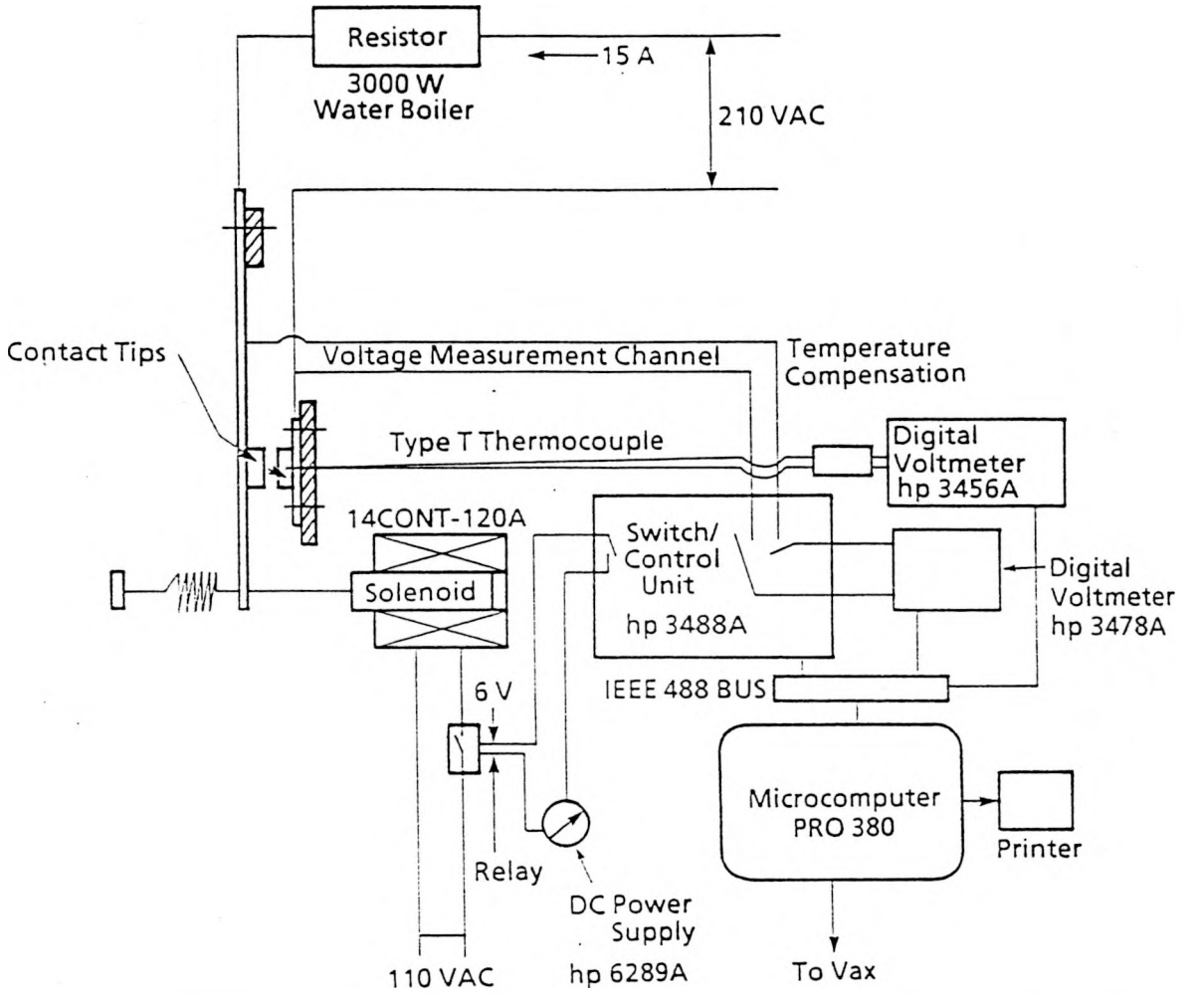

Figure 1: Arc erosion and contact test facility

diameter and 2.5 mm long, was riveted to a flat piece of Cu-10%Nb, 0.51 mm thick, 20 mm wide and 105 mm long. This flat piece served as the conducting spring for the contact pair while the specimen acted as the moving tip. The latter was pulled by a solenoid so as to close and open the circuit. The electrical circuit included a 3000 W resistor in the form of a water boiler for power consumption. The circuit was energized with 210 V AC and carried a current of 15 A.

The solenoid was activated by 110 V AC power which was switched on and off by a circuit relay. The relay was configured with a DC power supply of 6 V. Its operation was controlled by a switch/control unit with the help of a general purpose relay card which received commands from a microcomputer. Once the computer sent a command to the switch/control unit to close the circuit, the relay was activated for solenoid operation. The solenoid then pulled the spring thereby establishing contact between the moving and stationary tips. The computer then sent a command to the switch/control unit to open the circuit. The system now operated in reverse so that the contact was opened. The opening and closing duration for each cycle could be controlled by the computer. A time span of 2 s was used in this study, i.e., the contacts were closed and opened every two seconds. The contact tests were performed in a dry atmosphere. The arc erosion rate was determined from the mass loss of the pair of contact tips.

While the two contact tips were in contact, the contact voltage was measured by a digital voltmeter controlled by a computer through an IEEE-488 interface bus. The contact resistance was calculated by Ohm's law from the voltage drop across the contact interface. A type-T miniature thermocouple, inserted to a depth within 2 mm of the contact surface, and a digital voltmeter were used to measure temperature

in the vicinity of the stationary contact tip. The contact resistance and temperature data were printed and stored in a file. This data file was transferred to a digital computer for processing after the test was finished.

High-energy pulsed power stationary arcing test In order to evaluate the electrode arc erosion at high currents, the Mark VI facility [1] [6], was used to simulate typical spark gap switching applications. It consisted of a resistively-charged capacitor bank connected in series to a water-cooled test switch. When the capacitor bank was charged to the level of the self-breakdown voltage of the spark gap, it discharged through the test gap thereby producing a slightly damped oscillatory current. The discharge current was varied by changing the system capacitance. The operating parameters of this system are given in Table 1.

Table 1: Mark VI Facility System Parameters

Peak voltage	45 kV
Peak current	750 kA
Max. energy per shot	1.6-48 kJ
Effective charge transfer per shot	1-30 $Coul$
Capacitance	2-60 μF
Ringing frequency	50-250 kHz

For tests in this set-up, the electrodes in the form of 12.7 mm diameter and 60 mm long cylinders, with one end hemispherical and another flat, were machined from Cu-15%Nb and Cu-15%Cr bundled composite rods. A pair of stationary electrodes was positioned in the test rig with a gap of 10 mm [9]. The tests were performed in ambient atmosphere. The number of shots was varied from 50 to 1500. The arc erosion rate was evaluated as the volumetric loss of electrode material per shot.

[1] At Texas Tech University, Lubbock

RESULTS AND DISCUSSION

Contact Resistance

The contact resistance in make-and-break arc contact tests was measured because it is related to the energy consumption across a contact interface and contributes to the temperature rise on contacting surfaces. Figure 2 shows the variation of contact resistance with contact cycles for oxygen-free high-conductivity (OFHC) copper, and Cu-15%Nb and Cu-15%Cr composites, all with the same true deformation strain of 4.8. The true deformation strain η was defined as $\eta = ln(A_O/A)$ where A_O and A are the cross-sectional areas before and after deformation processing. Here, both the moving and stationary electrodes were made of an identical material. OFHC copper was tested to serve as a standard for contact resistance. It is seen from Figure 2 that the contact resistance values in the initial stage of operation for all of the three materials were fairly low. The contact resistance increased with increasing contacting cycles, the rate of increase being the highest for Cu-15%Cr and the lowest for OFHC copper. The contact resistance finally reached a steady state value for OFHC Cu and Cu-15%Nb. The mean contact resistance of Cu-15%Nb was close to that of OFHC copper but the the fluctuation in it was larger.

The increase in contact resistance is related to the development of a surface film on the contact surface and also surface deterioration. Because of the make-and-break operation, an arc is generated between the moving and stationary contacts. This produces surface damage and the build-up of surface film. With the increase in surface film thickness, the contact resistance is increased. Since the chemical structures of different surface films (to be reported) were different for different contact materials,

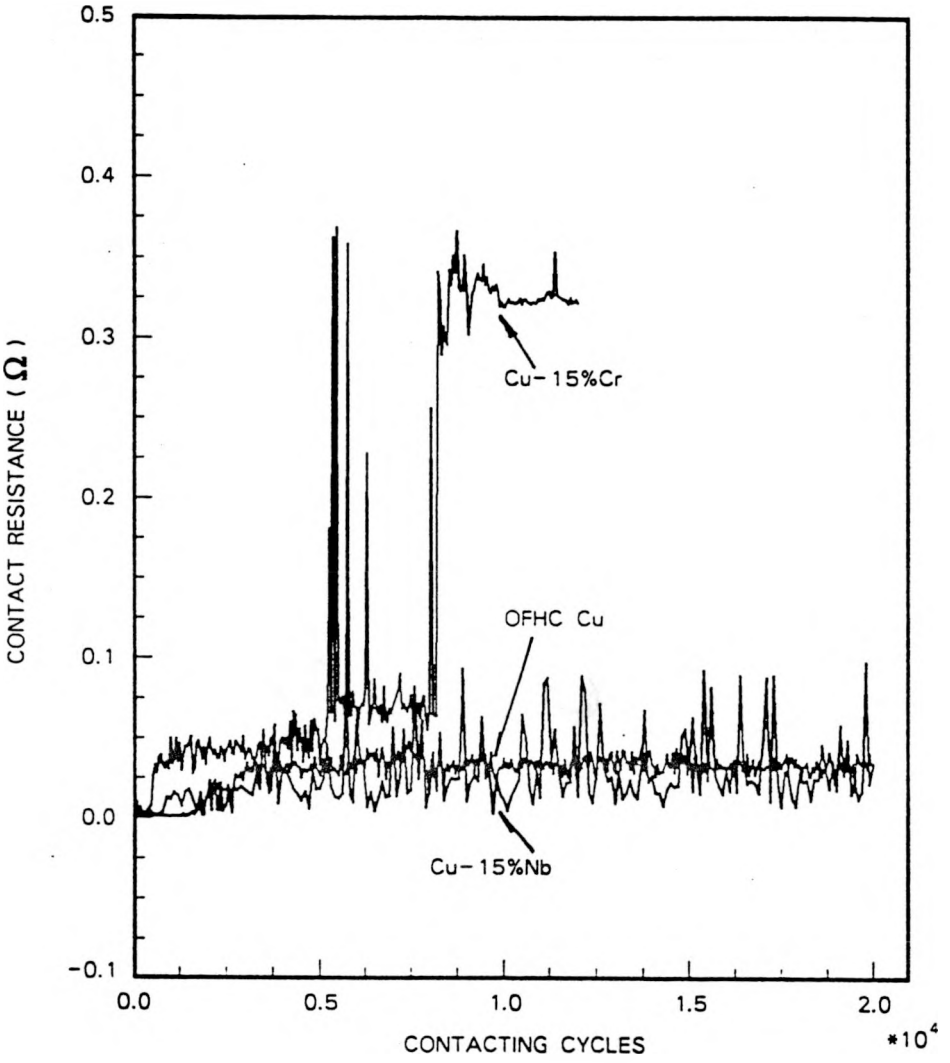

Figure 2: Variation of contact resistance with contacting cycles, test conditions: 210 V AC, 14.6 A, contact diameter 6.35 mm

the steady state contact resistance values and the cyclic fluctuations in them were also different.

Surface Film Analysis

The surfaces of the make-and-break contact specimens were analyzed for chemical structure by X-ray diffraction techniques. For this purpose, a Cu X-ray tube with an acceleration voltage of 35 kV and current of 20 mA was used. The X-ray diffraction spectra of the contact surfaces are shown in Figure 3. In all the cases, Cu was oxidized to Cu_2O. In Cu-15%Nb and Cu-15%Cr, Nb and Cr were also partially oxidized to NbO and Cr_2O_3. The electrical resistivities and the melting points of the related elements and their oxides formed on the contact surfaces are listed in Table 2.

Table 2: Electrical resistivities and melting points of some elements and their oxides

Substance	Electrical Resistivity (Ωm)	Melting Point (^{o}C)
Nb	12.5×10^{-8} [10]	2468 [10]
NbO	10^{-7} [11]	1937 [12]
Cr	12.9×10^{-8} [10]	1857 [10]
Cr_2O_3	non-metallic [11]	2266 [10]
Cu	1.534×10^{-8} [10]	1083 [10]
Cu_2O	10-50 [13]	1235 [10]

Table 2 shows that that NbO is a metallic conductor, Cu_2O a semiconductor while Cr_2O_3 is highly resistive. The resistivities of all the oxides are higher than those of the constituent metallic elements except for NbO where the difference is small. Thus, depending upon the resistivities, as the surface film formed on the contact surface, the contact resistance increased to different extents for different materials.

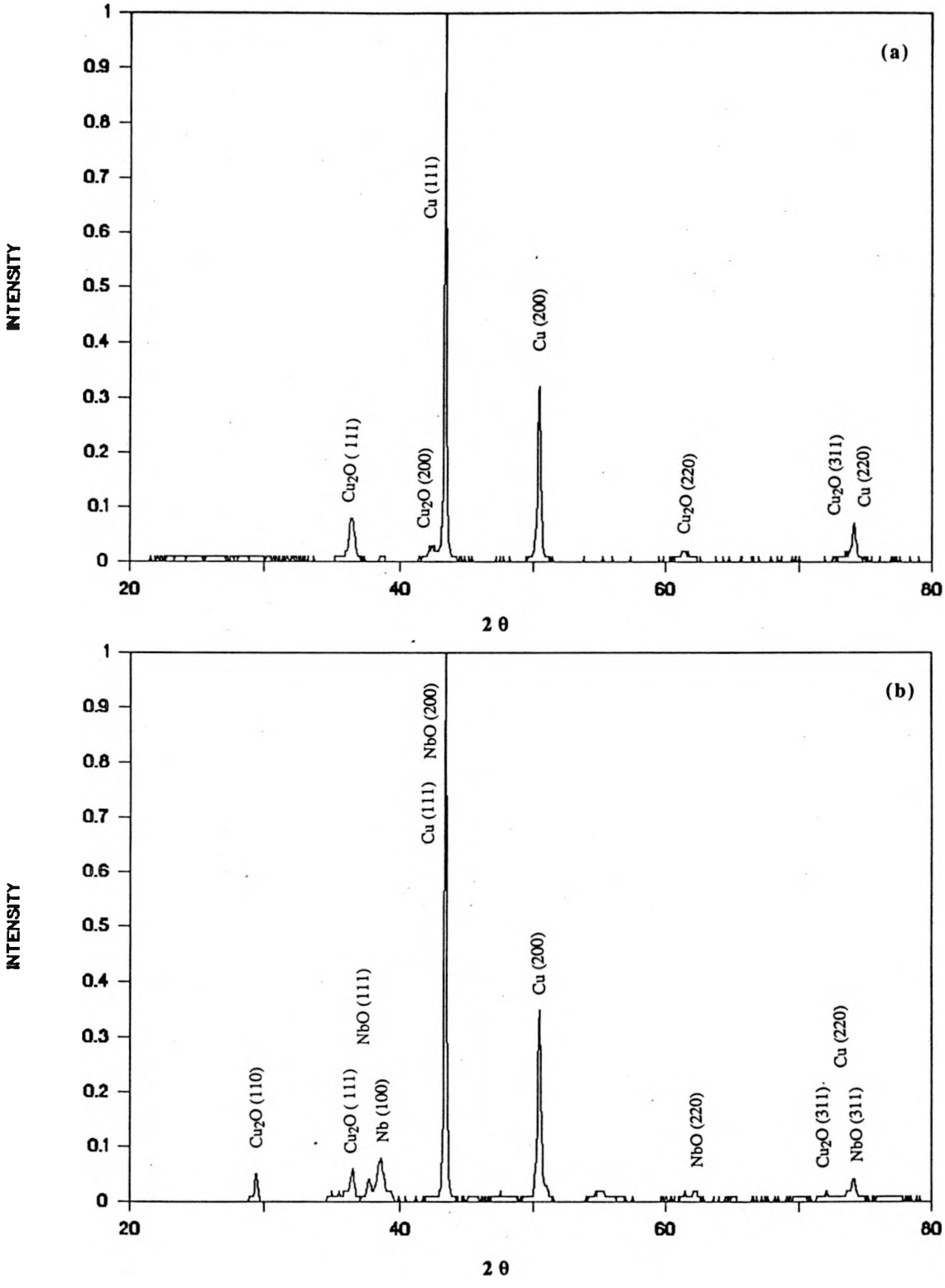

Figure 3: X-ray diffraction spectra of the contact surfaces of: (a) OFHC Cu; (b) Cu-15%Nb; (c) Cu-15%Cr. All specimens were tested at 210 V AC and 14.5 A

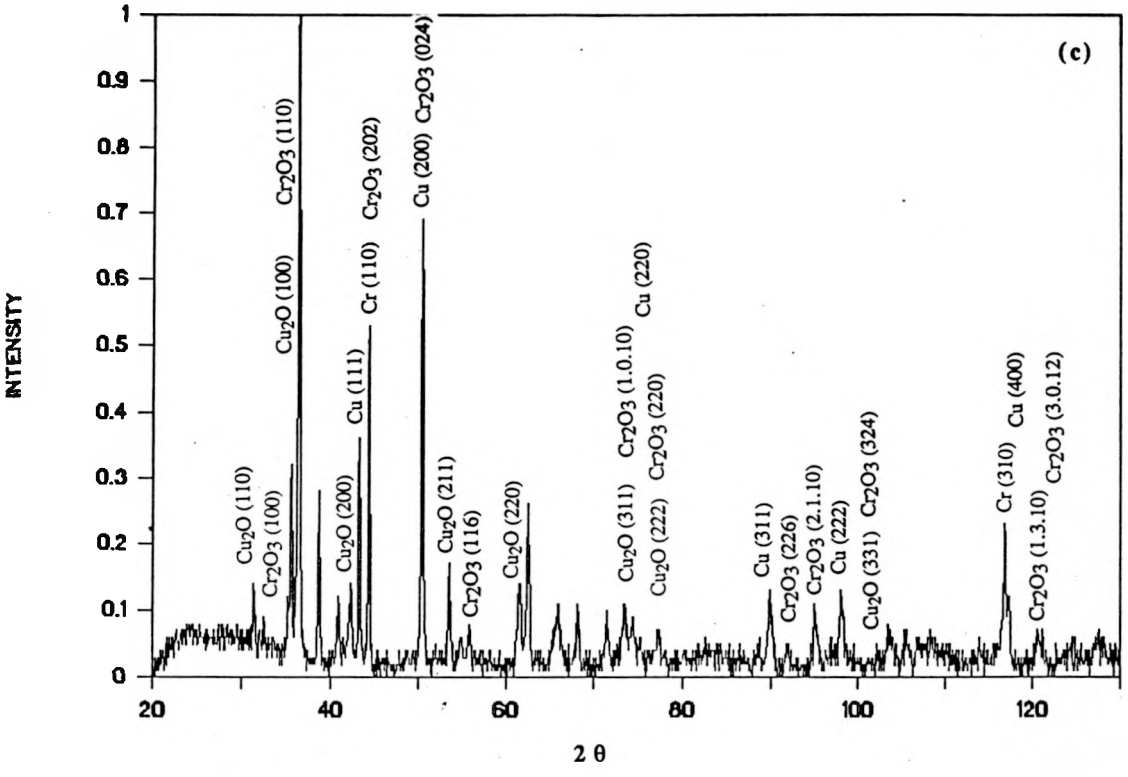

Figure 3 (Continued)

The contact resistance of Cu-15%Cr was much higher than that of Cu-15%Nb because Cr_2O_3 is highly resistive. Since Cr_2O_3 and Cu_2O have higher melting points than Cr and Cu respectively, the melting point of the oxide film on the Cu-15%Cr surface would also be expected to be higher than that of the substrate. Contrary to this, NbO formed on the Cu-15%Nb surface has a lower melting temperature (1937^oC) than Nb (2468^oC) in the substrate. Since the melting temperature of Cr_2O_3 is higher than that of NbO, Cr_2O_3 was more likely to stay in the solid state than NbO when subjected to an electrical arc of the same intensity. Because of the above differences, the contact resistance of Cu-15%Cr was higher than that of Cu-15%Nb.

Arc Erosion of Low-Energy Contacts

Figure 4 provides the comparison between the arc erosion rate of different materials tested in the low-energy make-and-break arc contact test facility. The arc erosion rates of the moving tips were either higher or equal to those of the stationary tips because the moving part was subjected to more vibrations. Since the moving spring was broken after 1400 cycles in the test of Cu-15%Cr, the arc erosion rate of the moving tip was not evaluated. The arc erosion rate of non-bundled Cu-15%Nb composite with $\eta = 4.88$ was close to that of OFHC copper, and it was higher for the bundled Cu-15%Nb composite with $\eta = 8.2$ than for the previous two materials. The arc erosion rate of Cu-15%Cr composite was the highest among all the materials tested.

In order to understand the arc erosion behavior, the arc eroded specimens were sectioned and examined for changes in the subsurface structure during arc erosion. The specimens were plated with Ni before sectioning in order to preserve the surface

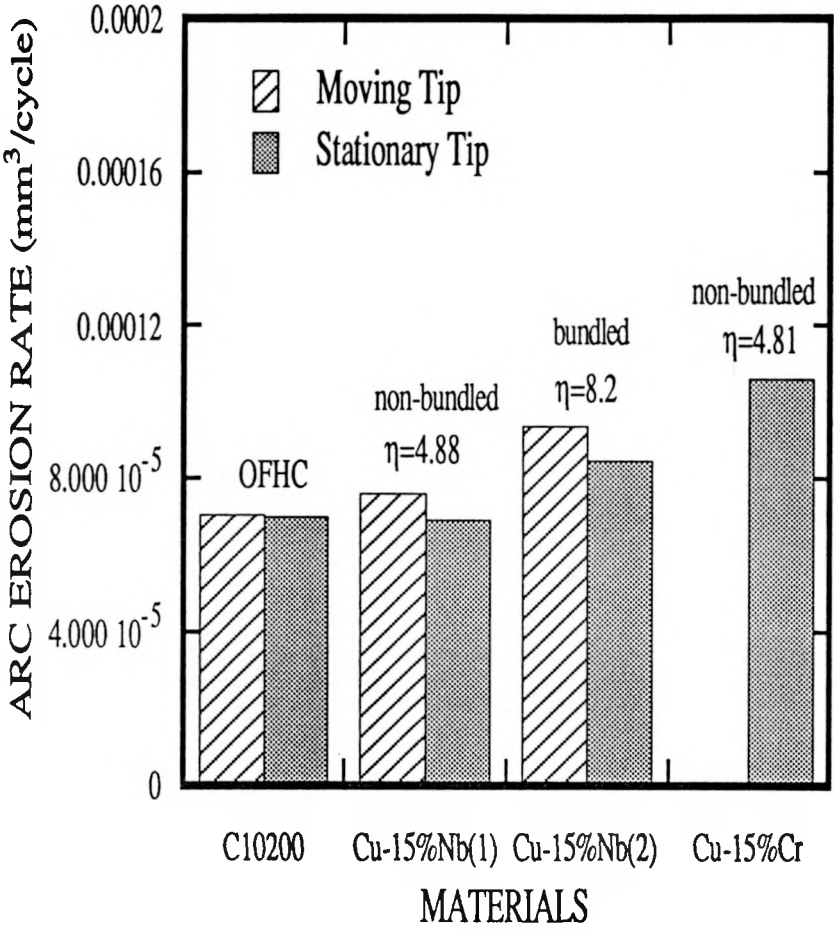

Figure 4: Comparison of arc erosion rates of OFHC Cu, Cu-15%Nb and Cu-15%Cr tested at 210 V AC and 14.6 A with a contact head diameter of 6.35 mm

film and the subsurface structure. Figure 5 shows the cross-sections of the eroded tips. The thickness of the oxide films formed on Cu-15%Cr, Cu-15%Nb and OFHC copper were about 40 μm, 20 μm and 8 μm, respectively. The differences in oxide film thickness should be related to the differences in the oxidation rates of different elements. In the low-energy contact situation, the arc heat and the consequent temperature rise were not high enough to cause large scale melting. Oxidation was thus a major event, which caused surface film formation, deterioration and materials loss. Since both Nb and Cr are more reactive with O_2 than Cu, the oxidation in Cu-15%Cr and Cu-15%Nb occurred at a faster rate than in Cu, resulting in thicker oxide films. A thicker film is easier to be separated from its substrate during the make-and-break operation than a thinner film. Therefore, in the low-energy situation, Cu-15%Nb and Cu-15%Cr did not show any better arc erosion resistance than OFHC copper, as shown in Figure 4. With the increase in true deformation strain of Cu-15%Nb, the Nb filament spacing decreased and the surface area of Nb exposed to oxidation increased so that more oxidation or material loss occurred. Cu-15%Nb with the higher η of 8.2 had thus had a higher arc erosion rate than that with the lower η of 4.88.

Figure 5 also shows that OFHC copper and Cu-15%Nb eroded by arc more uniformly than Cu-15%Cr. The Cu-15%Cr composite eroded preferentially and the surface became more ragged. During subsequent contacts, the surface irregularity resulted in higher contact resistance. In addition, the thicker oxide film formed in this case also contributed to higher contact resistance. Both of these factors were thus responsible for the higher contact resistance of Cu-15%Cr than that of Cu-15%Nb, as shown in Figure 2.

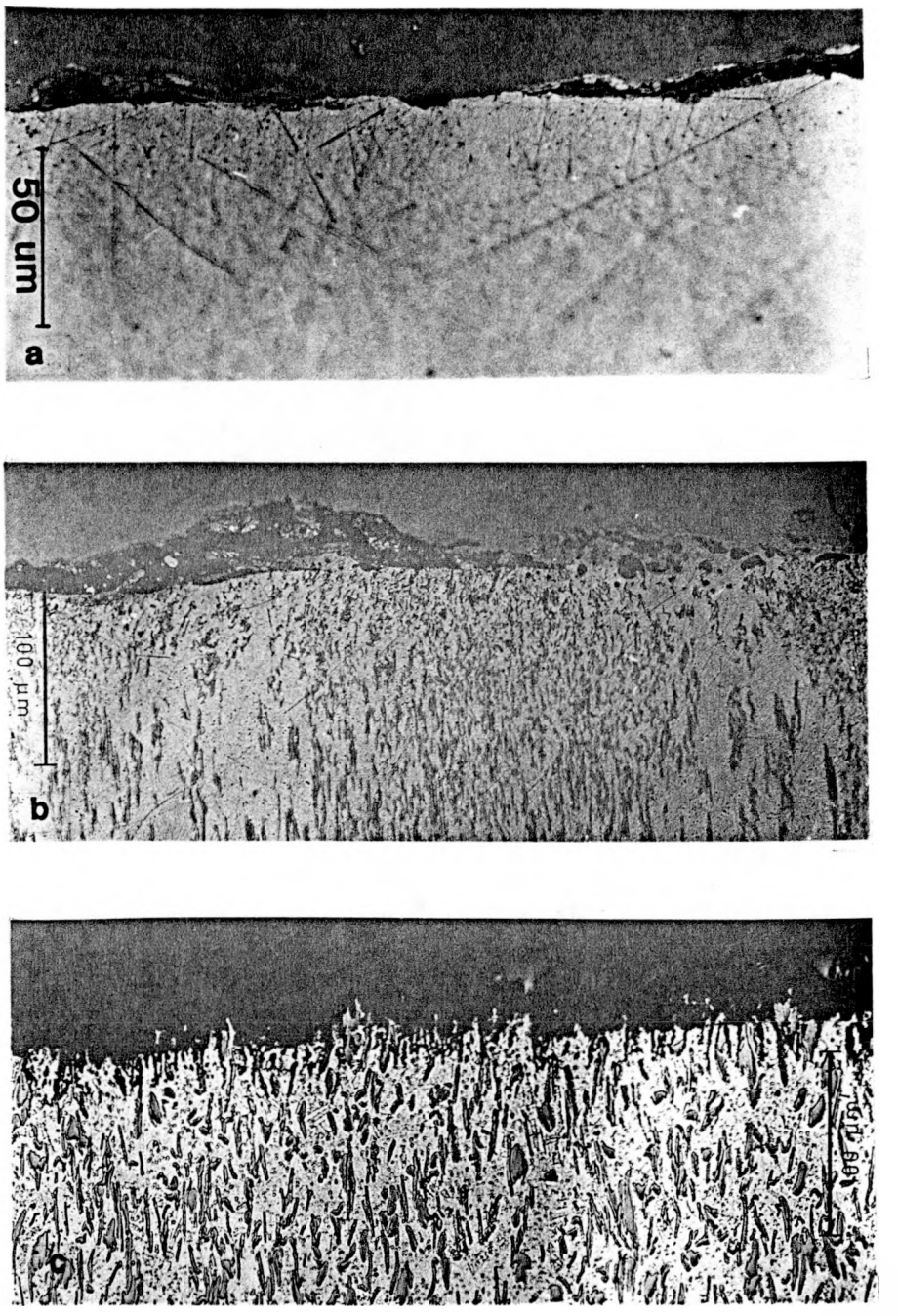

Figure 5: Optical micrographs of the cross-sections of make-and-break contact tips made of (a) OFHC Cu (20,000 cycles); (b) Cu-15%Nb with $\eta = 4.88$ (20,000 cycles); (c) Cu-15%Cr (12,000 cycles) tested at 210 V AC and 14.6 A with head diameters of 6.35 mm

Figure 6 shows the general features of the contact heads of Cu-15%Nb (tested for 20,000 cycles) and Cu-15%Cr (tested for 12,000 cycles). There was an oxide film on the contact surface of Cu-15%Nb. The oxide scale on the surface of Cu-15%Cr was much thicker and it separated easily from its substrate which appeared as shown in Figure 6(b). Figure 7 provides the details of the black and gray areas observed on the arc eroded surface of Cu-15%Nb in Figure 6 (a). The black region was heavily covered by a thick film which was cracked in some locations. There is an indication of adhesive bonding and the consequent removal of material in the lower middle part which exhibits severe plastic deformation. The gray region appears to be covered by a molten film and the solidified globules are also seen in Figure 7 (b). Figure 8 shows the details of the Cu-15%Cr contact surface given in Figure 6 (b). The upper part of the diagram shows the fracture surface of the oxide film because here the thick oxide film was shaken away from the surface. All of the above observations indicated that oxidation was the major factor responsible for deterioration of the contact surfaces of Cu-Nb and Cu-Cr composites in the low-energy contact situation.

Erosion of High-Energy Arc Gaps

The variation of volumetric arc erosion rate with the effective charge per shot is plotted in Figure 9 for pure copper, Cu-W, Cu-15%Nb and Cu-15%Cr, as determined in the Mark VI stationary arc erosion test facility. Here the data for pure Cu and Cu-W composite were taken from reference [9] and are included to serve as the basis for comparison and to reveal the effect of different refractory phases on the arc erosion behavior. As shown in the figure, the amount of arc erosion for all the materials tested increased with increasing electrical energy. The arc erosion rate of pure Cu

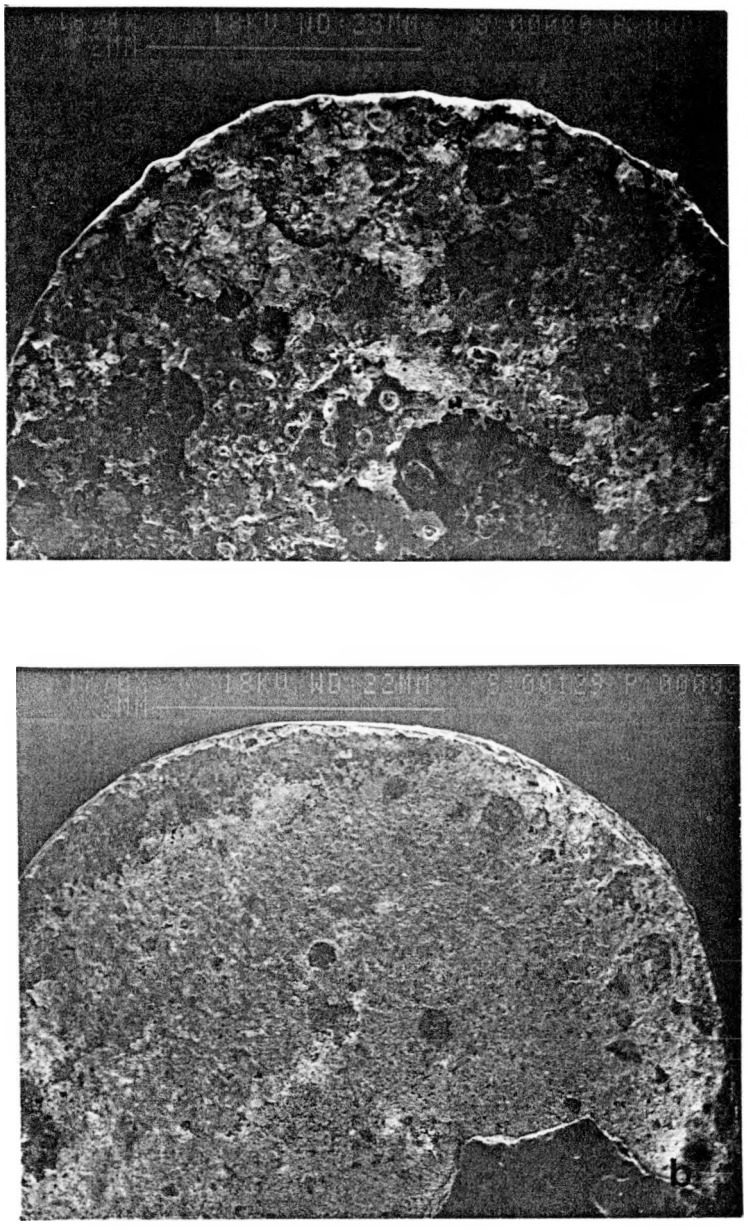

Figure 6: SEM photographs of the electrode contact surfaces of: (a) Cu-15%Nb with $\eta = 4.88$ (20,000 cycles) and (b) Cu-15%Cr (12,000 cycles) tested at 210 V AC and 14.6 A with contact head diameter of 6.35 mm

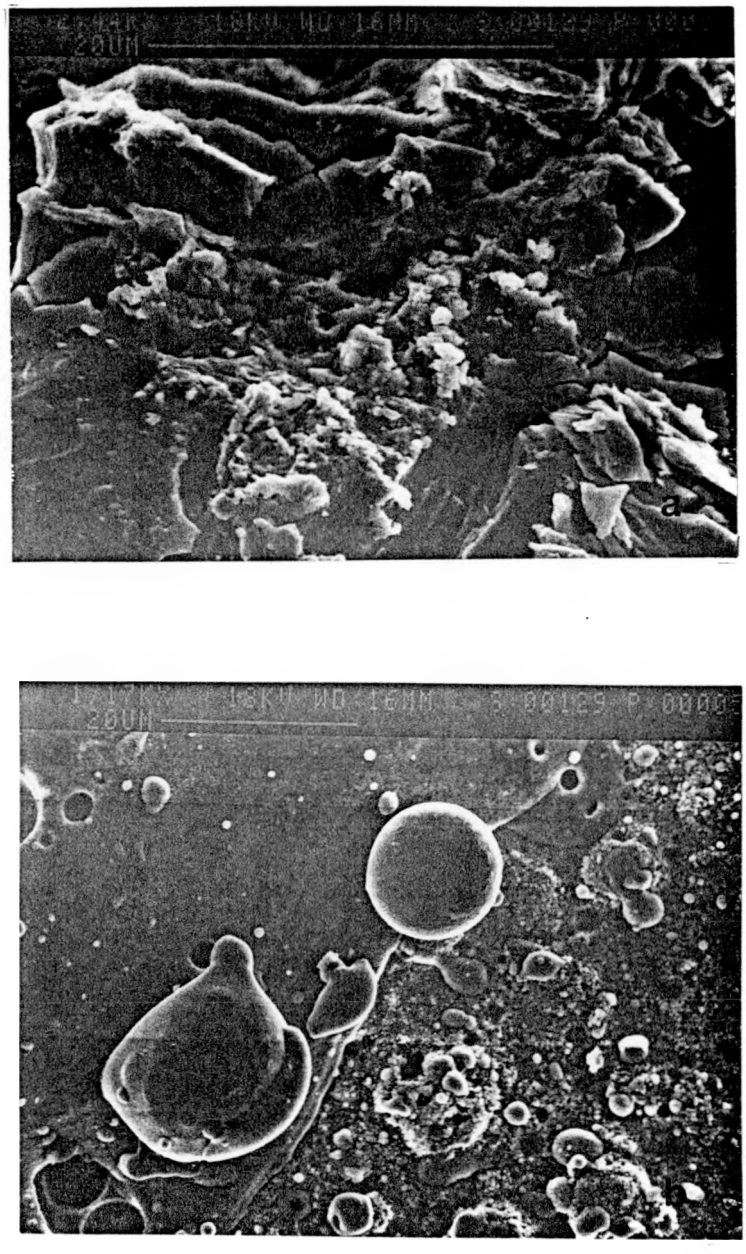

Figure 7: Details of the (a) black and (b) gray areas in Figure 6 (a)

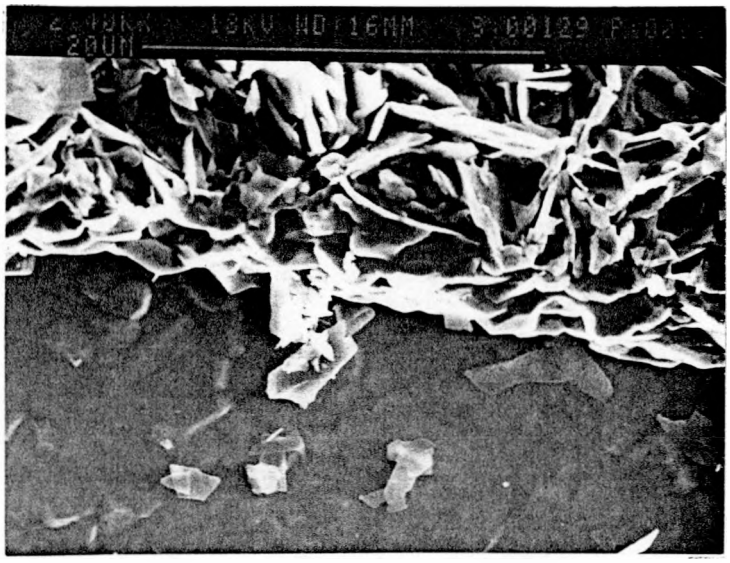

Figure 8: SEM micrograph showing the details of of the gray and black regions on the contact surface of Cu-15%Cr tested at 210 V AC and 14.5 A for 12,000 cycles

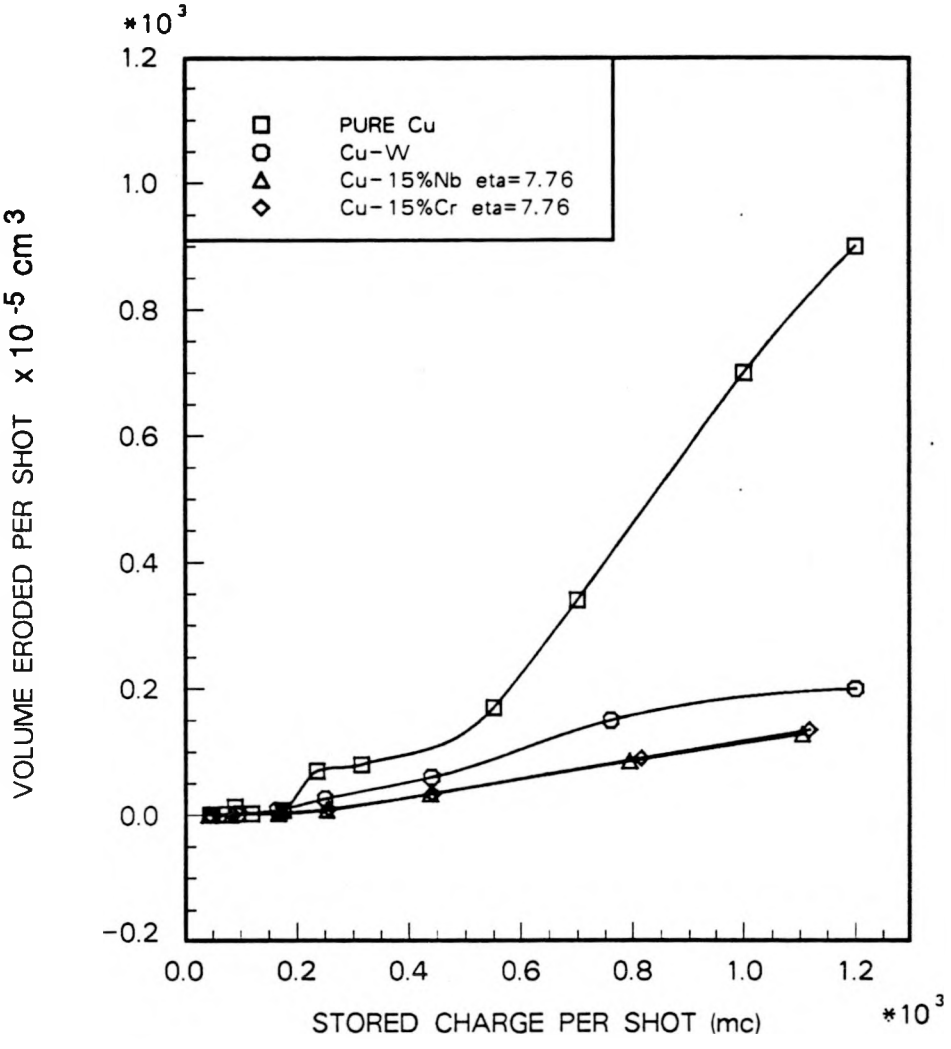

Figure 9: Variation of eroded volume per shot with stored energy for pure Cu, Cu-W, Cu-15%Nb and Cu-15%Cr electrodes tested in Mark VI high energy stationary arc test facility

was the highest and that of Cu-15%Nb or Cu-15%Cr the lowest. The differences among the arc erosion rates of different materials increased with increasing electrical energy level, and at very low energy levels the arc erosion rates of all the materials were the same.

Figure 10 shows the hemispherical tip surfaces of Cu-15%Nb and Cu-15%Cr electrodes eroded in the high-energy arc situation. Whereas the erosion rates for both of these composites were about the same, the eroded features are somewhat different. There was an indication of large scale melting in the case of Cu-Cr while that was not the case with Cu-Nb. Instead, there were some craters formed on the Cu-Nb surface because of localized erosion and melting. The bulk melting on the Cu-Cr contact surface can be seen in Figure 11 where the convex spherical tips seem to have been flattened slightly because of material flow to the sides. Cu-Nb electrode maintained its spherical shape better after the test, and there is no indication of a superficial layer.

Figure 12 shows the arc eroded surface of Cu-15%Nb. Here, erosion craters are seen on the surface and there is an indication of melting in the regions serving as the boundary between the hexagonal subelements bundled together for composite processing. Figure 13 shows the back-scattered electron image of the vertical section of the bundled Cu-15%Nb ($\eta = 7.76$) contact shown in Figure 12. This imaging mode was used because it showed Nb well. The figure shows an erosion crater in which Cu appeared to have melted and eroded away from the boundary so that Nb was left inside, aggregated and interlocked between the surface layers. This observation indicated that Nb filaments by virtue of their high melting point played a protective role in the high-energy arc erosion.

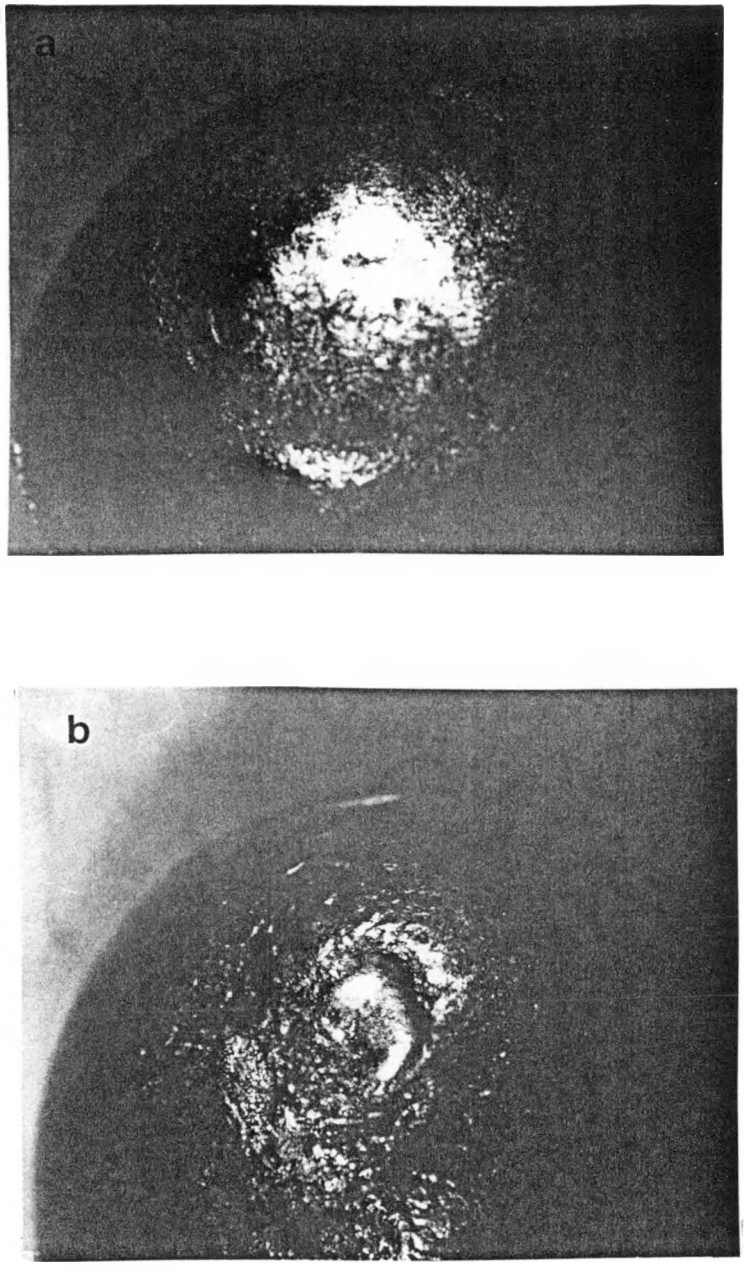

Figure 10: Optical micrographs showing arc erosion damage on the hemispherical tips tested in Mark VI facility for 1500 shots: (a) Cu-15%Cr; (b) Cu-15%Nb, both with $\eta = 7.76$

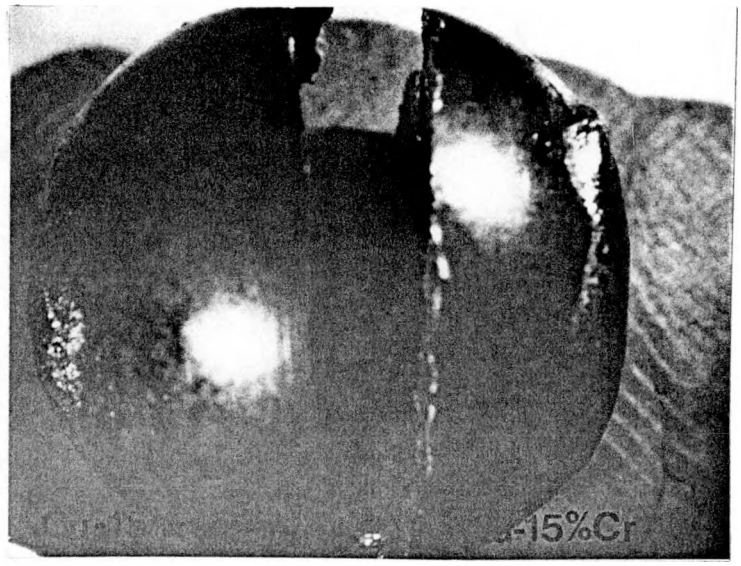

Figure 11: Side-view of the hemispherical ends of electrodes tested in stationary Mark VI facility for 1500 shots: left electrode Cu-15%Nb; right electrode Cu-15%Cr

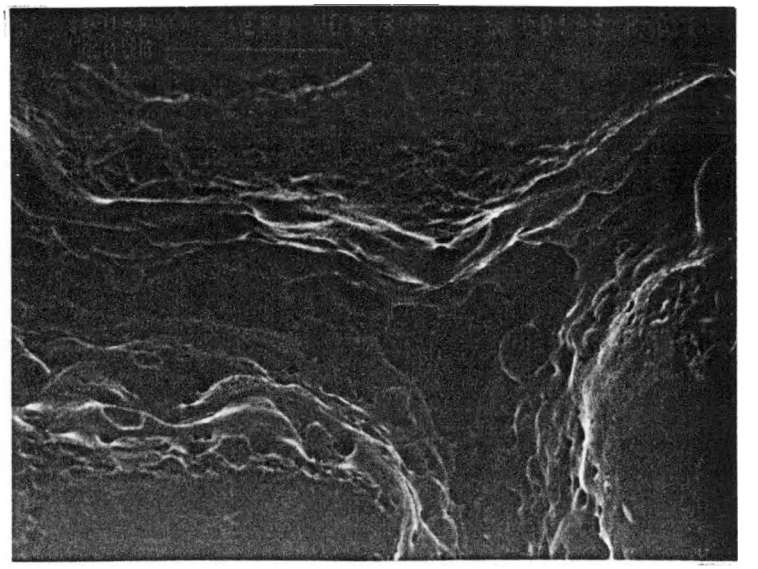

Figure 12: SEM micrograph of the eroded surface of Cu-15%Nb (η = 7.76) hemispherical tip tested in Mark VI facility for 1500 shots. The area shows the boundary between three hexagonal subelements bundled during composite processing

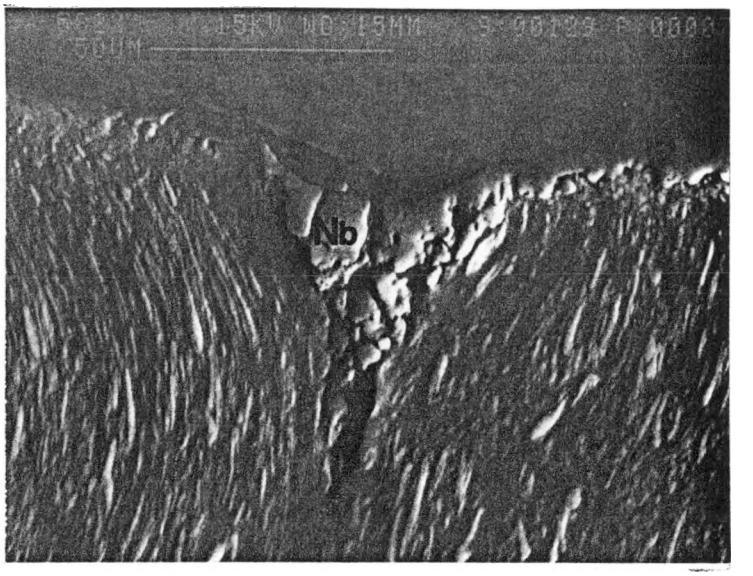

Figure 13: SEM back-scattered electron image of the cross-section of Cu-15%Nb (η = 7.76) hemispherical tip tested in Mark VI facility for 1500 shots

Figure 14 exhibits the cross-sections of Cu-15%Nb and Cu-15%Cr electrodes tested in the high-energy stationary arc situation. It shows only the partial thickness of molten layers. It provides the evidence of melting on the electrode surfaces. Some fine refractory metal particles are seen in the melted and solidified layer, but the number of Cr particles is fewer than that of Nb particles. Because the solubility of Cr is much higher than that of Nb at a given temperature, it is likely that most of the Cr particles dissolved in the molten material but not so with Nb particles. The high temperature presumably caused the Cu matrix phase to melt and form the molten layer. The dissolved Cr either remained in solid solution in the Cu phase because of rapid freezing or precipitated in the form of submicroscopic particles too small to be seen in optical microscopy. EDS results showed that the average composition of the molten layer in the particular location was 97%Cu and 3%Nb for Cu-15%Nb and 94%Cu and 6%Cr for Cu-15%Cr. Figure 15 is the SEM back-scattered electron image of the cross-section of Cu-15%Nb electrode tested in high-energy stationary arc situation. This micrograph shows the agglomeration of Nb on the surface. In other words, Cu-Cr formed either a solid solution or submicroscopic precipitate while Cu-Nb had the agglomeration of individual phases in the molten layer.

According to the above observations, melting is the major mode of arc erosion in high-energy situation. It is basically in this situation that refractory metals like Nb or Cr play a protective role to increase arc erosion resistance. Because of this, Cu-15%Nb and Cu-15%Cr had higher arc erosion resistance than pure Cu and even better than Cu-W composite which is commercially used.

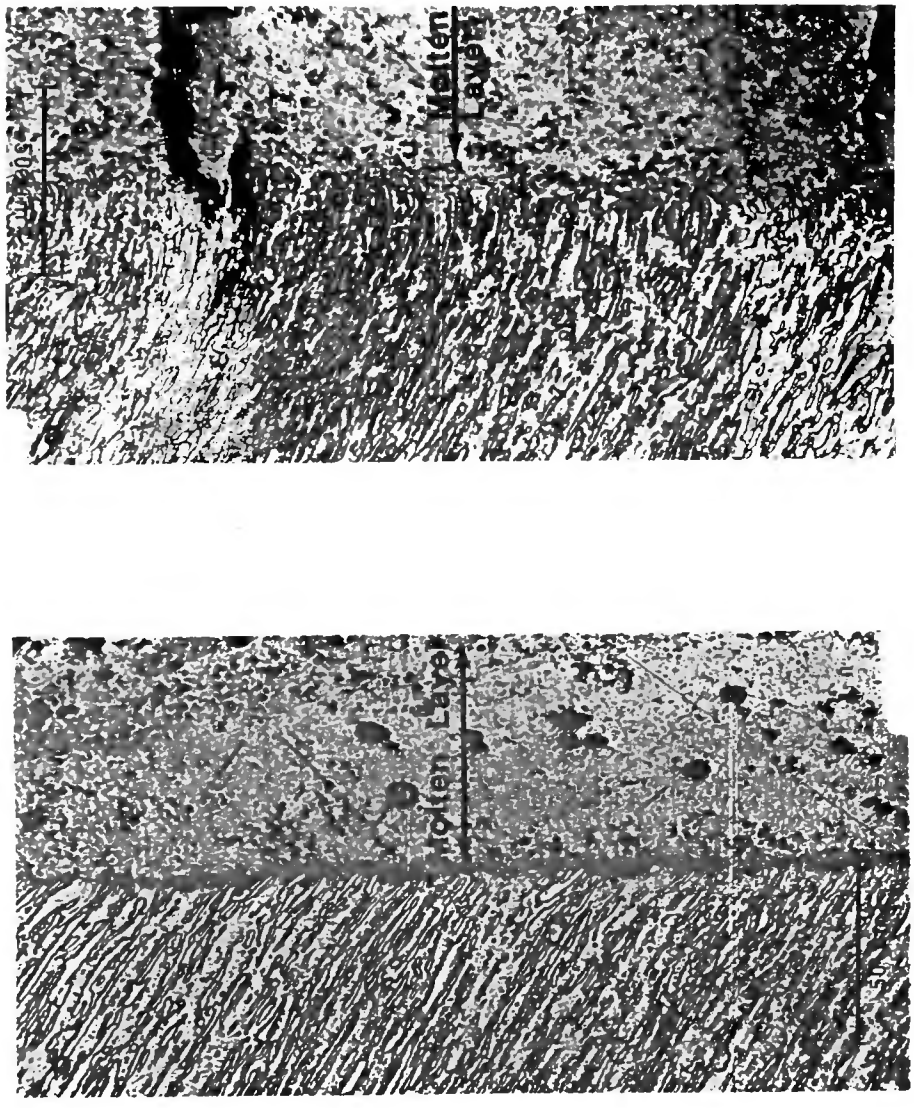

Figure 14: Optical micrographs of the cross-sections of electrodes tested in the Mark VI facility for 1500 shots: (a) Cu-15%Nb, $\eta = 7.76$; (b) Cu-15%Cr, $\eta = 7.76$

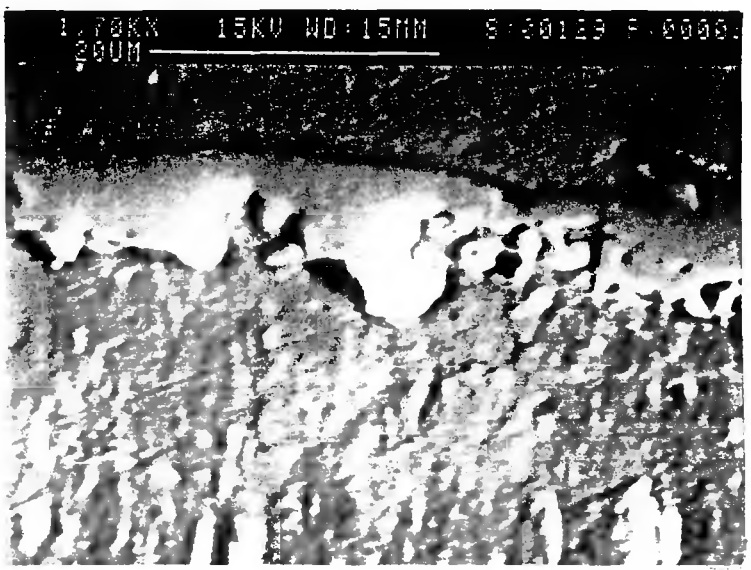

Figure 15: SEM back-scattered electron image of the cross-section of Cu-15%Nb electrode tested in high-energy stationary arc Mark VI facility for 1500 shots

CONCLUSIONS

In low-energy make-and-break contacts, oxidation was the major factor responsible for the deterioration of contact surfaces. The surface film formed on the Cu-15%Cr contact surface consisted of Cr_2O_3 and Cu_2O. It was much thicker and more resistive than the film formed in the case of Cu-15%Nb which contained NbO and Cu_2O. In this situation, the arc erosion resistance of Cu-based composites was not increased by the presence of Nb or Cr filaments. The Cu-15%Nb composite was eroded uniformly in contrast to the nonuniform erosion observed in case of Cu-15%Cr. The contact resistance of Cu-15%Cr was higher than that of OFHC copper or Cu-15%Nb because of nonuniform erosion and the different structure of oxide films.

In high-energy stationary arcing gaps, the arc erosion resistance of bundled Cu-15%Nb and Cu-15%Cr electrodes was much better than that of pure Cu and also better than that of the commercially used Cu-W composite. Melting was a major mode of erosion damage in this situation. In the event of melting caused by high-energy arc, Cu-15%Cr tended to form either a solid solution or submicroscopic precipitate whereas Cu-15%Nb tended to form the agglomerate of individual phases in the molten layer.

REFERENCES

[1] Pitney, K. E. Ney Contact Manual, Electrical Contacts for Low Energy Uses. The J. M. Ney Company (1973): 14.

[2] Michal, R. and K. E. Saeger. "Application of Silver-Based Contact Materials in Air-Break Switching Devices for Power Engineering." Electrical Contacts-1988. Proceedings of the 34th IEEE Holm Conference on Electrical Contacts (1988): 121-127.

[3] Gray, E. W. "Voltage Fluctuations in Low-Current Atmospheric Arcs." J. Appl. Phys. vol.43(11) (1972): 4573-4575.

[4] Sone, H. and T. Takagi. "Role of the Metallic Phase Arc Discharge on Arc Erosion in Ag Contacts." Electrical Contacts-1989. Proceedings of the 34th IEEE Holm Conference on Electrical Contacts (1989): 157-161.

[5] Shen, Y. S. and L. J. Gould. "Erosion Modes of Internally Oxidized Ag-CdO and Ag-(Sn,In)O Material." Electrical Contacts-1987. Proceedings of the 33rd IEEE Holm Conference on Electrical Contacts (1987): 157-161.

[6] Donaldson, A. L., M. Kristiansen, A. Watson, K. Zinsmeyer and E. Kristiansen. "Electrode Erosion in High Current, High Energy Transient Arcs." IEEE Trans. on Magnetics. vol.22(6) (1986): 1441-1447.

[7] Bahadur, S., P. Liu and J. D. Verhoeven. "Cu-Refractory Metal Alloy Application in Sliding Electrical Contacts." Final Report. Center for Advanced Technology Development, Iowa State University, Ames (1990).

[8] Verhoeven, J. D., F. A. Schmidt, E. D. Gibson and W. A. Spitzig. "Copper-Refractory Metal Alloys." Journal of Metals. Sept. (1986): 20-24.

[9] Donaldson, A. L., T. G. Engel and M. Kristiansen. "State-of-the-art Insulator and Electrode Materials for Use in High Current, High Energy Switching." IEEE Trans. on Magnetics. vol. 25(1) (1989): 138-141.

[10] Weast, R. C. (editor-in-chief) CRC Handbook of Chemistry and Physics. CRC Press, Inc., Boca Raton, Florida (1989): F-146-147, B-85.

[11] Tallal, N. M. (editor) Electrical Conductivity in Ceramics and Glass. Marcel Dekker, Inc., New York (1974): 380-384.

[12] Dean, J. A. (editor) Lange's Handbook of Chemistry (12th edition). McGraw-Hill Book Company (1979): 4-82-83.

[13] Carmichael, R. S. CRC Handbook of Physical Properties of Rocks. CRC Press, Inc., Boca Raton, Florida (1982): 231.

SUMMARY

The tribological and arc erosion behaviors of Cu-Nb and Cu-Cr composites have been studied in this dissertation. The mechanical and the sliding friction and wear behaviors of the composites under non-electrical sliding condition provided a basis for the understanding of the friction and wear behaviors of these composites under electrical load. The coefficient of friction decreased with Nb proportion in both electrical and non-electrical sliding. Cu-20vol.%Nb had the best wear resistance among Cu-Nb composites tested with and without electrical current.

In non-electrical sliding, in the subsurface layer affected by sliding, along with the Cu matrix Nb filaments were also deformed. As a result of this deformation, the filaments were oriented along the sliding direction and were refined. There was no debonding observed between the filament and the matrix and the composition of wear debris was about the same as that of the composite. Subsurface deformation flow, cutting, plowing and surface crack initiation and propagation were the mechanisms responsible for the wear of composites. The coefficient of friction was not affected significantly by sliding speeds in the range of 0.028 to 2.50 m/s, but the wear rate decreased with increasing sliding speed. The coefficient of friction and wear resistance of the composites with filament orientation perpendicular to the sliding plane were higher than those with the parallel filament orientation. The wear resistance and the

coefficient of friction of Cu-Nb composites increased with increasing true strain. The wear rate of the composites increased rapidly with increasing annealing temperature up to $300^{o}C$, but the rate of increase was very modest for the composites annealed in the range of 300 to $600^{o}C$.

The subsurface deformation in sliding with electrical current was similar to that of non-electrical sliding except that a much thicker oxide film was formed in the presence of electrical current. There were three characteristic zones observed on the worn surface: plowing zone, transition zone, and particle accumulation and arc erosion zone. Besides transferring from the composite pin to the steel disk, material was transferred from the tool steel disk to the Cu-Nb composite surface in the form of oxide. The sliding track on the tool steel disk was severely damaged and oxidized because of electric arcing. Oxidation and material transfer were the two mechanisms governing the friction and wear behavior of the composites. The coefficient of friction of Cu-Nb in situ composites sliding against tool-steel was lower in electrical sliding than in non-electrical sliding. At a relatively low electrical current level, the coefficient of friction and wear were high. As the electrical current density increased to 2.89 MA/m^2, both the coefficient of friction and wear rate decreased. The temperature rise in sliding contact was dominated by electrical Joule heating, which is proportional to contact resistance. The sliding motion produced a large increase in both the contact resistance and the temperature rise. The composite with Nb filaments perpendicular to the sliding direction exhibited higher wear resistance than that with a parallel filament orientation. There was no significant difference in the coefficient of friction with parallel and perpendicular filament orientations.

As for the sliding contact behavior of Cu-20%Nb composite, the sliding contact

resistance was much higher than that for the stationary contact. At lower sliding speeds, it was controlled by oxide film growth and wear particle accumulation. At high speeds, unsteady contact caused by sliding motion was the dominant factor affecting contact resistance. With higher current density, the contact resistance for sliding contact between Cu-20%Nb composite and tool steel was lower. The Cu-20%Nb composite with Nb filaments parallel to the contact plane had lower contact resistance and temperature rise than that with perpendicular filament orientation. High contact resistance and temperature rise was attributed to dust wear for the composite of lower true strain.

Arc erosion occurred in both the make-and-break contacts and sliding electrical contacts. In low-energy make-and-break contacts, oxidation was the major mode of deterioration, and the Nb and Cr filaments did not increase the arc erosion resistance of the Cu-based composites. The surface films of Cr_2O_3 and Cu_2O were formed on the Cu-15%Cr surface. These were much thicker and more resistive than the films of NbO and Cu_2O formed in the case of Cu-15%Nb. Cu-15%Nb was eroded uniformly by arc in contrast to Cu-15%Cr where erosion was non-uniform. In high-energy stationary arcing gaps, melting occurred on the surfaces of electrode ends and this was the major failure mode for these contacts. The bundled Cu-15%Nb and Cu-15%Cr electrodes had much better arc erosion resistance than pure Cu and even better than the commercially used Cu-W composite.

ACKNOWLEDGMENT

It has been an honor to work under supervision of Dr. Shyam Bahadur and Dr. John D. Verhoeven and I extend my deepest gratitude to them for their continuous guidance, constant encouragement and patient assistance. Their unyielding ways of search for a better understanding on any subjects will benefit my whole life.

I am very grateful to Dr. William A. Spitzig in Ames Laboratory for his valuable discussions and suggestions and also for his willingness to be my committee member.

I would like to thank Dr. Raymond T. Greer in the Department of Aerospace Engineering and Mechanics for his consultation and willingness to serve as my committee member.

I would also like to thank Dr. Palaniappa A. Molian in the Department of Mechanical Engineering for his support and willingness to serve as my committee member.

Thanks are also due to Mr. E. D. Gibson in Ames Laboratory for his assistance in performing materials analysis, Mr. H. Sailsbury in Ames Laboratory for his continuous support on metallographic service, Mr. R. D. Steed in the Department of Mechanical Engineering for his help in setting up measurement and data acquisition system, and Mr. G. N. Scandrett in the Department of Mechanical Engineering for his hands-on teaching how to use machining facilities.

The support for this project was from the U. S. Department of Commerce through the Center for Advanced Technology Development in the Institute of Physical Research and Technology at Iowa State University. Part of the work was done in the Department of Mechanical Engineering at Iowa State University. The other part was performed at Ames Laboratory under contract no. W-7405-eng-82 with the U. S. Department of Energy. The United States government has assigned the DOE Report number IS-T 1565 to this dissertation.

I dedicate this work to my wife Susan X. Shao for her understanding and support, especially for her typing the first draft, to our daughter Annie [redacted] for her dear cooperation, and to my parents for their dreams, their sacrifice, their encouragement, their love and their affection.